NATIONAL AERONAUTICS AND SPACE ADMINISTRATION

Technical Report No. 32-854

Development Of An Electrochemical Energy Source For The Mariner II Spacecraft

Charles W. Brooke, Jr.

P. Goldsmith, Manager
Spacecraft Power Section

JET PROPULSION LABORATORY
CALIFORNIA INSTITUTE OF TECHNOLOGY
PASADENA, CALIFORNIA

March 15, 1966

CONTENTS

TABLES

TABLES (Cont'd)

FIGURES

FIGURES (Cont'd)

ABSTRACT

$N66-22207$

This Report describes in detail the development of an electrochemical energy source for the *Mariner II* spacecraft. The data presented trace the development of this battery, beginning with the definition of the electrical and mechanical requirements for the battery and concluding with the telemetered data obtained from the battery during 109 days of spaceflight to Venus. The design changes resulting from the type approval test program on the development model battery and the additional changes dictated by the *Mariner II* spacecraft system requirements were combined in the final silver-zinc battery design.

Author

I. INTRODUCTION

The *Mariner II* spacecraft electrical power system was designed to supply electrical energy for the spacecraft from two types of energy sources. A photovoltaic array provided electrical energy during those periods after launch when Sun orientation could be maintained by the spacecraft attitude control system. For those periods during the flight when Sun orientation could not be maintained, a source of stored energy was required. Based upon various limiting factors, which will be presented later in this Report, an electrochemical source of the secondary type was selected to supplement the solar power portion of the spacecraft electrical power system.

II. BATTERY PERFORMANCE REQUIREMENTS

The battery was required to supply energy for several distinct periods during the flight, as well as supplying the additional energy required in excess of that available from the solar array.

During prelaunch testing of the spacecraft, as part of the countdown operation, the battery was required to supply 150 whr of energy. Because of the launch time sequence restraints, the battery design should be such as to not require that this 150 whr be replaced by charging prior to launch.

The battery should also be capable of retaining sufficient charge to meet the flight requirements during a 10-day period in the spacecraft prior to launching. This battery was to be capable of being recharged at 10-day

minimum intervals during a 70-day period. The battery should still be capable of meeting the flight requirements at the end of this 70-day period.

The actual space flight period requiring battery operation ranged from a minimum of approximately 92 days to a maximum of approximately 158 days, depending on the actual calendar day when launch was accomplished. During the 90-min time interval from lift-off until Sun acquisition, the battery is required to supply 305 whr. Approximately midway during this period, a pulse load of the pyrotechnics systems would raise the peak power load on the battery to 475 w. The second battery operating period would start during the period from 17 to 70 hr after lift-off. This second period would require 170 whr of energy during a time interval of approximately 45 min. A pulse load during this period would raise the peak power demand to approximately 510 w. Figure 1 is a graphic presentation of the various battery energy demand preliminary requirements throughout the flight, based on the minimum flight time of 92 days. Figure 2 depicts the preliminary requirements on the basis of 158 days. The data presented in Figs. 1 and 2

are summarized in Table 1. The use of a primary or a secondary battery to meet these requirements was considered during the preliminary power system design. As shown in Figs. 1 and 2, there are basically two significant areas during the flight, with respect to the electrical energy requirements to be supplied by the battery. Commencing with spacecraft lift-off, the battery must have sufficient capacity to supply all energy requirements until Sun acquistion has been accomplished. Those loads that have a variable time of occurrence, such as period 2 (shown in Figs. 1 and 2), cause an increase in the minimum acceptable battery capacity as their starting times approach the end of the launch phase. This condition results from the reduction in charging time available between load periods if a secondary type of battery system is used. This effect was of a greater degree in the case of a primary battery system, since the internal battery losses cannot be replaced by charging. In the case of the primary battery system, the required capacity was minimized by keeping the time between battery load periods small. It should be recognized that the foregoing comparison of primary and secondary bat-
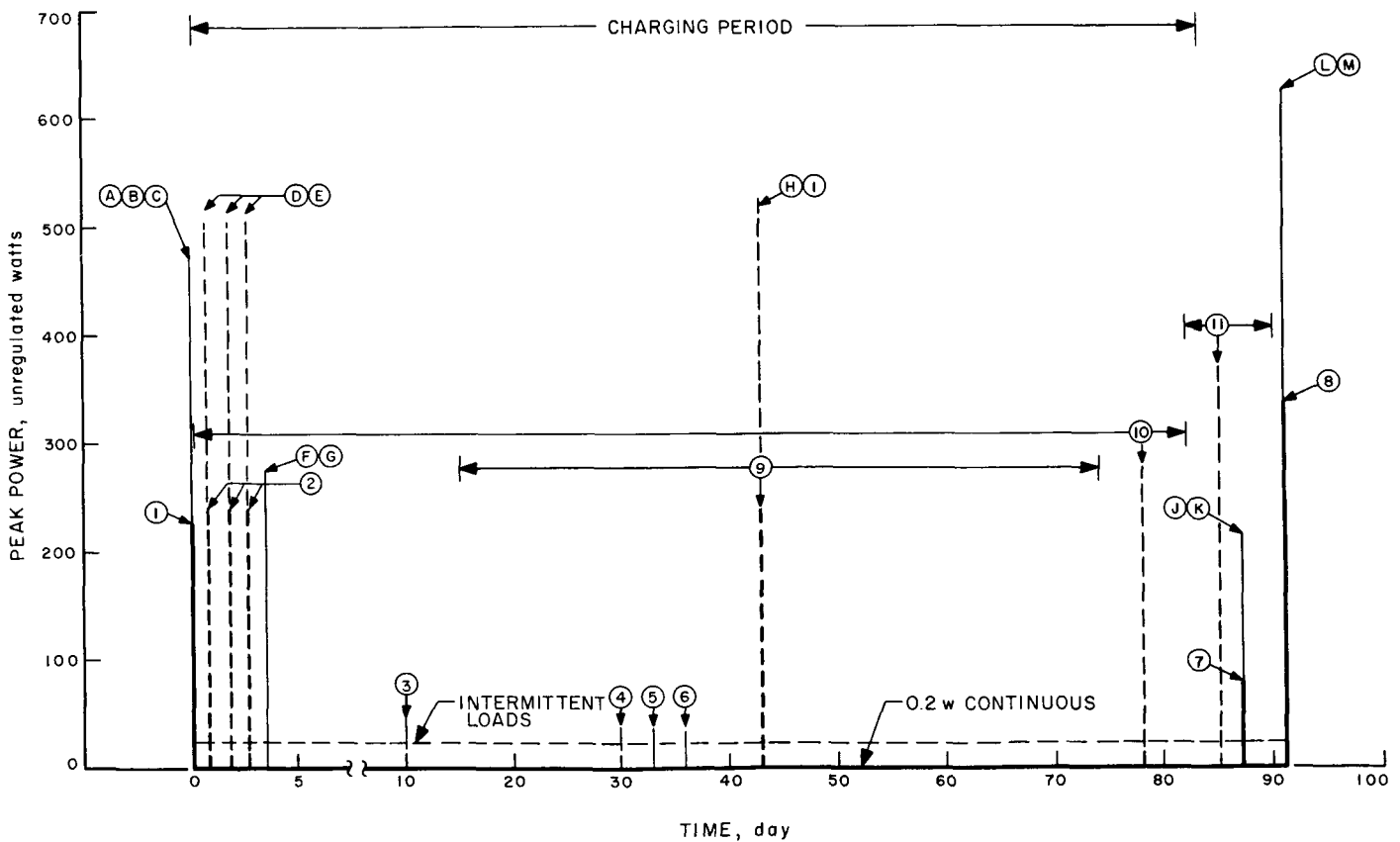
Fig. 1. Energy source power requirements vs shortest flight time
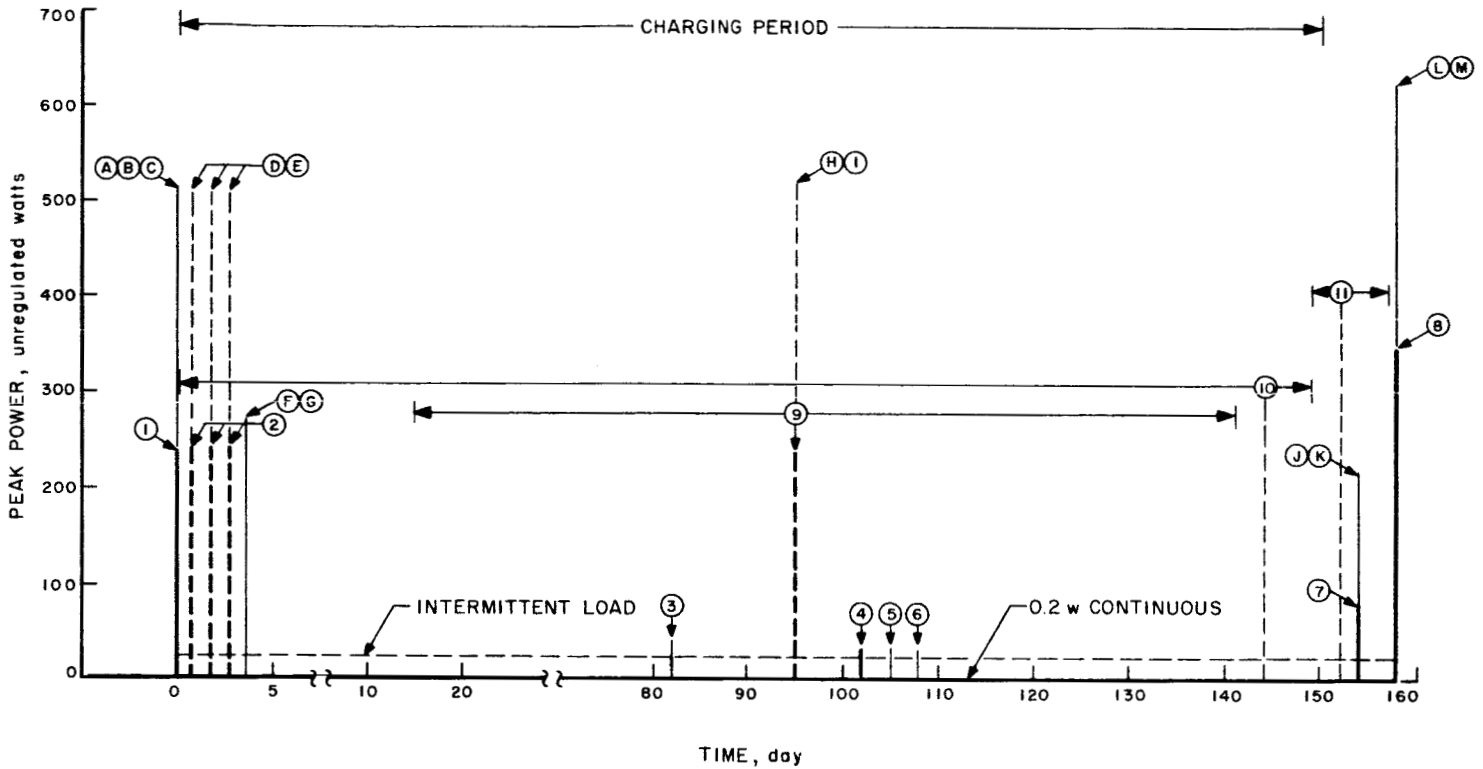
Fig. 2. Energy source power requirements vs longest flight time

tery systems on the basis of minimizing capacity is a generalization and ignores many other characteristics which may be significant in various applications. The second area of major interest shown in Figs. 1 and 2 is the battery requirements at the end of the flight. These loads are scheduled to occur during a 10-day interval after the battery can no longer be recharged. This condition presents two basic battery performance capabilities. The first is that the sum of these battery loads at the end of flight, plus an additional amount representing the

Table 1. Battery load schedule

Period No.	Flight Phase	Total load energy, whr	Load peak power, w	Starting time of load period[a]		Total load time, min
				Earliest, day	Latest, day	
—	Pre-launch testing	150	625	−10	−8 hr	—
1	Launch	305	475	—	—	90
10	Sun acquisition	68	275	+1.5 hr	82	15
2	Midcourse correction	170	510	+17 hr	+70 hr	45
3	Science load	20	44	10	82	60
9	Midcourse correction	170	510	15	141	45
4	Science load	15	38	30	102	60
10	Sun re-acquisition	68	275	30	149	15
5	Science load	15	38	33	105	60
6	Science load	10	35	36	108	60
7	Planet encounter	678	205	87	154	1080
11	Sun re-acquisition	94[b]	380	82	157	15
8	Science load	250[c]	625	91	158	45

[a] Referenced to lift off.
[b] Period 11 is an alternate requirement to one of the period 10 requirements.
[c] Period 8 is an alternate to period 9.

internal losses that will occur in the battery during this 10-day interval, will directly affect the determination of minimum battery capacity required. Considering the maximum spaceflight time shown in Fig. 2, the selection of a secondary battery appeared to be the only choice, based on the battery weight consideration. Because the peak power demand values (indicated by the circled letters on Figs. 1 and 2) exceed the capacity of the solar energy source, a battery system of small capacity and a large peak power capability was required throughout the flight. The other basic battery performance capability was the continuous battery load throughout the flight, created by the characteristics of the pulse load circuitry in the off mode. The power system connections between the battery and the pulse loads result in this small continuous load being drawn from the battery. However, because the battery charger is connected in parallel with the battery loads, the battery charger actually supplies the continuous load, as long as power is supplied to the charger from the solar cell array.

A review of the preceding discussion of requirements indicated that the battery loads at the end of the flight are the largest, collectively. The sum of 678 whr for planet encounter, 250 whr for the science load and 94 whr for Sun reacquisition is 1022 whr. The 0.2 w continuous load would be required for approximately 8 days after the battery charger ceases operation due to reduced input voltage from the solar array. Adding 38 whr to the previous total yields 1060 whr for a minimum battery capacity. Using an average value of 27.5 v, this can be converted to 38.6 amp-hr. This capacity number does not include any allowance for capacity loss due to temperature deterioration or the application of a safety factor. These factors will be discussed in the portion of this Report describing the design.

III. SELECTION OF THE ELECTROCHEMICAL SYSTEM

The selection of the specific electrochemical system to be used in the *Mariner II* battery was based on the following factors:

1. Maximum weight of 40 lb

2. Operating temperature range of 50 to 120°F

3. Minimum available capacity of 38.6 amp-hr

4. Voltage range of 25.8 to 33.3 v under load

5. Capability of being float charged throughout maximum flight time

6. Sealed system to withstand the hard vacuum condition of space

7. Minimum capacity loss during open-circuit stand

8. Availability of the system selected, based on schedule requirements.

Of the various electrochemical energy storage systems initially considered, three of the more conventional battery systems were reviewed in detail. These three systems were the nickel-cadmium, silver-cadmium, and silver-zinc couples. The general characteristics of these three systems met the majority of the factors listed above.

In the case of the nickel-cadmium system, several problem areas were determined. Nickel-cadmium cells exhibit significant self-discharge rates on the order of 20 or 30% of capacity in as little time as a week at temperatures much above room ambient (Ref. 1). The per cell voltage range on discharge would be from 1.35 to 0.8 or 0.9 v. Thus, the total number of cells connected in series to obtain the required battery voltage would be a minimum of 26 cells. Reliability considerations would suggest that a minimum number of series-connected cells be required. On the basis of specific energy comparison, the nickel-cadmium system can be rated at 10 whr/lb at the 1-hr discharge rate at 70°F. Thus, a nickel-cadmium battery would weigh approximately 100 lb to meet the previously specified minimum capacity of 1,060 whr.

The silver-cadmium system characteristics more closely approached the required factors than the nickel-cadmium system previously discussed. The silver-cadmium cell voltage covers the range from an open-circuit value of 1.4 v to a plateau voltage of 1.0 v (Ref. 2) under load. In order to utilize the full capacity of the silver-cadmium cell, it is necessary to operate over a voltage range of from approximately 0.9 v at the end of discharge to

approximately 2.0 v at the end of charge (Ref. 2). End-of-charge voltage of 1.60 v, to prevent the development of high cell pressure, is indicated by data on charge/discharge cycles of sealed silver-cadmium cells (Ref. 3). Based on the plateau voltage value of 1.0 v, the silver-cadmium system would require approximately the same number, 26, of series-connected cells to meet the required minimum voltage as does the nickel-cadmium system. The end-of-charge voltage of 26 × 1.6 v or 31.6 v is less than the specified maximum. The specific energy for this system would be in the range of 25 to 33 whr/lb (Ref. 2); thus, a silver-cadmium battery to meet the minimum specified capacity would weigh in the range of 42 to 32 lb with respect to whr/lb range limits. The larger weight exceeds the required maximum by two lb. As a result of limiting the end-of-charge voltage to 1.60 v/cell, the available capacity would be reduced, in turn causing an increase in the battery weight values stated above. Assuming 20 whr/lb as the corrected specific energy, the battery weight would be 53 lb, considerably more than the required maximum. The operating temperature range of the silver-cadmium system was compatible with the 50 to 120°F requirements. In the area of float charging and the control of cell pressure, both the encapsulation type seal and the seal with a safety relief valve approaches were considered. Cell pressure and charge current measurements during periods of low rate charging (Ref. 3) indicated that with overcharge current rates as low as 10 to 20 ma, cell pressure became as high as 140 psi. Capacity retention data (Ref. 2) indicated acceptable self-discharge rates over the required temperature range. The sealed silver-cadmium type system was apparently available from only one manufacturer (Ref. 2).

The silver-zinc sealed secondary system was selected for the *Mariner II* spacecraft. This decision was based primarily on the higher energy-to-weight ratio of the silver-zinc system. This characteristic would permit the maximum amount of stored energy for the allowed weight of 40 lb. Thus, a considerable design margin in available energy could be incorporated in the battery. Other features, such as the minimum number of cells due to silver-zinc cell voltage and the charged stand capabilities, also were considered. The decision to use the silver-zinc battery with a continuous, or float type, charger throughout the flight, introduced a degree of risk to the battery development program. Data obtained during battery development, qualification testing and the successful performance of the battery in the *Mariner II* spacecraft demonstrated the validity of that decision.

IV. BATTERY DESIGN

A. Electrical Requirements

The maximum energy rating for the battery was stated earlier in this Report as 1060 whr. This value represented the sum of the requirements for the load periods occurring at the end of the flight. A pessimistic estimate of 24 amp-hr capacity loss due to deterioration during storage and space flight was made. Changing this estimate to 660 whr (based on 27.5 v) and adding to the previous 1060 whr increases the required capacity to 1720 whr. A safety factor of 1.25 was applied to this total, yielding a final design capacity of 2150 whr or 78 amp-hr. The battery voltage under load was to remain within the range of 25.8 to 33.3 v throughout the temperature range of 50 to 120°F.

B. Mechanical Requirements

The maximum allowable weight of the battery was 40 lb. The mechanical restrictions to the design are shown in Fig. 3, which describes the basic shape and dimensional limits. Sufficient space was available to allow as many as four of these units to be located around the spacecraft, as shown in Fig. 4. The choice of materials used in the battery was made on the basis of minimum magnetic field, to as great an extent as possible. Internal construction of the battery was required to be such as to restrict any change in the center of gravity to not more than $\pm\frac{1}{4}$ in.
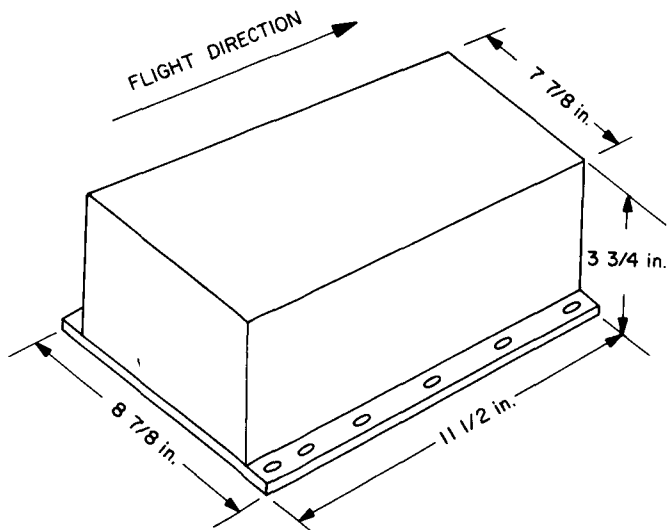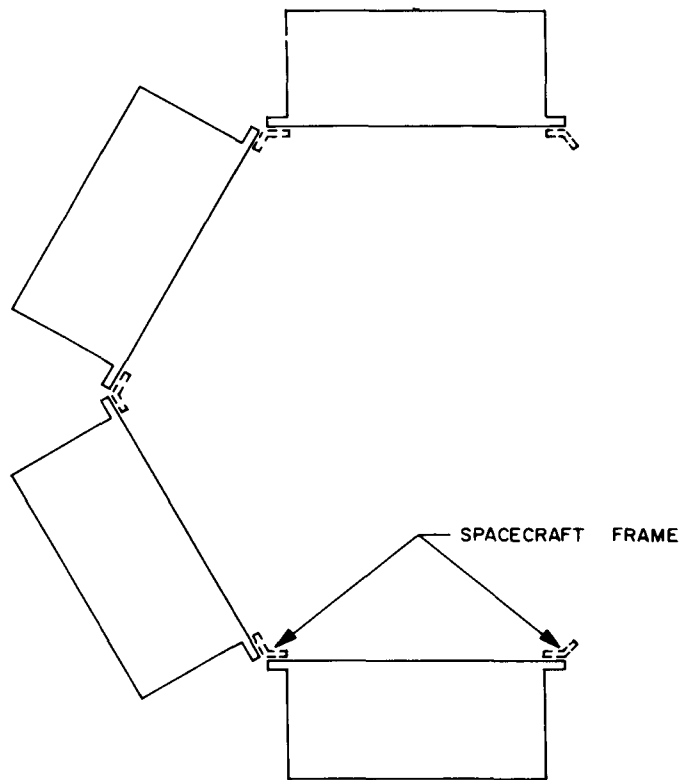
Fig. 4. Battery locations on spacecraft

Fig. 3. Mechanical restrictions

C. Basic Cell Design

The basic cell design evolves from the relationship of the various performance requirements and the characteristics of the materials involved in the design of a given electrochemical system. The required battery capacity is reflected in each cell of a series-connected system and, therefore, the quantity of electrode material will be determined in this case to provide 78 amp-hr. The combined parameters of minimum voltage under load, minimum temperature, and the peak power demand will determine the electrode area required. The minimum cell voltage was 1.43 v (25.8 v/18 cells). The maximum current is the peak power of 625 w, divided by 25.8 v, or 24 amp.

Based on the requirements stated above a design factor of 1.45 v/cell at 34.8 w (24 amp) and 50°F was established. The electrode area required for each cell was approximately 422 in². Approximately 260 g of Ag were required for the positive plates and 160 g of Zn

for the negative plates of each cell. The cell was composed of 11 positive plates and 12 negative plates to meet the dimension limits for the battery. Each plate was approximately 9.5 in². in area.

The separator system was composed of three materials. The main purpose of the separator was to separate or prevent a direct conductive path between the positive and negative plates. The positive plate was first covered with one layer of a microporous polyvinyl chloride material. The major purpose of this first layer was to prevent direct contact between the silver electrode and the second, or outer, layer of separator material. The second separator was cellophane and in this cell design four, and later five, layers of this material were used. The purpose of the cellophane is to permit ionic conduction to take place and at the same time to prevent the migration of silver

to the negative electrode. The negative electrode was covered with one layer of a nonwoven cellulose material. The primary purpose of this material is to retain the soluble zinc negative material in the electrode. All three of the previously described separator materials serve the common purpose of holding the electrolyte for the cell. The cell is filled with a minimum amount of electrolyte to increase the recombination rate of the gas produced in the cell. Therefore, the electrolyte retention capability of the separator materials is an important factor. Figure 5 shows the arrangement of two positive plates and separators. Figure 6 shows the method of covering the negative plate with the retainer material.

After the positive plates (Fig. 5) have been wrapped, a fold is made between the ends of the two plates forming the assembly into a U shape. A negative plate is then placed in the center of the folded positive assembly, with the positive and negative plate leads at opposite corners. The three plate assemblies are placed in a stack, separated by additional negative plates to form the complete set of plates required for one cell pack.

The cell pack is placed in a molded polystyrene container, or jar. The cell jars were actually molded in multi-cell monoblocks (multiple cells) as shown in Fig. 7.
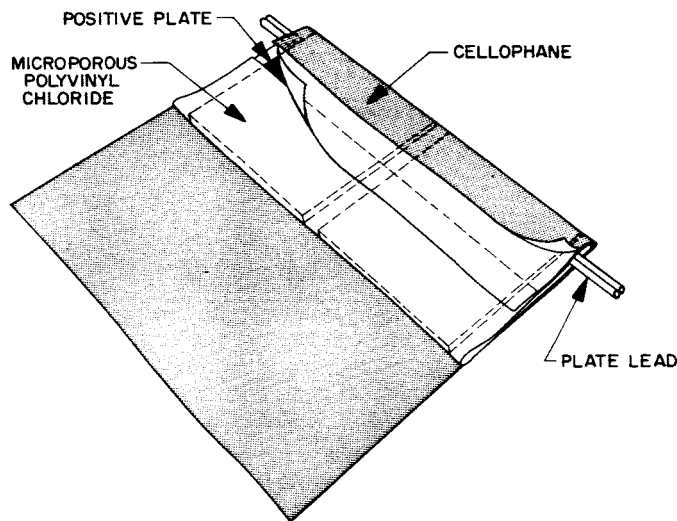
Fig. 5. Positive plates and separators, development model

Fig. 7. Five cell monoblock

D. Development Model Battery Design

The development model battery design was composed of two identical 9-cell units connected in series. The electrical and mechanical requirements of the development model battery were described in the preceding

Fig. 6. Negative plate and retainer, development model
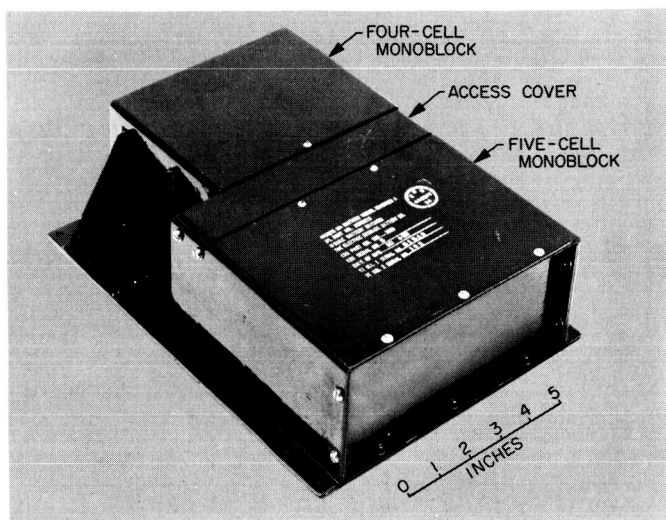
Fig. 8. Nine cell assembly, front view, development model

paragraphs of this Section. Figure 8 shows the front view of one of the 9-cell assemblies of the development model. This unit was composed of 2 monoblocks, one 5-cell and one 4-cell unit, positioned in the metal case so that the top of the monoblocks were parallel and facing each other. Space was provided between the 2 monoblocks for the wiring, connectors and temperature transducers. Access to this area was provided by removing a cover plate held by two screws on each end. This access cover can be seen in the center of Fig. 8. The rear view of this assembly is shown in Fig. 9, the connectors locate the
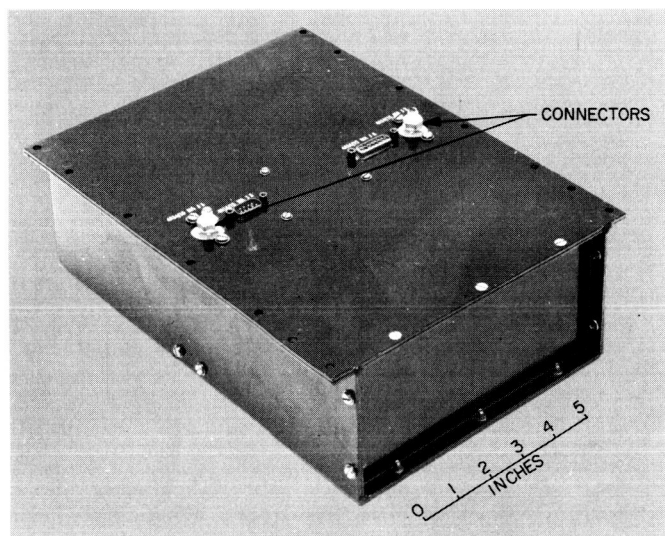
Fig. 9. Nine cell assembly, rear view, development model

Table 2. Battery characteristics

Item	Development model	Mariner II
Capacity, amp-hr	78	40
Weight, lb	40.8	33.4
Voltage, range, v	25.8 to 33.3	
Specific energy, whr/lb	54	33
Number of cells	18	
Cellophane layers on positive	4	5
Number of assemblies	2	1
Temperature range	50 to 120°F	
Peak power, w	625	510
Number of positive plates, per cell	11	14
Number of negative plates, per cell	12	15
Specific energy, whr/in^a	3	1.9
Volume^a	700 in.^{3}	470 in.^{3}

^{a} Computation based on liquid displacement volume equivalent.

wiring access area. Table 2 contains a summary of the characteristics of the development model battery.

E. Mariner II Battery Design

The mechanical and electrical design requirements for the flight battery were changed after the initial battery development program was well underway. These new requirements reduced the maximum allowable battery weight to 33 lb and the capacity to 40 amp-hr. The 40 amp-hr was not directly related to the spaceflight power profile, but rather to the revised weight limit and the state of the art in battery design. Table 2 contains a comparison of the old *development model* and the new *Mariner II* battery characteristics. Figures 10 through 15 and Table 3 describe the revised power profile design

Table 3. _Mariner II_ squib events

Event	Function	Initiation time	No. of squibs	Peak power, @ 27 v, w	Average power, w	Comments
A	Unfold solar panel & radi- ometer erection	Launch + 44 min	4	272	150	—
B	Unfold solar panel	Launch + 44 min	3	198	150	Fired after A
C	Unfold solar panel & radi- ometer erection	Launch + 44 min	4	272	150	Fired after B
D	Unfold solar panel	Launch + 44 min	3	198	75	Fired after C
E	Midcourse motor N_2 pressure ON	Launch + 7.8 days	2	148	75	Fired prior to F
F	Midcourse motor ignition	Launch + 7.8 days	4	297	75	Fired prior to G
G	Midcourse motor shutoff	Launch + 7.8 days[a]	4	297	75	—

[a] May occur prior to completion of F .
(If time elements overlap, power requirements will add.)
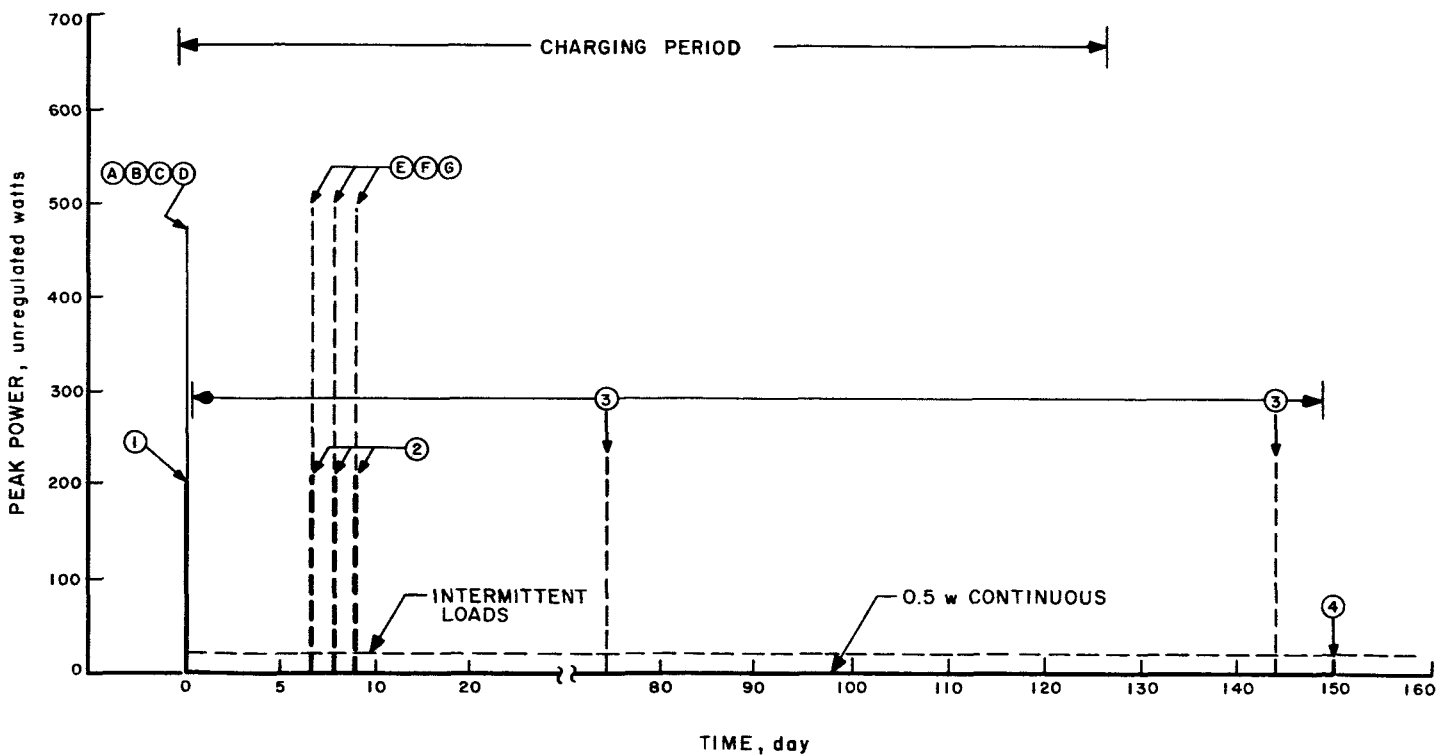
Fig. 10. Battery power requirements vs longest flight time, _Mariner II_
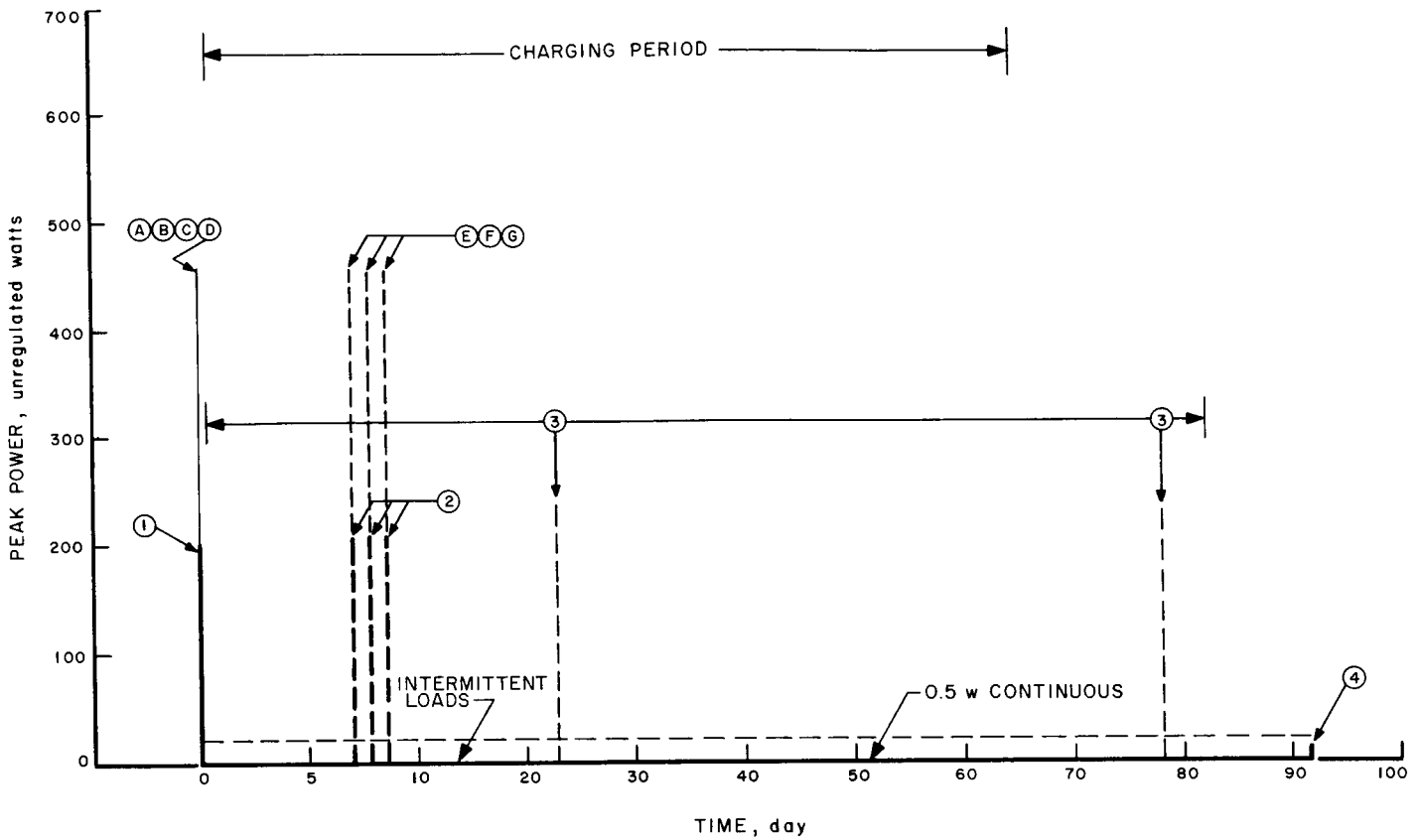
Fig. 11. Battery power requirements vs shortest flight time, *Mariner II*
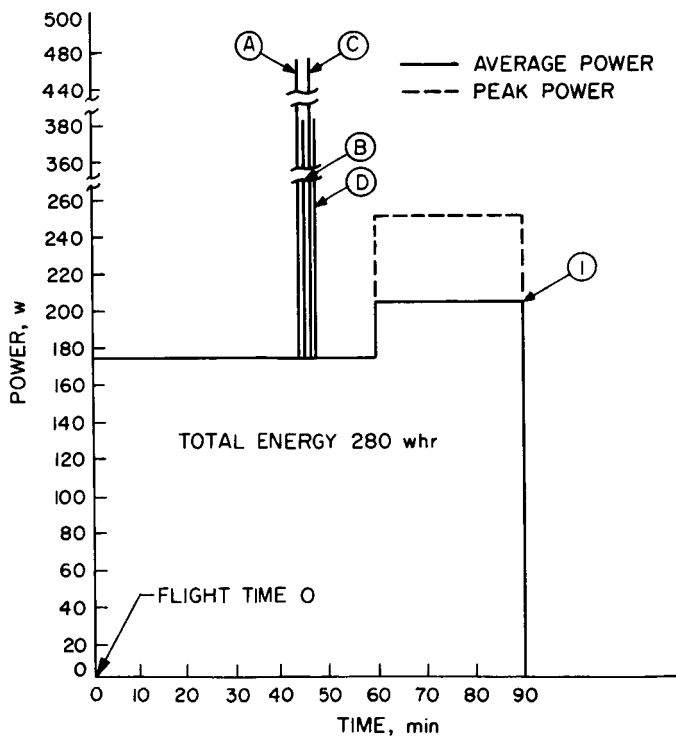
Fig. 12. Launch phase battery requirement, *Mariner II*
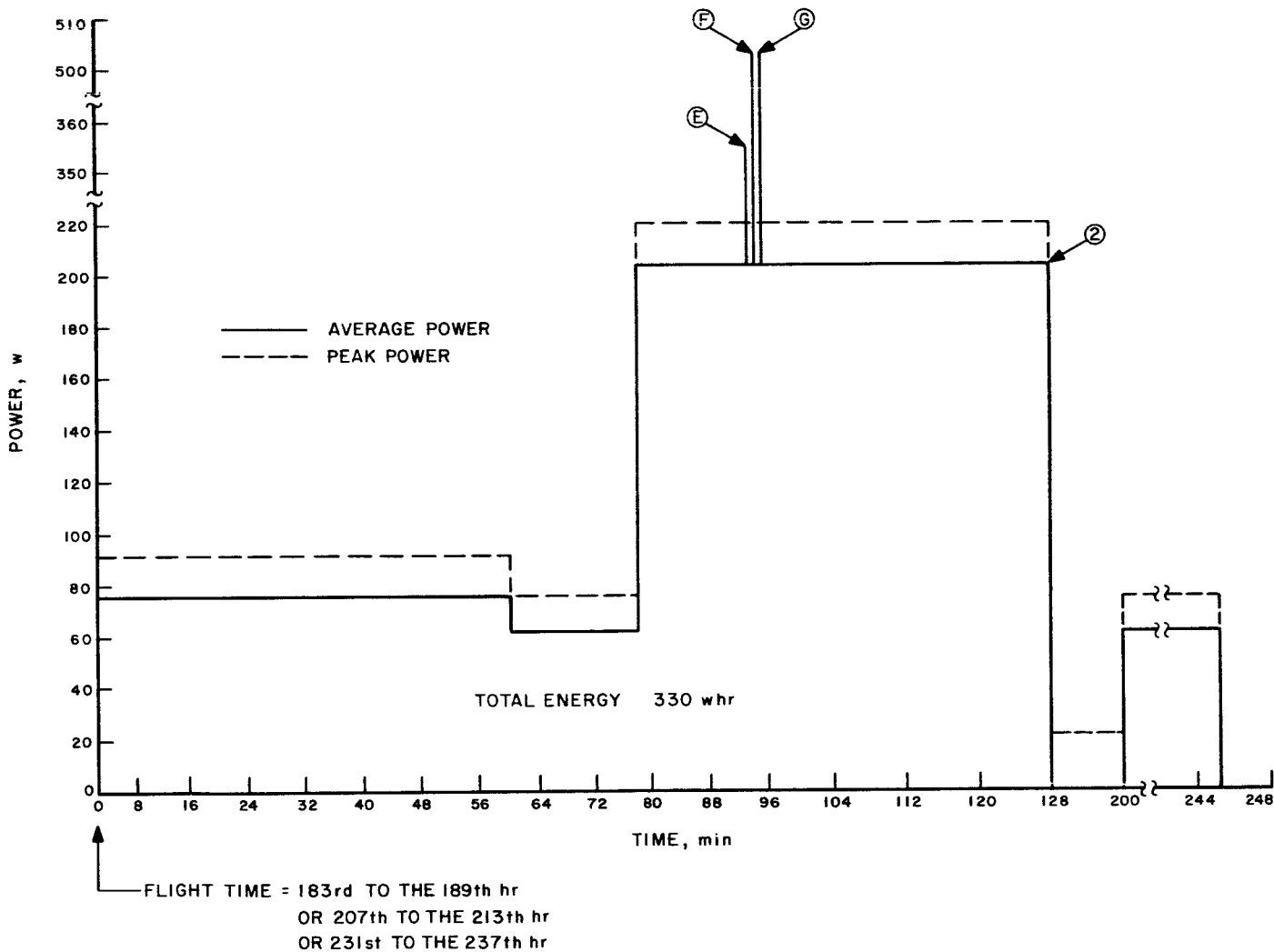
Fig. 13. Midcourse maneuver battery requirement, *Mariner II*
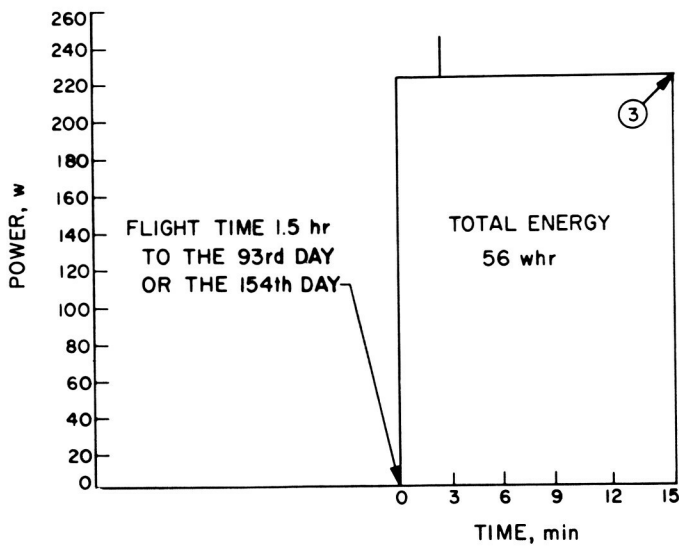
Fig. 14. Sun reacquisition battery requirement, Mariner II

requirements for this smaller battery. A review of these Figures indicates that the most critical operating period for the battery would be on the longest flight (Fig. 10), after charging of the battery can no longer be accomplished. That portion of the flight would cover a period of approximately 23 days. During that period the total energy drain on the battery would be approximately 350 whr, considering the worst possible combination of loads. At the start of this final 23-day period the battery would have a capacity of approximately 1000 whr. Therefore, the permissible loss within the battery due to deterioration would be 650 whr or a margin of 185%. It would be appropriate to reduce this percentage slightly to include permanent capacity losses occurring earlier in the flight. The metal case of the *Mariner II* battery design is shown in Fig. 16. The cells were arranged in two rows, each row containing a 4-cell and a 5-cell monoblock. The three access holes in the cover, as seen in Fig. 16, are located over the open connector and wire area, extending for the full length along the center of the battery case.

Fig. 15. Planet encounter battery requirement, Mariner II
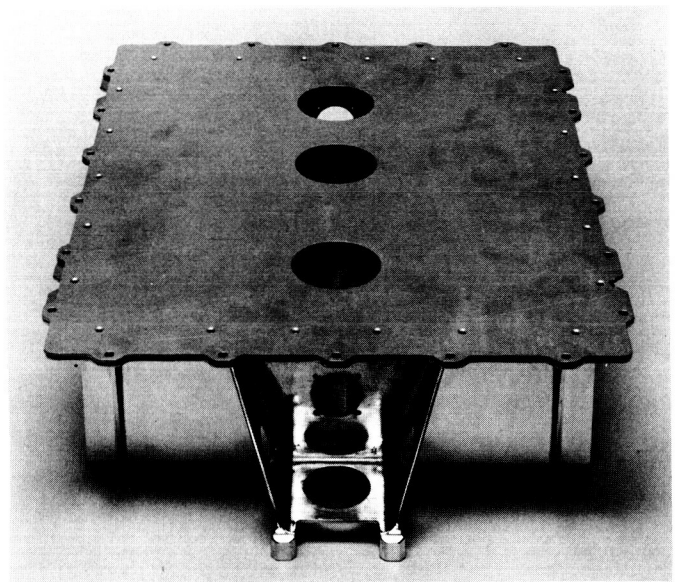
Fig. 16. Mariner II battery case with cover

V. FLIGHT CHARGER DESIGN

The design of a flight charger for the battery was an integral part of the battery development program.

Several modes of charging were considered for the battery. Constant current charging with automatic and/or manual (ground control) start and stop action was eliminated for several reasons. The maximum power available from the charger was approximately 20 w, due to the limit on power available from the solar panels to supply the basic spacecraft power requirements. Although constant current charging would require the least time to return the battery to full capacity after a discharge period, failure to turn off the charger at the prescribed end-of-charge battery terminal voltage would result in a rapid buildup of gas pressure in the battery and the subsequent failure of the battery. The automatic start and stop circuitry of the charger would add components to the basic charger circuitry, tending to reduce reliability when at the same time this additional circuitry would be required to have a high degree of reliability. Because of the severe limits on available power and weight, it did not appear possible to obtain the accuracy necessary for the automatic start and stop circuitry. The use of a manual start and stop control for the charger based on ground signals transmitted via the radio command system to the spacecraft was a less reliable plan.

Constant potential charging was the second method to be considered. With this method the current is at its largest value at the beginning of the charge operation and decreases as charging progresses and the battery terminal voltage increases. In this case the current must be limited to maintain the charger output to not more than 20 w, as specified at the beginning of this discussion. So that start and stop charger control circuitry would not be necessary, the basic constant potential charging circuitry was further modified to provide a specific current-voltage relationship of the charger throughout the range, from maximum current to zero current (maximum voltage).

Initially, the flight charger design was composed of a voltage regulator and a current limiter in series from input to output. The output characteristic of this first design is shown in Fig. 17. The optimum curve based on the battery requirements is shown for comparison purposes. The maximum output voltage at zero current for this design was 34.3 v. As the evaluation of this charger and battery continued, the voltage regulator portion of
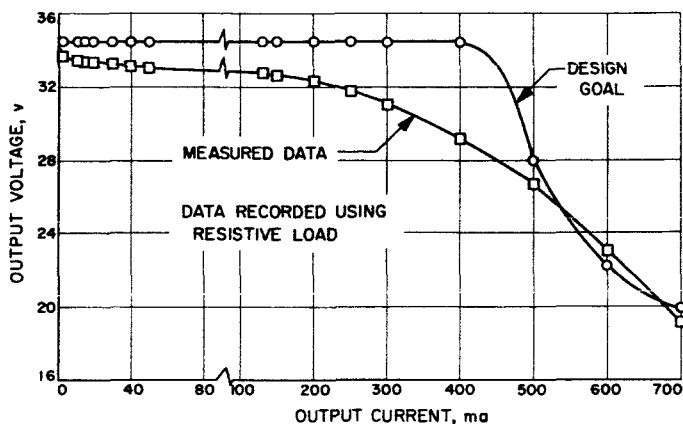
Fig. 17. Flight charger prototype characteristic and design goal

the charger was changed to increase the maximum voltage at zero current to 35.5 v. Figure 18 shows the output voltage-current characteristic for this higher voltage setting, measured while charging an 18-cell silver-zinc battery. A curve was plotted for each of three input voltages to the charger, covering the minimum to maximum values of the input voltage design range.

During the final design phase of the charger development, the voltage regulator and current limiter sections were electrically interchanged, placing the current limiter first and the voltage regulator second on the basis of
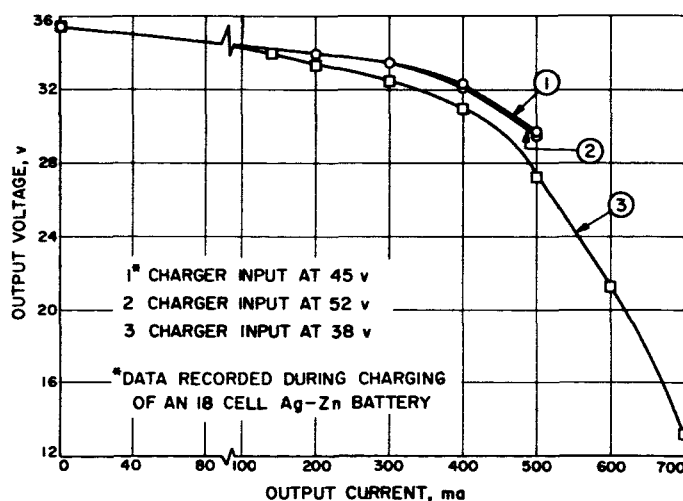
Fig. 18. Flight charger characteristic (35.5 v maximum)

current flow through the charger. This change in circuitry produced an output characteristic for the charger as shown in Fig. 19. The critical operating point is at the minimum output current. The voltage at 5 ma was designed to be 34.65 ±0.17 v (±0.5%). The two curves marked *upper limit* and *lower limit* on Fig. 19 outline the permissible variation of voltage for an acceptable charger throughout the current range from 5 ma to the short-circuit condition. At current values greater than 500 ma, the upper limit line significance changes from that of maximum acceptable voltage to the maximum power available. At current values greater than 100 ma, the lower limit line significance changes from the minimum required voltage to obtain a fully charged battery to the minimum voltage-current relationship of a properly operating charger.
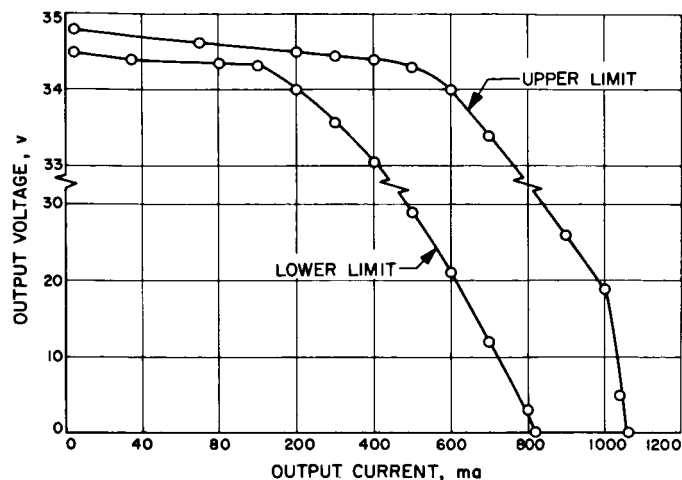
Fig. 19. Mariner II flight charger characteristic

VI. DEVELOPMENT MODEL BATTERY TEST PROGRAM

During the development of the battery for the *Mariner II* spacecraft, several types of single cell, monoblock, and battery tests were conducted. The cell and monoblock tests were conducted by the manufacturer (Ref. 4) during the design and development phase of the program. These tests were made to determine design factors such as cell pressure characteristics during charge and discharge, burst strength of cell containers, optimum quantity of electrolyte and cell voltage current characteristics for various cell configurations, etc. Testing of complete batteries was conducted at JPL to determine whether their electrical and environmental characteristics met the design requirements. The results of these battery qualification tests are presented in this Section.

A. Prototype Tests

The prototype of the *development model* battery was subjected to a series of charge and discharge cycles at temperatures from 50 to 120°F. The test equipment was arranged as shown in Fig. 20.

The battery was stabilized at 72°F and then discharged at a constant current of 12 amp for 5½ hr or 66 amp-hr. The battery was then charged at a constant current rate of 2 amp and accepted approximately 66 amp-hr. Capacity was considerably less than the design value of 78

amp-hr. A subsequent review of the preliminary *Service and Operating Instructions,* supplied with the prototype by the manufacturer, disclosed that the specified end of
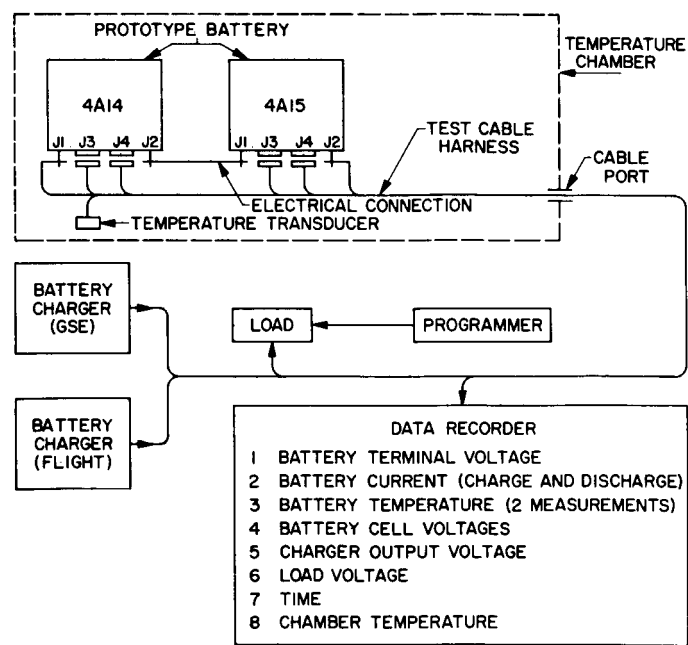
Fig. 20. Test setup block diagram, prototype battery, development model
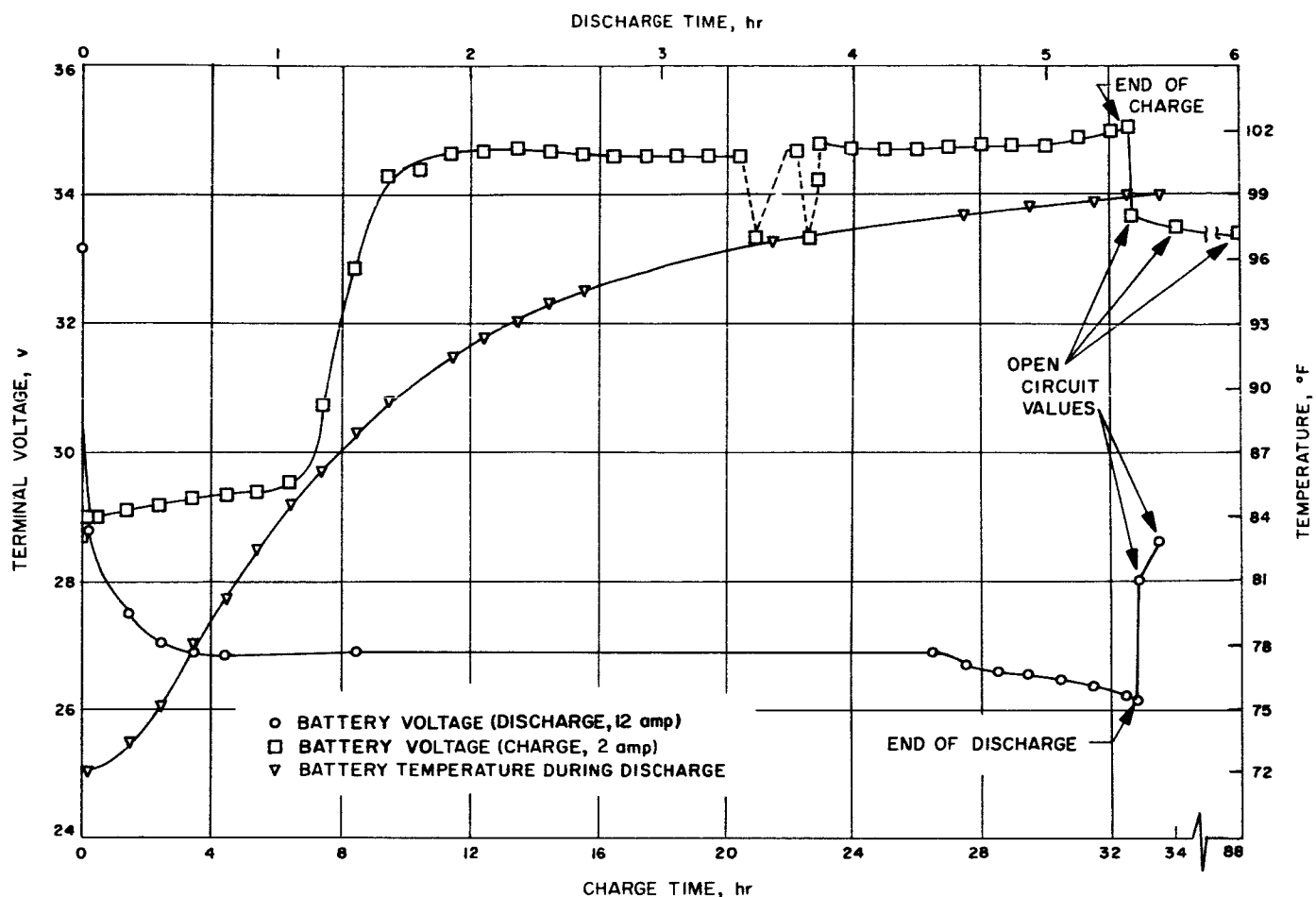
Fig. 21. Prototype discharge and charge data, development model

discharge voltage was in error. This voltage setting was approximately 2-v greater than the design limit, thus, approximately 12 amp-hr had not been removed during the discharge. The data obtained during the discharge/charge cycle at 72°F is graphically presented in Fig. 21. The voltage variation shown in Fig. 21, during the 20 to 24 hr period of charging, were the result of interruptions in the input power to the charger. Because of test time limitations, this cycle was not repeated using the corrected end-of-discharge voltage.

At the completion of the charge at 72°F, the battery temperature was lowered to 50°F and the battery was discharged at various rates to a maximum of 491 w. The test was conducted in accordance with the load schedule shown in Table 4. The listed wattages represent all of the possible combinations of continuous and pulse-type load design requirements for the development-model battery. Figure 22 is a plot of battery voltage vs load watts for each combination of Table 4. These measurements were repeated at 120°F after the battery was

recharged at 72°F following the 50°F tests. The results at both temperatures are shown in Fig. 22 for ease of comparison. At each of the average power levels, sufficient time was allowed for the battery voltage to stabilize or establish a definite trend before the measurements were recorded or the pulse load was added. The time for the pulse load was held to 5 ±2 sec. The battery temperature during each of the load sequences is also shown in Fig. 22. Because of the heat transfer characteristics of the battery materials, the temperature of the battery was not maintained at 50 and 120°F, respectively, for the two tests. Therefore, the voltage regulation data obtained were not conclusive; however, an appreciable margin did exist between battery voltage at maximum load and the minimum voltage limit of 25.8 v. Additional data on voltage under load vs temperature are presented later in this Report.

The battery temperature was lowered to 75°F at the completion of the load tests described in the previous

Table 4. Test load schedule

Test No.	Average power, w	Peak power, w	Total power, w		Test No.	Average power, w	Peak power, w	Total power, w
1	0	0	0		17	200	—	200
2	0.2	—	0.2		18	200	20	220
3	10	—	10		19	200	272	472
4	10	25	35		20	225	—	225
5	15	—	25		21	225	15	240
6	15	18	33		22	225	151	376
7	20	—	20		23	265	—	265
8	20	24	44		24	265	10	275
9	30	—	30		25	315	—	315
10	30	40	70		26	335	—	335
11	30	136	166		27	335	20	355
12	30	176	206		28	335	156	491
13	35	—	35		29	375	—	375
14	35	40	75		30	375	10	385
15	45	—	45		31	0	0	0
16	45	40	85					
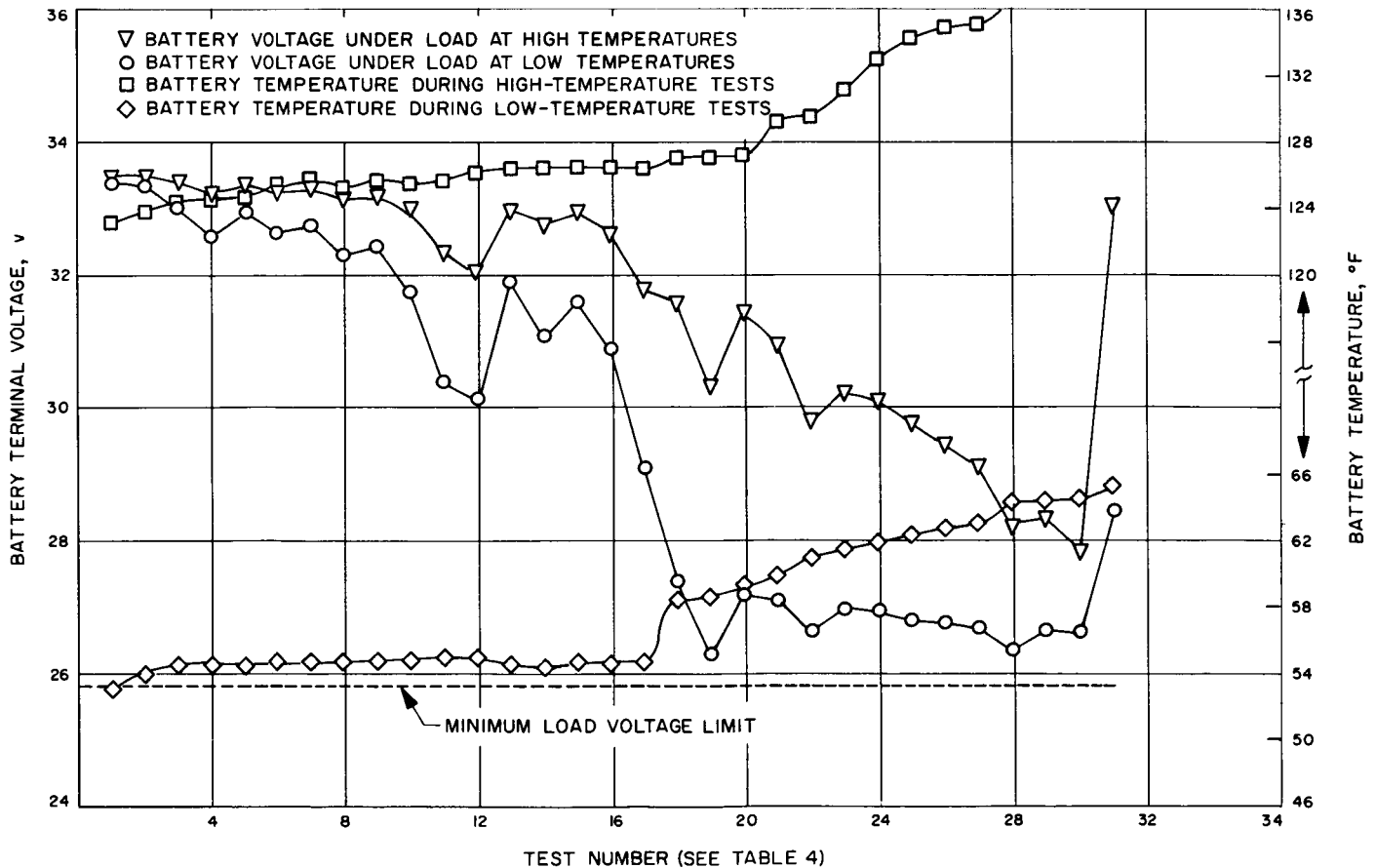
Fig. 22. Prototype battery load tests

paragraph. The battery was then charged using a proto-type version of the flight charger design. The data obtained from this charging operation is presented in Fig. 23. This charge operation was stopped before the battery had reached full charge, based on the charge current and voltage values, as a precautionary measure, since internal construction of the prototype was not considered sufficient to accept continuous overcharge. The prototype battery remained in the test chamber at 75°F in the open-circuit condition for 110 hr, after the flight charging operation was completed. When the battery was removed from the chamber at the conclusion of this test, electrolyte leakage was observed in one of the 9-cell assemblies. The battery was returned to the manufacturer where the aluminum chassis was removed by milling and the plastic monoblocks were examined. The electrolyte leakage had occurred in the area of the epoxy seal joining the poly-

styrene cell case and cover. The epoxy appeared to have pulled away from the case in one corner of the cell. It was concluded that shrinkage during the cure of the EC 3050 epoxy may have caused the separation. Open-circuit cell voltages ranged from 1.862 to 1.893 v indicating that no shorts had occurred.

The information obtained from the prototype battery tests indicated that an acceptable basic design had been obtained. Because of the difficulties experienced with the battery temperature control equipment during the discharge test, the voltage regulation measurements were not conclusive. The performance of the flight charger did indicate proper operation of the voltage regulating and current limiting characteristics of the design. However, the physical limitations of the prototype construction prevented full evaluation of the battery's overcharge performance.
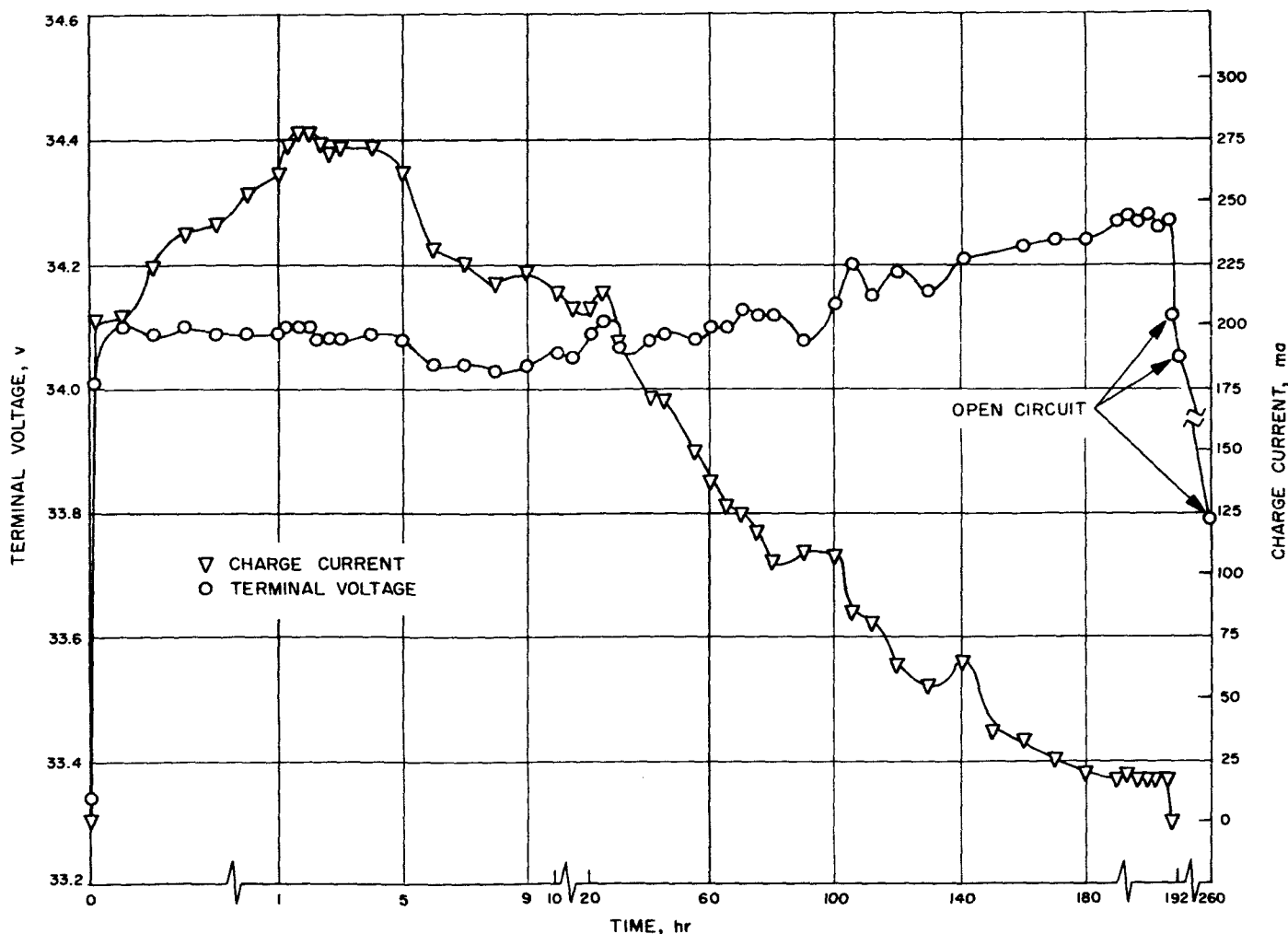
Fig. 23. Charge current and battery terminal voltage using flight charger

B. Type Approval Tests

Three batteries were designated as type approval (TA) units. These three batteries were subjected to a complete series of environmental and operational tests to determine the capability of the battery to meet the design requirements. The environmental test levels during the TA program are more severe than the anticipated actual operating conditions. Table 5 is a condensed schedule of the TA program with a summary of the environmental conditions for each phase and the electrical tests to be conducted during each environmental sequence.

1. Prelaunch, Simulated

a. Electrical inspection. Type approval battery 1 delivered 65 amp-hr at the 12 amp rate during the first discharge. This discharge was conducted as part of the basic checkout procedure for the battery prior to starting the TA test sequence. The battery was charged at a constant current rate of two amp, following the discharge, and accepted 63 amp-hr. Type approval battery

2 delivered 72 amp-hr on discharge. The battery accepted 65 amp-hr during charge at the two amp rate. Type approval battery 3 delivered 75 amp-hr on discharge and accepted 66 amp-hr of charge. The discharge data obtained for these batteries are shown in Fig. 24. Although some variation in voltage occurred at the beginning of the discharge the batteries were almost indistinguishable during the final 80% of the discharge. It should be noted that TA battery 3 was discharged beyond the minimum voltage limit for the test due to an equipment malfunction. Type approval battery 1 discharge was stopped at 26.6 v as the result of an error in the manufacturer's instructions, which was corrected prior to the discharge testing of TA batteries 2 and 3. All three batteries accepted more than the required minimum of 60 amp-hr during the charge. The large difference in the discharge and charge capacity numbers result from the fact that the batteries were charged to a higher end voltage during manufacture than the 35.2 v limit used in this test. Figure 25 shows the data obtained during the charging of these batteries.

Fig. 24. Discharge of the three type approval batteries at 12 amp

Table 5. Type approval test program schedule

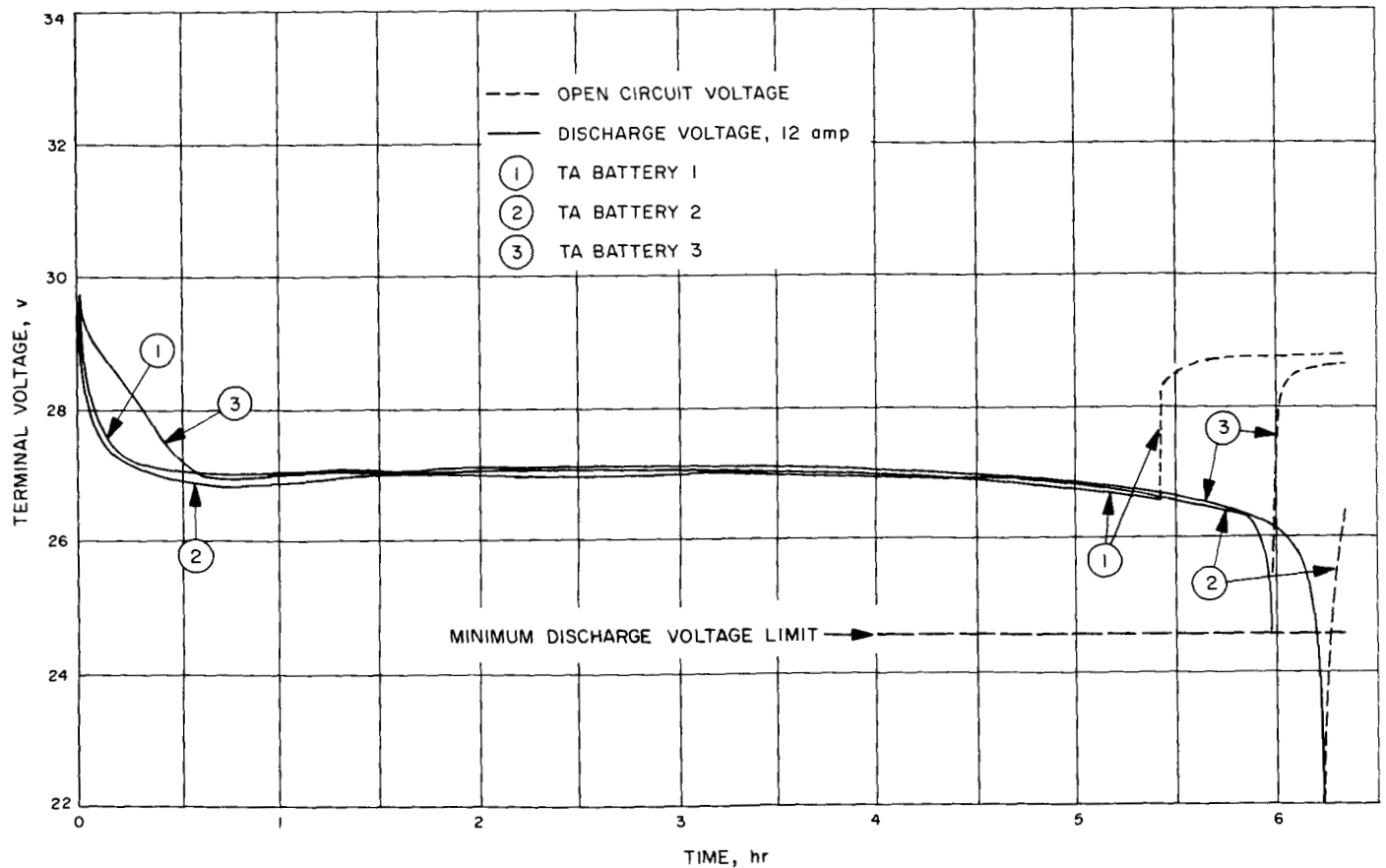| Battery TA No.	Environmental conditions	Electrical tests	Test objectives
1, 2 & 3	Transportation vibration and handling shock	Evaluated later in test program	Determine ability to survive vibration and shock during commercial transport
1	Low temperature, 10 days at 50°F and 10% humidity	Open circuit charged stand with 300 w discharge during final 30 min	Simulate prelaunch conditions and evaluate effect of prior environments on battery performance
2	Mid-range temperature, 10 days at 85°F and 95% humidity	Open circuit charged stand with 300 w discharge during final 30 min	Simulate prelaunch conditions and evaluate effect of prior environments on battery performance
3	High temperature, 10 days at 120°F and 95% humidity	Open circuit charged stand with 300 w discharge during final 30 min	Simulate prelaunch conditions and evaluate effect of prior environments on battery performance
1, 2 & 3	Static acceleration, +14g & −4g, roll axis ±6g, pitch & yaw axes	Launch period discharge sequence[a]	Evaluate battery discharge performance during simulated booster operation
1, 2 & 3	High-frequency vibration, 9 min at levels of 4.5g to 15g in the range of 15 to 1500 cps in each of three mutually perpendicular planes	Continuation of launch period discharge sequence[a]	Evaluate battery discharge performance during simulated booster operation
1, 2 & 3	Low-frequency vibration, 8 min at levels of ±3 in. from 1 to 3 cps and 3g from 3 to 40 cps in each of three mutually perpendicular planes	Continuation of launch period discharge sequence[a]	Evaluate battery discharge performance during simulated booster operation
1, 2 & 3	Shock, two (200g) 0.5- to 1.5-msec terminal peak sawtooth shocks in each of three mutually perpendicular planes	Average load wattage of launch period plus peak wattage at pyrotechnic loads applied during shock pulse	Evaluate battery performance under peak load and the effect of shock associated with pyrotechnics
1	Low temperature and vacuum (50°F and 10^{-4} mm Hg, or less) for 158 days	Power profile for spaceflight period from end of launch until end of maximum (158 days) anticipated flight time	Evaluate battery performance during all phases of simulated spaceflight operation with battery temperature stabilized at minimum design value of 50°F
2	High temperature and vacuum (100°F and 10^{-4} mm Hg, or less) for 158 days	Power profile for spaceflight period from end of launch until end of maximum (158 days) anticipated flight time	Evaluate battery performance during all phases of simulated spaceflight operation with battery temperature maintained at values near the upper design value of 120°F
3	Mid-range temperature and vacuum (80°F and 10^{-4} mm Hg, or less) for 158 days	Power profile for spaceflight period from end of launch until end of maximum (158 days) anticipated flight time	Evaluate battery performance during all phases of simulated spaceflight operation with battery temperature maintained at the predicted average battery temperature of 80°F

[a] To conduct the previously described launch phase environmental tests, the discharge time for the battery was extended beyond the actual total energy required for the flight. Therefore, the battery was partially recharged to replace this excess load prior to the initiation of the type approval tests.
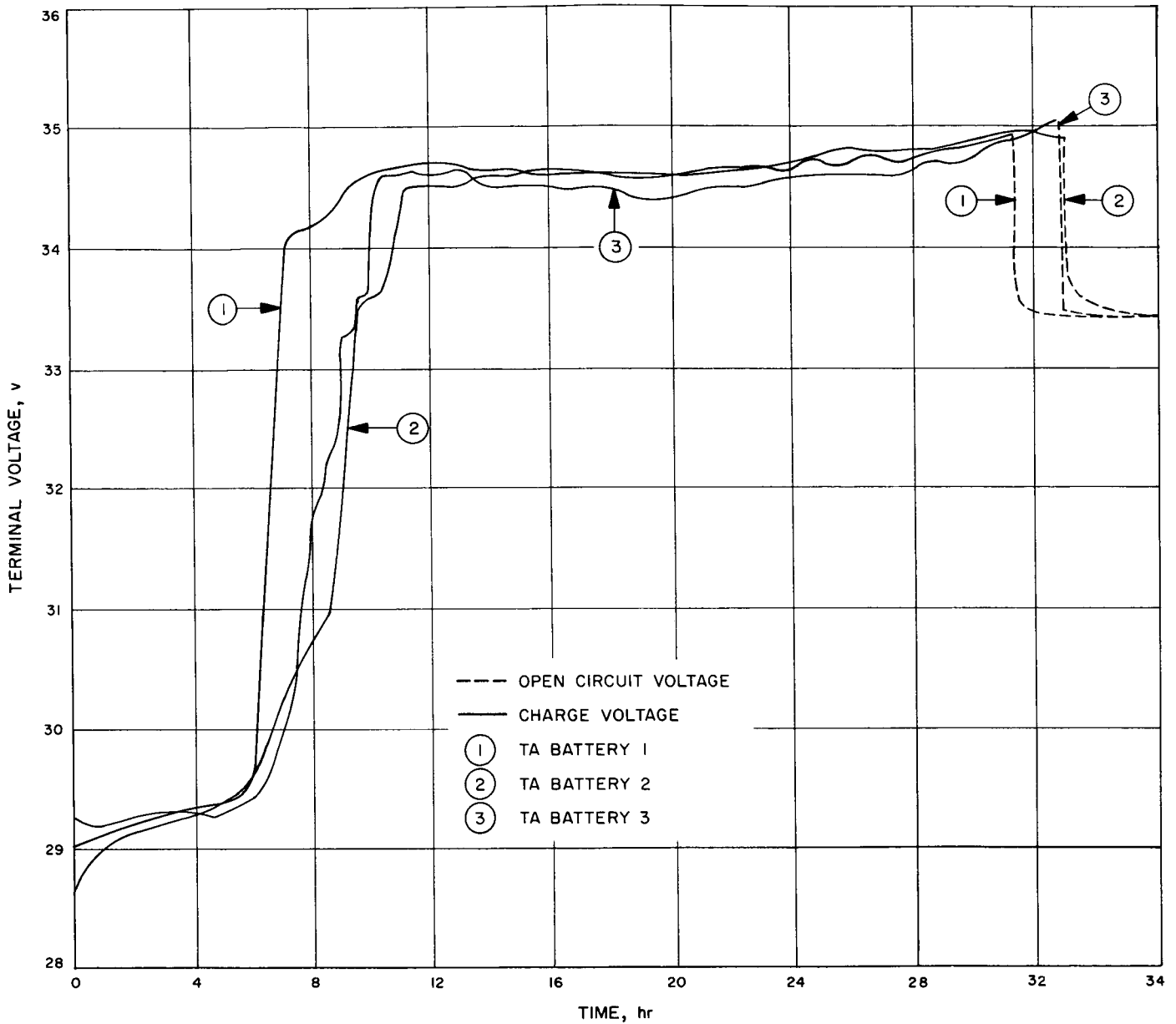
Fig. 25. Charging of the three type approval batteries at 2 amp

b. Transportation vibration and handling shock. The batteries, in their wood shipping containers, were subjected to a total of 1 hr of vibration testing in each of three mutually perpendicular directions. The vibration waveform was sinusoidal and the sweeping rate was such that the time rate of change of frequency varied directly with the frequency.

The vibration levels were:

1. 2 to 10 cps at 1.3 g peak, sweeping for 18 min

2. 10 to 35 cps at 1.3 g peak, sweeping for 14 min

3. 35 to 48 cps at 3.0 g peak, sweeping for 3 min

4. 48 to 500 cps at 50 g peak, sweeping for 25 min

The handling shock test was composed of two separate drop tests. The first of these tests was conducted with the battery in the wood shipping container. The battery was dropped six times from a height of 36 in. onto a concrete floor, landing each time on a different corner or edge.

The second test was conducted with the battery removed from the shipping container. The battery was dropped on a 2 in. thick wood (fir) bench or table from such a position that at least one point of the battery was in contact with the wood surface and that the angle between the wood surface and an edge or surface of the battery was at least 45 deg. One drop from each of six different positions constituted the test sequence.

Batteries 1 and 3 completed these tests with no observed effect on battery condition. Examination of battery 2 after removal from the shipping container, prior to the bench drop test revealed electrolyte leakage in both of the 9-cell assemblies. Open-circuit cell voltages of 1.854 or 1.855 indicated the absence of any shorted cells. Battery 2 was then discharged at the 12 amp rate and yielded 67 amp-hr. The cell voltages remained normal for this current rate throughout the discharge. Figure 26 is a graph of battery terminal voltage vs time during this discharge. The 14 hr of open-circuit during the discharge resulted from a power interruption to the test equipment. Examination of this battery by the manufacturer disclosed a condition similar to that described for the prototype battery (see Section VII B-1). At this point in the program a design change was made replacing the EC 3050 epoxy with Bisonite K1/K4. This later material had been used successfully in the batteries for

the *Ranger* spacecraft. Type approval battery 2 was repaired and continued in the test program.

c. Temperature and humidity. Type approval battery 1 was then placed in a test chamber where the air temperature was lowered to 41°F and the humidity was raised to greater than 95%. As soon as a stabilized condition was obtained, the temperature was then reduced to 32°F. and these conditions were maintained for 4 hr, after the battery stabilized at 32°F. At the end of this period the temperature was raised to 50°F and the humidity was reduced to less than 10%. This temperature/humidity combination was maintained for the balance of the 10 days of this test sequence. The battery was in the open-circuit condition and the terminal voltage, 18-cell voltages, temperature measurements at 4 locations in the battery and chamber temperature were recorded throughout the test.

During the open-circuit portion of the test the battery terminal voltage remained constant at 33.41 v.

During the final 30 min of this test the battery was discharged at the 300 w level. The battery voltage decreased from 28.76 to 26.94 v during the discharge. The open-circuit battery voltage immediately after the discharge was 29.02 v. The battery temperature increased
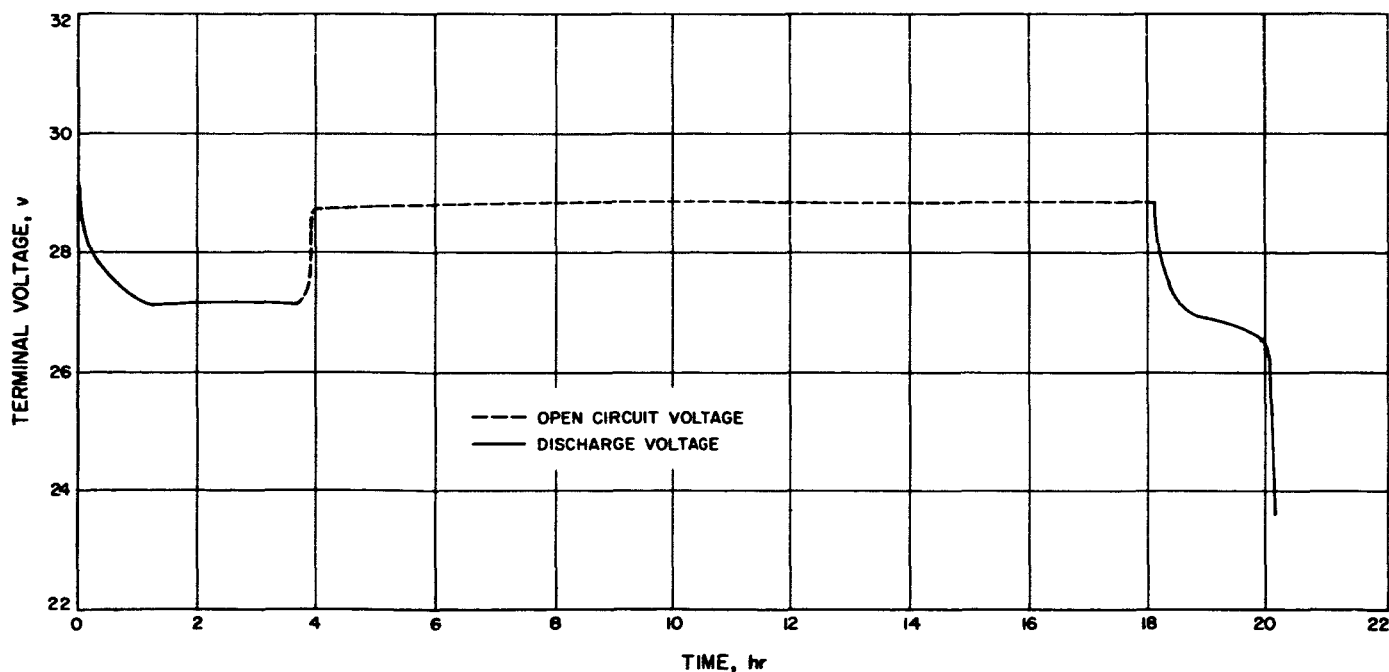
Fig. 26. Type approval battery 2 discharge at 12 amp

from 50 to 54°F during the discharge. All observed parameters remained within the required limits during this test.

Type approval battery 2 was subjected to a test sequence similar to that described in the previous paragraph. The temperature/humidity sequence was changed to the one combination of 85°F and greater than 95%, respectively. During the open-circuit portion of the test, the battery voltage remained constant at 33.40 v. The battery voltage decreased from 27.44 to 27.08 v during the 30 min of discharge at the 300 w level. All observed parameters remained within the required limits during this test.

Type approval battery 3 was also subjected to a test sequence similar to that described in the two previous paragraphs. The temperature/humidity sequence was changed to the one combination of 120°F and greater than 95%, respectively. During the open-circuit portion of the test, the battery voltage remained constant at

33.45 v. The battery temperature increased during the test period from 121 to 127°F. The heat transfer characteristics of the battery and the capacity of the test chamber prevented the stabilization of the battery temperature during the discharge portion of the test when thermal energy is released by the battery. The battery voltage decreased from 29.60 to 29.42 v during the 30 min discharge at the 300 w level. At the completion of the discharge, the battery was returned to the open-circuit condition and remained in the test chamber for an additional 36 hr. During this open-circuit time in the chamber, the chamber temperature increased to approximately 135°F. This temperature rise resulted from a power failure in the circuits supplying the temperature control equipment; however, the interior observation light remained on in the chamber. Examination of the battery after removal from the chamber revealed electrolyte leakage in one of the 9-cell assemblies. The battery was returned to the manufacturer where the aluminum chassis was removed. The leak was located in a corner of the 5-cell monoblock and was similar to the

Fig. 27. Ten day temperature/humidity test

leaks in the other batteries. All three of the TA batteries had been built prior to the decision to change the type of epoxy sealing material discussed earlier in 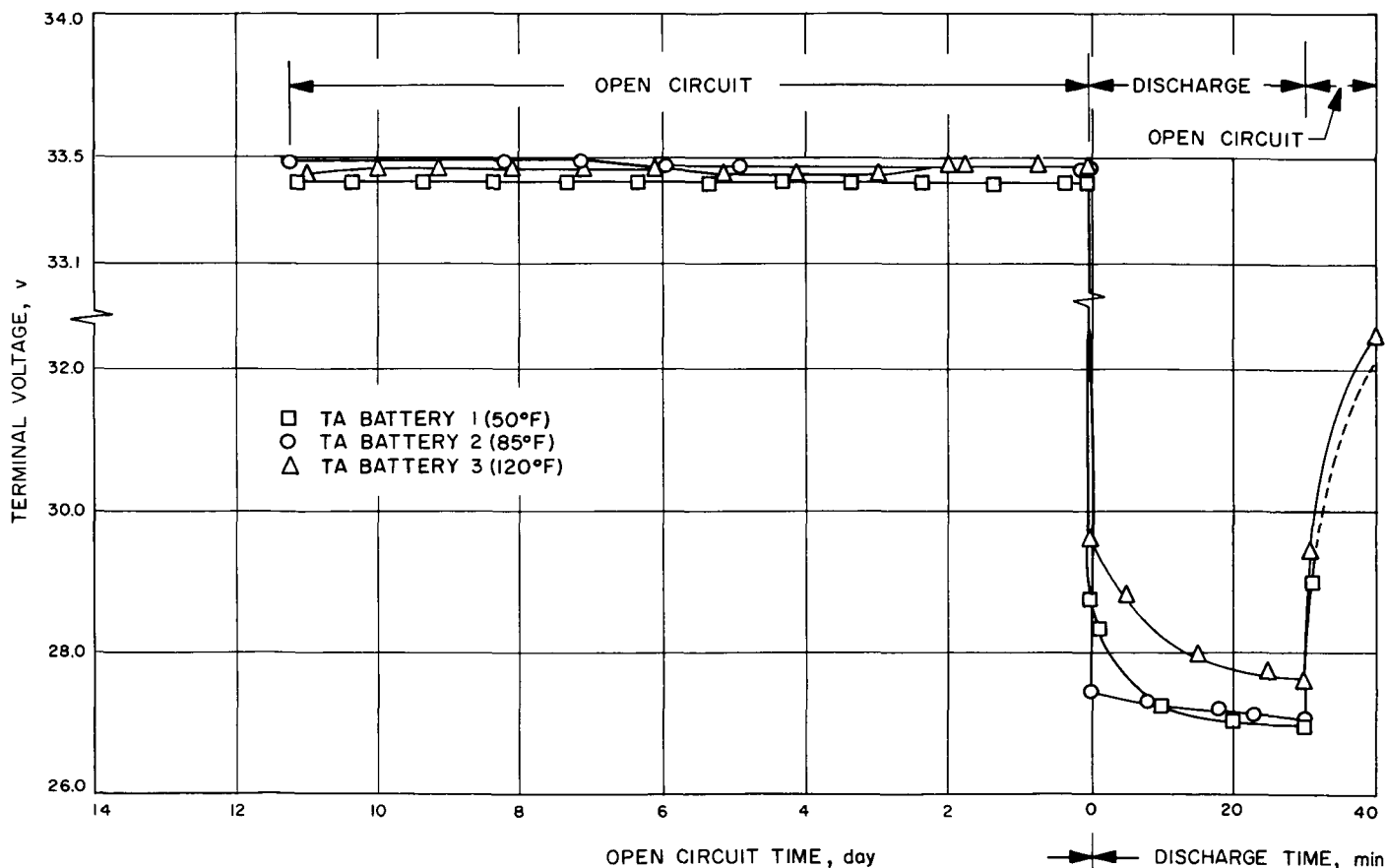this Report. The leak in TA battery 3 was repaired, placed in a new aluminum chassis, and reinstated in the test program. The data obtained from the testing of these three batteries during the 10-day temperature/humidity test, are shown in Fig. 27.

2. Launch, Simulated

a. Static acceleration. The three TA batteries were subjected to a static acceleration test in each of three mutually perpendicular planes, while supplying 200 w of power to a resistive load simulating the spacecraft power system load, during the acceleration phase of the launch operation. Each battery was subjected to a static acceleration of 14 g for 5 min along the thrust axis of the spacecraft in the forward direction and 4 g for 5 min along the same axis in the reverse direction. This was followed by +6 and −6 g for 5 min in each of the two other orthogonal directions. The battery voltage remained within the required limits during all portions of this test. The data obtained during this test are shown in Table 6.

b. Vibration test. The three TA batteries were subjected to vibration tests that simulated the vibration which accompanies *Atlas* and *Centaur* motor burning. Each battery was subjected to vibration in a direction parallel to the vehicle thrust axis and in two other orthogonal directions which are perpendicular to the thrust axis. The battery was discharged at the 200 w rate during the vibration periods.

High frequency. This test consisted of a programmed sequence of (1) band-limited Gaussian noise and (2) combined noise and sinusoidal vibration. The total time in each orthogonal direction was 9 min 12 sec. The test was conducted in four parts as follows:

1. White Gaussian noise, 15 g rms, band-limited between 15 and 1500 cps for 6 sec.

2. White Gaussian noise, 10 g rms, band-limited between 15 and 1500 cps for 3 min.

3. White Gaussian noise, 4.5 g rms, band-limited between 15 and 1500 cps — plus a 4.5 g rms, sinusoid, superimposed on the noise. The frequency of the sinusoid was swept from 40 to 1500 cps in 2 min, at a rate increasing directly with frequency. The sweep was repeated three times, making a total of 6 min.

4. White Gaussian noise, 15 g rms, band-limited between 15 and 1500 cps for 6 sec.

Battery voltage remained within the required limits throughout the high frequency tests. The test data obtained are shown in Table 7.

Low frequency. This test consisted of sinusoidal vibration at frequencies between 1 cps and 40 cps for 8 min

Table 6. Battery voltage at 200 w discharge during static acceleration

Test	Thrust axis		Pitch axis		Yaw axis	
	+14g	−4g	+6g	−6g	+6g	−6g
TA battery 1						
Open circuit	33.30	33.07	32.95	↑	29.81	↑
Start 200 w discharge	29.26	28.05	27.74	(ᵃ)	27.35	(ᵃ)
After 5 min of discharge	28.18	27.76	27.68		27.64	
Open circuit after discharge	33.07	32.88	29.23	↓	29.31	↓
TA battery 2						
Open circuit	32.96	↑	30.04	↑	29.63	↑
Start 200 w discharge	27.61	(ᵃ)	27.65ᵇ	(ᵃ)	27.41	(ᵃ)
After 5 min of discharge	27.50		27.45ᵇ		27.34	
Open circuit after discharge	29.64	↓	29.27	↓	29.38	↓
TA battery 3						
Open circuit	33.00	32.89	32.74	32.62	↑	↑
Start 200 w discharge	29.00ᶜ	29.61ᶜ	29.14	29.14	(ᵃ)	(ᵃ)
After 5 min of discharge	29.42ᶜ	29.30ᶜ	29.04	28.82		
Open circuit after discharge	32.76	32.63	32.51	32.54	↓	↓

ᵃ Data was not obtained, due to test equipment malfunctions.
ᵇ Data obtained at 14g level, due to instrumentation error.
ᶜ Data obtained at 6g level, due to instrumentation error.

Table 7. Battery voltage at 200 w discharge during high-frequency vibration

Test	Thrust axis	Pitch axis	Yaw axis
TA battery 1			
Open circuit	33.28	32.96	30.12
Start discharge	27.73	27.65	27.60
End discharge	27.39	27.30	27.42
Open circuit	28.90	29.54	28.67
TA battery 2			
Open circuit	32.53	30.23	29.79
Start discharge	27.56	27.14	27.15
End discharge	27.06	26.99	26.81
Open circuit	28.65	28.53	28.25
TA battery 3			
Open circuit	32.73	32.83	29.25
Start discharge	28.81	28.59	27.10
End discharge	28.49	27.50	27.00
Open circuit	30.86	28.72	28.37

in each of three orthogonal directions. The displacement of the vibration was ±3 in. from 1 to 3 cps and 3-g, peak, from 3 to 40 cps. The sweep rate from 1 to 40 cps was proportional to frequency. Battery voltage remained within the required limits throughout the low frequency tests. The test data obtained are shown in Table 8.

c. Shock. Each of the three TA batteries was subjected to two 0.5 to 1.5 msec terminal peak sawtooth shocks, 200 g, in each of three orthogonal directions, with one direction parallel to the vehicle thrust axis. A load of 200 w was applied to the battery throughout each of the

Table 8. Battery voltage at 200 w discharge during low-frequency vibration

Test	Thrust axis	Pitch axis	Yaw axis
TA battery 1			
Open circuit	33.06	28.78	28.73
Start discharge	27.53	27.69	27.57
End discharge	27.36	27.32	27.29
Open circuit	28.63	28.72	28.46
TA battery 2			
Open circuit	32.53	28.57	28.49
Start discharge	26.89	26.96	27.06
End discharge	26.86	26.86	26.84
Open circuit	28.42	28.36	28.37
TA battery 3			
Open circuit	32.97	28.69	28.59
Start discharge	27.16	27.22	27.10
End discharge	27.07	26.99	26.97
Open circuit	28.51	28.43	28.57

shock tests. A pulse load of an additional 260 w was applied for a period of 5 ±2 sec. During the time interval of this added electrical load, the shock of 200 g was applied to the battery. The terminal voltage of the battery was observed with an oscilloscope to determine the effect of the shock on battery performance.

Because of instrumentation difficulties, the shock tests on TA battery 1 were not conducted during the period of maximum electrical load. The data obtained during the shock testing of battery 1 are shown in Fig. 28. The sequence of testing in the three planes was thrust, followed by pitch and yaw. The minimum load voltage observed during these tests was 26.46 v, which was well above the allowable minimum of 25.8 v.

During the shock testing of batteries 2 and 3, the test techniques were improved and the data shown in Fig. 29 were obtained. Battery open-circuit voltage, prior to the application of the electrical load in each plane, ranged from 28.5 to 28.8 v. Battery voltage under load at the 200 w level ranged from 27.5 to 27.7 v. At the
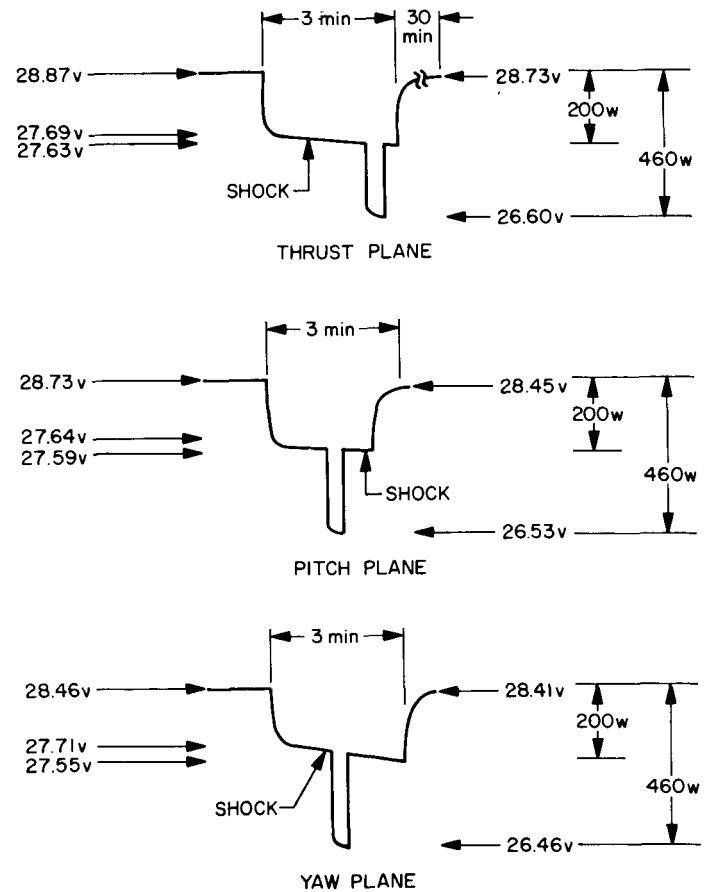

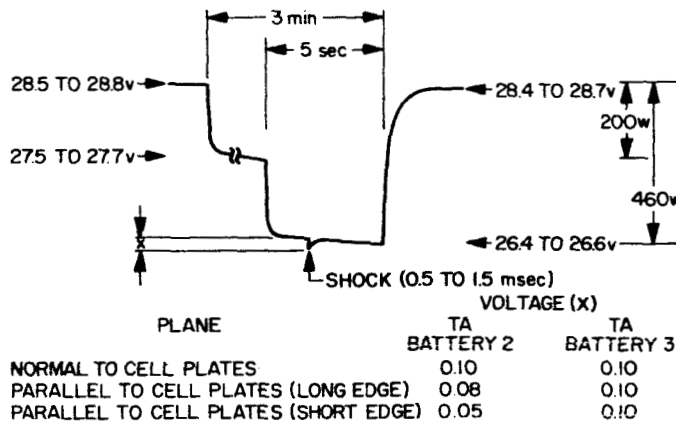**Fig. 28. Type approval battery 1 shock test**

Fig. 29. Type approval batteries 2 and 3 shock test

PLANE	TA BATTERY 2	TA BATTERY 3
NORMAL TO CELL PLATES	0.10	0.10
PARALLEL TO CELL PLATES (LONG EDGE)	0.08	0.10
PARALLEL TO CELL PLATES (SHORT EDGE)	0.05	0.10

460 w load level, battery voltage ranged from 26.4 to 26.6 v. A momentary additional voltage drop of 0.1 v maximum was observed during the shock pulse. The value of this voltage drop for each of the six tests is shown in Fig. 29.

3. Space Flight Vacuum/Temperature

The vacuum/temperature test environmental conditions simulated that portion of the space flight, commencing with Sun acquisition by the solar panels at the end of the boost phase through the end of the flight. The power profile for a maximum flight time of 158 days (Fig. 2) was simulated during this test, using resistive loads of the appropriate value and switching these loads off and on according to the time requirements of the power profile. Loads with a variable initiation time, as shown in the power profile, were applied at a time within the indicated limits which presented the most severe operating conditions. Period 2 was conducted as early as possible in the test; periods 10 and 11 were conducted as late as possible in the test. Because periods 8 and 9 were alternates, period 9 was deleted from the test to determine the capability of the battery to supply the greater average and peak power requirements of period 8 at the end of the flight, a significant period of time after the flight charger had stopped operation due to low input voltage from the solar panels.

Each of the TA batteries was mounted in a heat exchanger which was then placed in a vacuum chamber. Electrical connections were made to the battery to permit charging and discharging by equipment located outside the vacuum chamber. Provisions were also made to record battery temperature, terminal voltage, eighteen cell voltages, load current, load voltage, charge current

and charger voltage. Throughout the test time in the vacuum chamber the pressure was maintained at 10^{-4} mm Hg or less. Type approval battery 1 was held at a temperature of 10°C (50°F). Type approval battery 2 was held at a temperature of 37.8°C (100°F) during portions of the test, with the exception of period 7 when the temperature was increased to 48.9°C (120°F). Type approval battery 3 was held at a temperature of 26.7°C (80°F) throughout the test.

a. Type approval battery 1 tests, 50°F.

Sun acquisition phase. The Sun acquisition phase of the vacuum/temperature test corresponded to that point in flight immediately after launch of the spacecraft, when the battery has completed supplying the requirements of period 1, Fig. 30. The spacecraft has been oriented such that the solar panels are exposed to the Sun and are supplying all spacecraft power, including the operation of the battery charger.

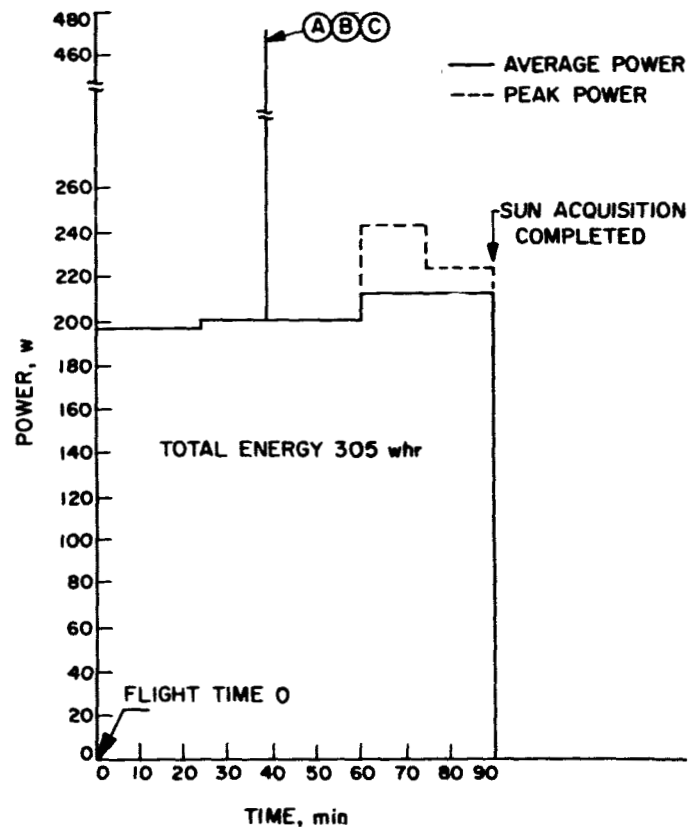Because of an error in interpretation of the test instructions, the period 1 launch phase load was repeated

Fig. 30. Launch phase battery requirement, development model

at the beginning of the vacuum/temperature test of TA battery 1. During this discharge at the 200 w level, the battery voltage decreased from 28.01 to 25.89 v after 90 min. The battery temperature was gradually reduced by the temperature control system in the vacuum chamber to the required 50°F. However, the battery temperature during the discharge decreased only 9°F to 70°F due to the battery heat produced during discharge. At the conclusion of this discharge, the flight charger was turned on and the initial output current was 630 ma and the battery terminal voltage was 26.67 v. Charging continued for 20 hr with the current decreasing to 376 ma and the battery voltage increasing to 34.10 v. Battery temperature had been reduced to 52°F. The charge current and battery voltage data for this 20 hr period are shown in Fig. 31.

Midcourse maneuver phase. At the beginning of the midcourse maneuver load (period 2, Fig. 32), the battery voltage was 30.66 v at the 230 w level and decreased to 27.11 v after 45 min. The pulse loads D and E increased the discharge rate to the 500 w level and the battery voltage decreased to 26.18 v. Battery temperature was 53°F at that time. During the final 36 min of discharge at the 5 w level the battery voltage increased from 28.67 to 28.96 v due to the effect of the flight charger, which
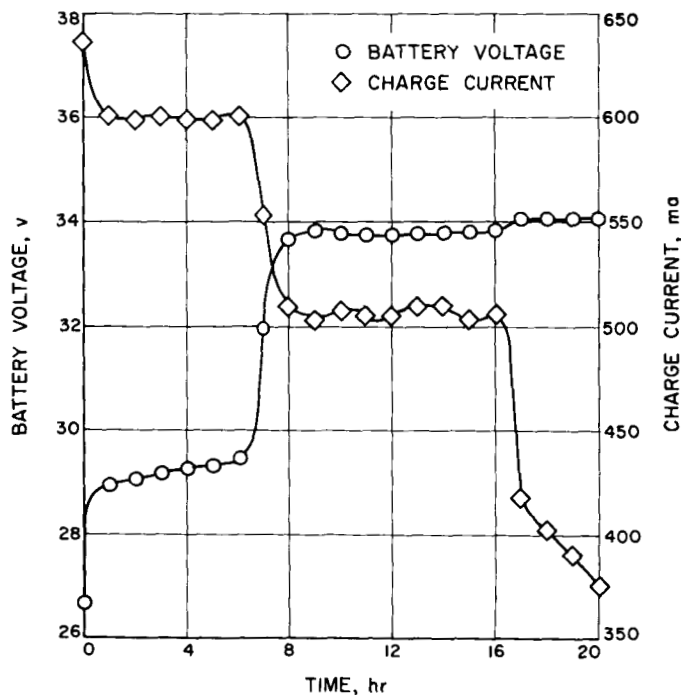
was not turned off during the discharge. Because of the limited current capability of the charger, the battery voltage observed during the high voltage discharge levels was not affected. These data are shown in Fig. 33. At the end of this discharge test the charger continued to operate. During the following 14 days the charge current decreased from 616 to 28 ma while the battery voltage increased from 28.99 to 34.36 v.

Cruise phase. Battery voltage, load current and charge current for the first 10 days of cruise mode operation following the midcourse maneuver are shown in Fig. 34. Figure 35 presents the record of battery terminal voltage and charge current for the next 60 days of the simulated flight. The period 3 discharge at the beginning of Fig. 35 resulted in a minimum battery voltage of 31.3 v. This voltage is partially a result of the presence of the charger output voltage and the contribution of 510 ma of charge current to the load total of 560 ma. At the 41st and 48th days of the test, adjustments were made in the setting of the charger output level. The adjustment on the 41st day resulted in a lower than desired float charge voltage and was therefore corrected on the 48th day.

During the 76th day of the test, the battery reached full charge as indicated by the reduction in charge current shown in Fig. 36. The momentary drop in battery

Fig. 31. Flight charging of type approval battery 1 after launch and Sun acquisition
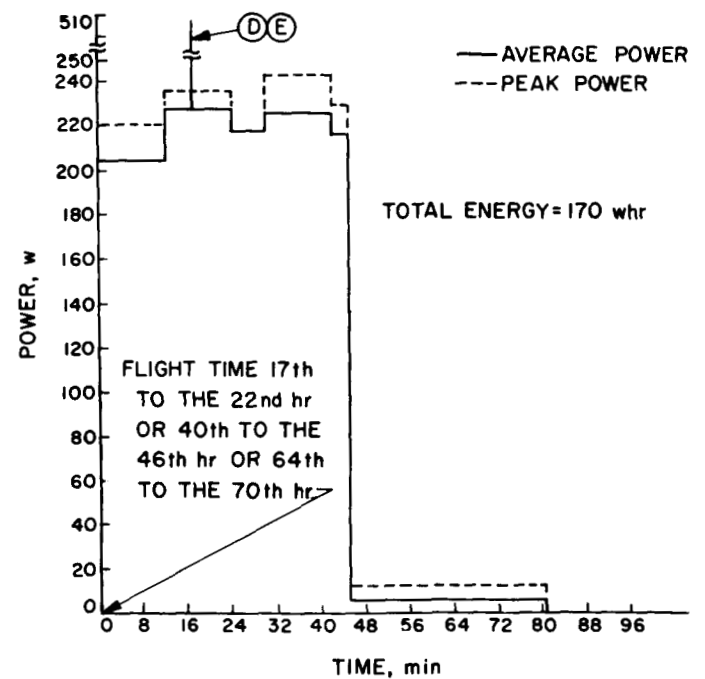
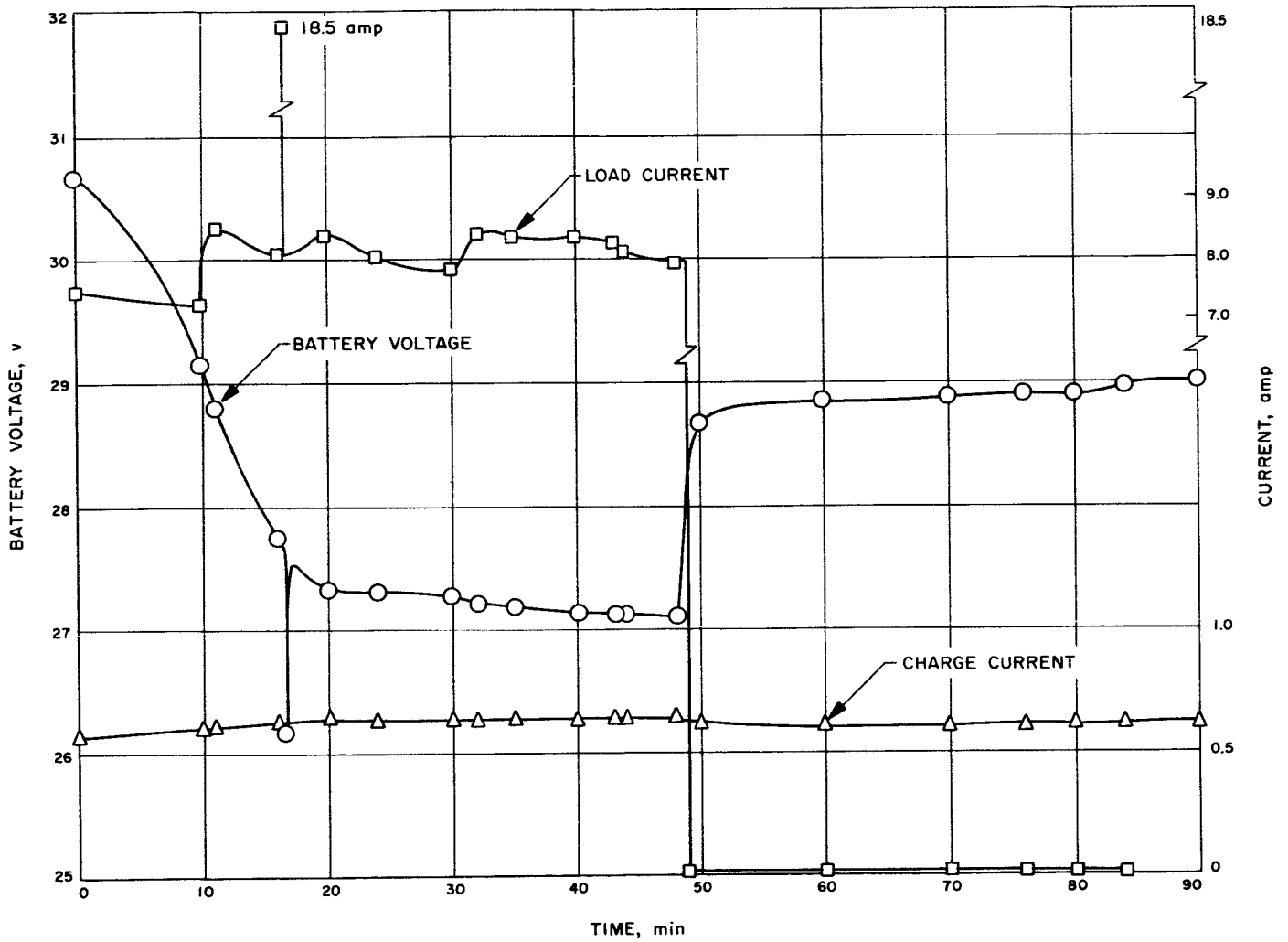**Fig. 32. Midcourse maneuver battery requirement, development model**

Fig. 33. Type approval battery 1 performance during midcourse maneuver
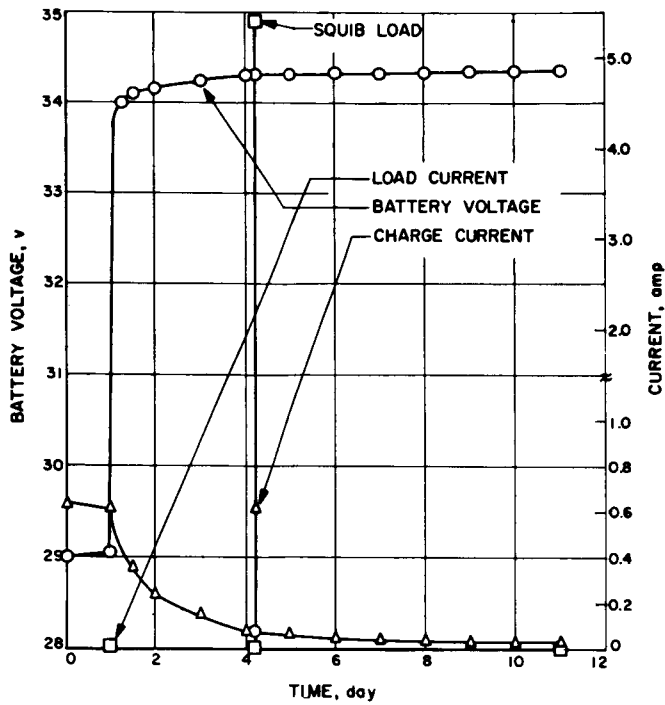
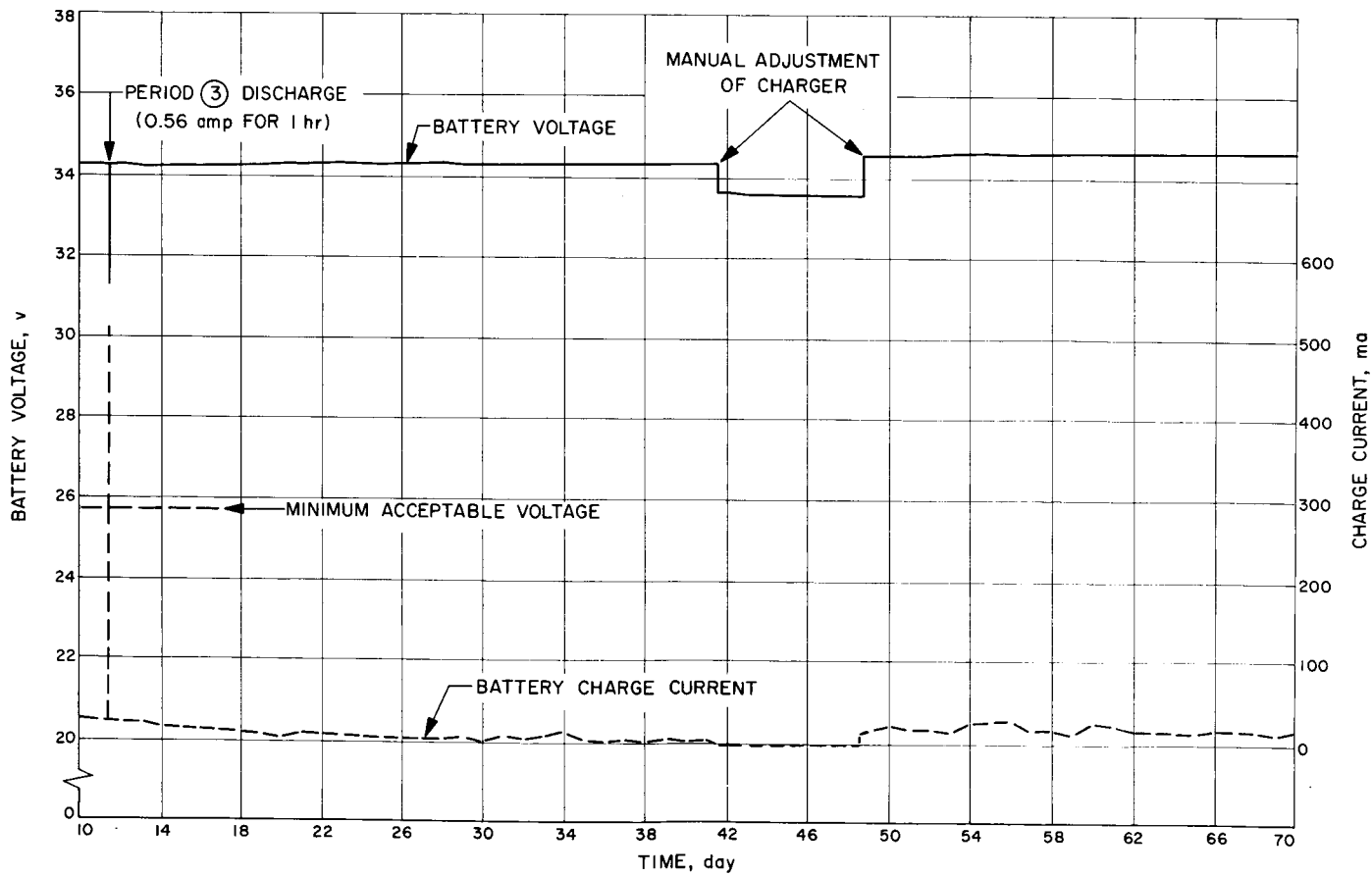Fig. 34. Type approval battery 1 performance during cruise after midcourse

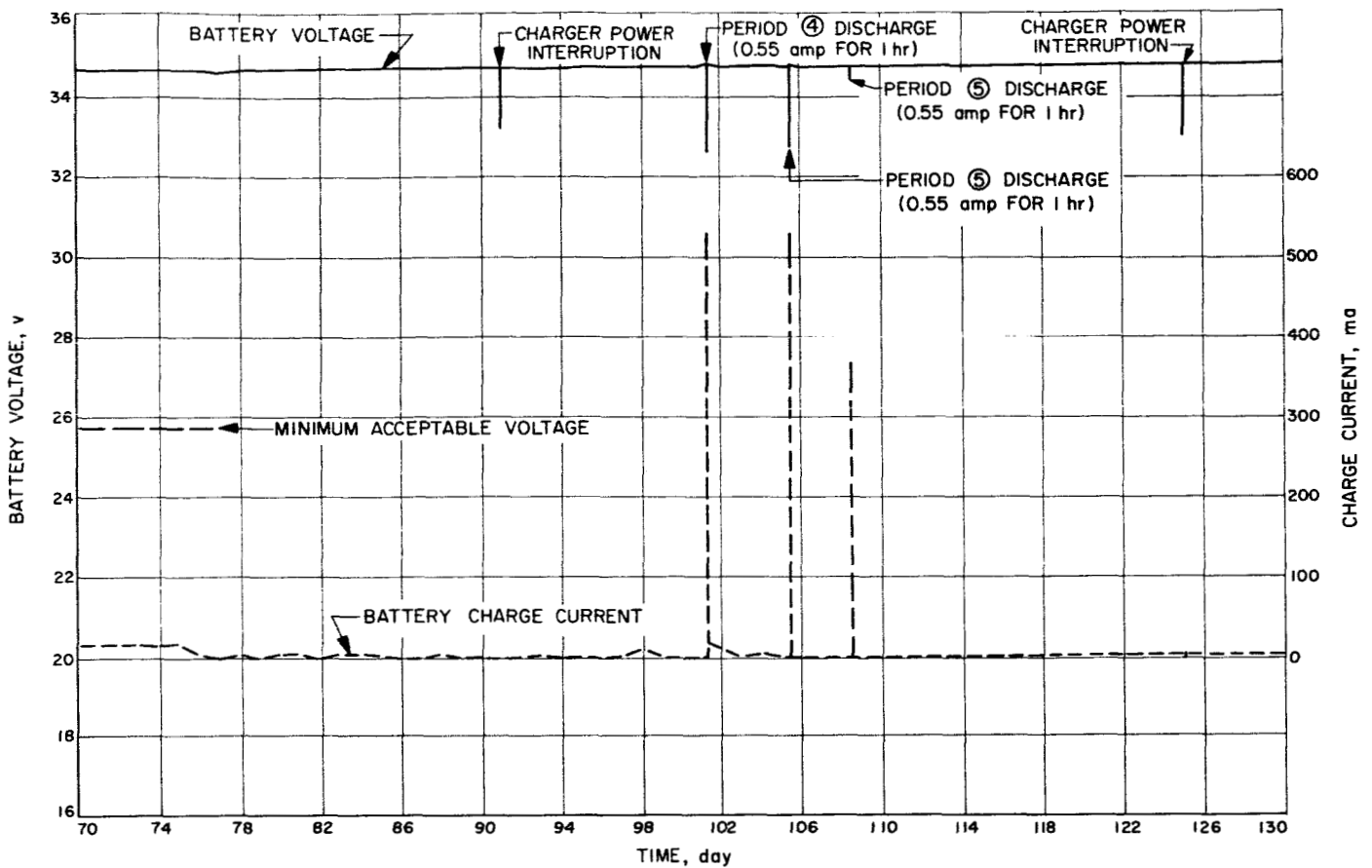Fig. 35. Type approval battery 1 performance during cruise (10 to 70 days)

Fig. 36. Type approval battery 1 performance during cruise (70 to 130 days)

terminal voltage recorded on the 91st day of testing, resulted from an interruption to the 400-cycle power source. This source provided the simulated solar panel power input for the battery charger. A like situation occurred again on the 125th day of testing. Battery voltage under load during periods 4, 5, and 6 discharges remained well above the minimum allowable voltage. Again, the battery charger was on and actually supplied the majority of the current during each of these discharges.

Planet encounter phase. Battery performance during the planet encounter phase of the test is shown in Fig. 37. Battery voltage during the period 10 discharge reached a minimum of 26.75 v. During the period 7 discharge on the 151st day of the test, the minimum battery voltage was 25.58 v when the squib load *J* was applied. At the end of period 7 on the 152nd day, squib load *K* reduced the battery voltage to 24.25 v. Both of these voltages were below the design minimum of 25.8 v. At the completion of this period 7 discharge, it was observed that the battery charger had not been turned off during the discharge. The charger was turned

off and the period 7 discharge was repeated on the 159th day of the simulated flight. Squib load *K*, at the end of this discharge on the 160th day, resulted in a minimum battery voltage of 25.32 v. The voltages of the first 6 cells were recorded during the application of squib load *J* on day 151. The readings obtained ranged from 1.487 to 1.510 v/cell or an average of 1.499 v. The battery terminal voltage of 25.59 v obtained at the initiation of squib-load *J* would have required an average cell voltage of 1.42 v, which is considerably below the values recorded. This data indicates the possibility of one or more cells with low voltage. A review of the cell voltage data recorded during the balance of the period 7 discharge (approximately 17 hr) at the 1.4-amp rate disclosed that cell 12 voltage was significantly below average for the group of 18 cells at any time. At the end of the first 3 hr at the 1.4 amp rate, cell 12 voltage was 1.515 v, whereas the average of the remaining 17 cells was 1.565 v. Near the end of the 17 hr of discharge the average cell voltage was 1.543 v and cell 12 voltage was 1.520 v. When squib load *K* was applied at the end of the 17 hr, the average cell voltage for cells 1 through 14, excluding cell 12, was 1.452 v; cell 12 voltage was 1.273 v.
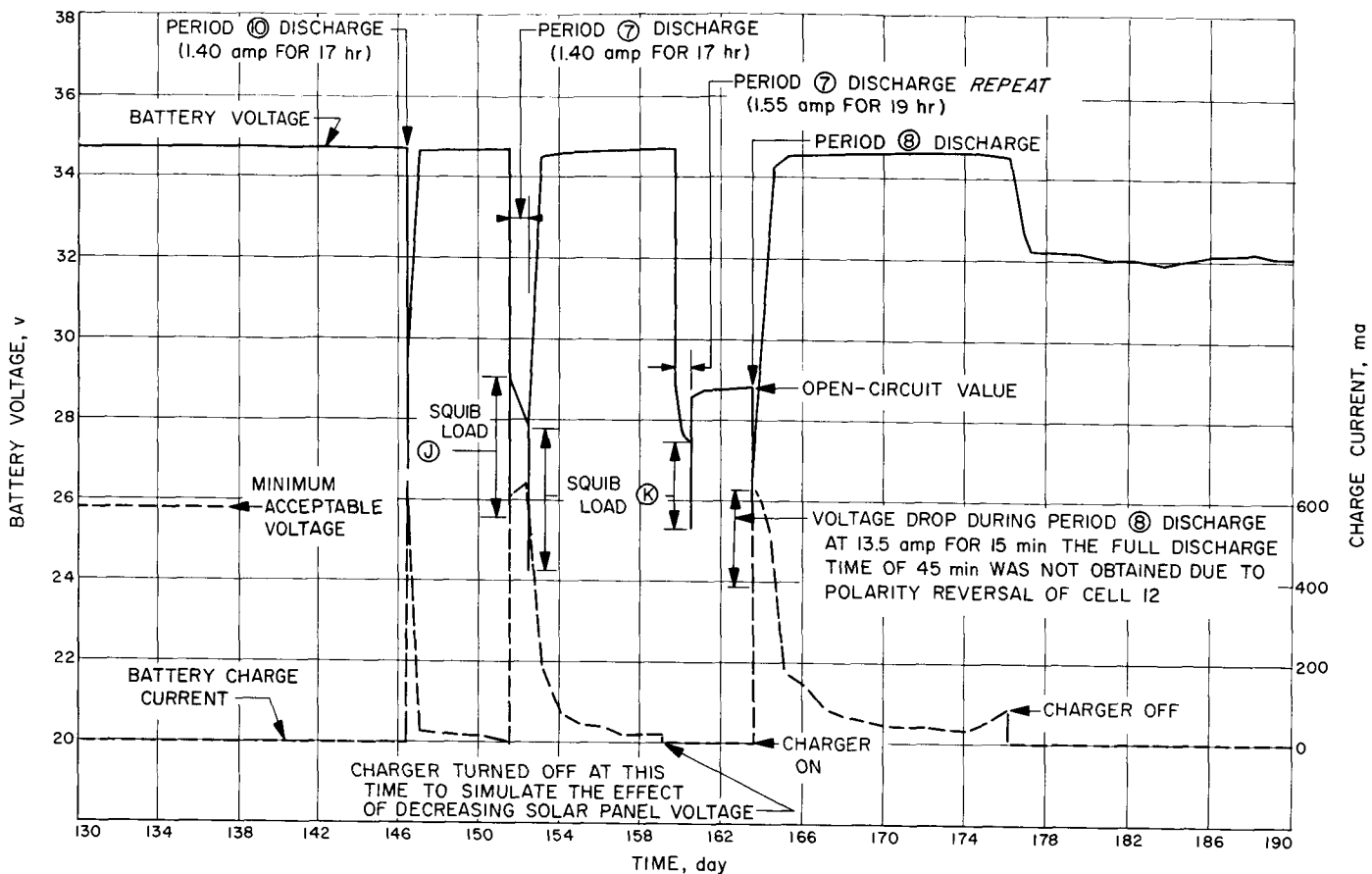
Fig. 37. Type approval battery 1 performance during cruise (130 to 190 days)

On the 159th day of testing, when the flight charger was turned off prior to the repeat of the period 7 discharge, cell voltages on open-circuit averaged 1.883 v. The exceptions were cell 8, which was low at 1.695 v indicating the possibility of an internal short forming, and cell 12, which was high at 1.990 v. At the beginning of the period 7 *repeat* discharge on test day 159, all cell voltages appeared normal with the exception of cell 12 at 1.72 v. Just prior to the application of squib load K on test day 160 (Fig. 37), average cell voltage was 1.53 v with the exception of cell 12 which was 1.45 v. During squib load K discharge, the average cell voltage, based on cells 1 through 4, was 1.445 v. If all 18 cells had maintained this value as a minimum, the battery terminal voltage would have been 26.01 v, as compared to the 25.32 v observed.

The battery remained in the open-circuit mode until test day 163, when period 8 discharge was attempted (Fig. 37). Only 15 min of discharge at the 13.5 amp rate were obtained before battery terminal voltage went be-

low the 25.8 v minimum, due to polarity reversal of cell 12. Charging was resumed on the 163rd test day to determine if cell 12 was shorted and would, therefore, not accept charge. After six days of charger operation, the voltage of cell 12 had risen to 2.074 v while the average for the remaining cells was 1.92 v. During the two days preceding charger turnoff on test day 176 (Fig. 37), charger current began to increase as the result of several cell voltages decreasing erratically, thus reducing the battery terminal voltage. During the 39 days following charger turnoff, battery voltages were monitored in the open-circuit condition. The voltage of cells 1, 6, 8, and 13 decreased gradually during the open-circuit period prior to test day 211. Beginning on day 212 (Fig. 38), cell 8 voltage decreased rapidly to 1.245 v and continued dropping to 0.025 v on day 214 when the recording of test data was stopped and the battery was removed from the test chamber.

Battery examination. The battery was returned to the manufacturer where a post-mortem examination was
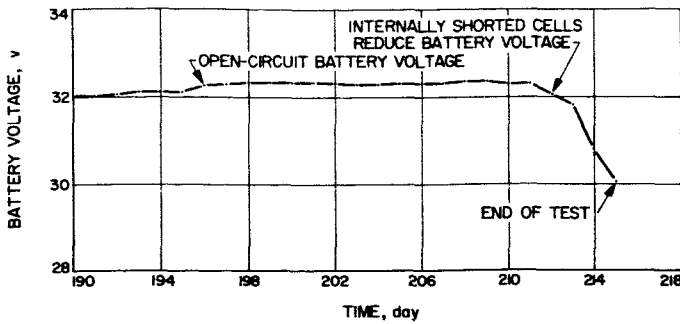
Fig. 38. Type approval battery 1 performance during 25 days after planet encounter (190 to 215 days)

conducted to determine the cause of the failures observed during testing. Cell voltages, when the battery was received at the manufacturer, are shown in Table 9. Voltage measurements from each cell to chassis, for cells 1 through 9 comprising assembly 3, indicated no electrolyte leakage. Electrolyte leakage was observed in assembly 4, comprising cells 10 through 18. The cell monoblocks were removed from this assembly by machining away the metal shell. Close inspection revealed the following: An outside wall of cell 8 was cracked; the intercell wall between cells 8 and 9 was broken; evidence of electrolyte leakage was observed in the corners of the cover seals for cells 1, 5, and 6. Cells 17 and 18 were disassembled and examined part by part. The cellophane on all positive plates of cell 17 contained holes in the fold area at the bottom of the plate. These holes apparently resulted from the stress placed on the cellophane, due to the tight folding radius. However, the main cause for the

Table 9. Type approval battery 1 condition when returned to manufacturer for post-mortem examination

Assembly 3, open-circuit voltages			Assembly 4, open-circuit voltages		
Cell No.	Cell Terminals	Chassis to cell	Cell No.	Cell Terminals	Chassis to cell
1	1.60	0	10	1.86	0
2	1.85	0	11	1.84	0
3	1.85	0	12	1.85	0
4	1.77	0	13	0.02	0
5	1.84	0	14	0.19	0.01
6	1.73	0	15	1.86	0.01
7	1.86	0	16	0.00	0.02
8	0.00	0	17	1.86	0.03
9	1.86	0	18	1.85	0.03
Total	14.36			11.33	

discharged condition was the zinc tree formations over the top of the open end of the cellophane. The epoxy sealing of the separator envelope had not effectively bonded to the top of the separator. Cell 18 (not shorted) separator system components were heavily laden with silver; however, the cellophane was intact and no zinc trees were visible. Epoxy seal area was minimal, but had not been penetrated.

Design recommendations. Examination of the cover seal resulted in a change in the design of the cover plate to more closely match the cell jar opening, reducing the amount of cement buildup required. The thickness of the epoxy seal was increased to enlarge the surface bonding area between the separator and the epoxy. The degree of silver penetration observed in these cells prompted a recommendation that an additional layer of cellophane be added to this cell design to improve the float charging life. A change in the cellophane wrapping procedure was also made to control the fold radius at the bottom of the positive plates.

b. Type approval battery 2 tests, 100°F.

Sun acquisition phase. The launch phase load, period 1 (Fig. 30) was incorrectly repeated at the beginning of the vacuum/temperature testing of TA battery 2. The full discharge period of 90 min was not obtained due to the polarity reversal of the voltage of cell 9. Figure 39 shows the data obtained during the first 15 days in the vacuum chamber at 100°F. The additional energy removed from the battery during this discharge was beyond the specification requirements, thus, the cell reversal could not be considered a failure which would disqualify the battery design. It was not possible to predict the effect of this excessive discharge on future performance of the battery. However, the proper test sequence was initiated by turning on the flight charger. The initial conditions at that time were: charge current of 708 ma and battery terminal voltage of 28.77 v. All cell voltages were in the range of 1.59 to 1.60 v. Battery temperature had risen above the 100°F test temperature during the discharge and was 106°F at the time the flight charger was turned on.

Midcourse maneuver phase. The charging operation continued for 6 days before the battery reached full charge, as indicated by the reduction of charging current below 10 ma. The charger output adjustments noted in Fig. 39 were made during the 5th day of the vacuum/temperature test to reduce the final float charging voltage. However, the adjustment procedure used resulted in the final voltage being too low to obtain maximum
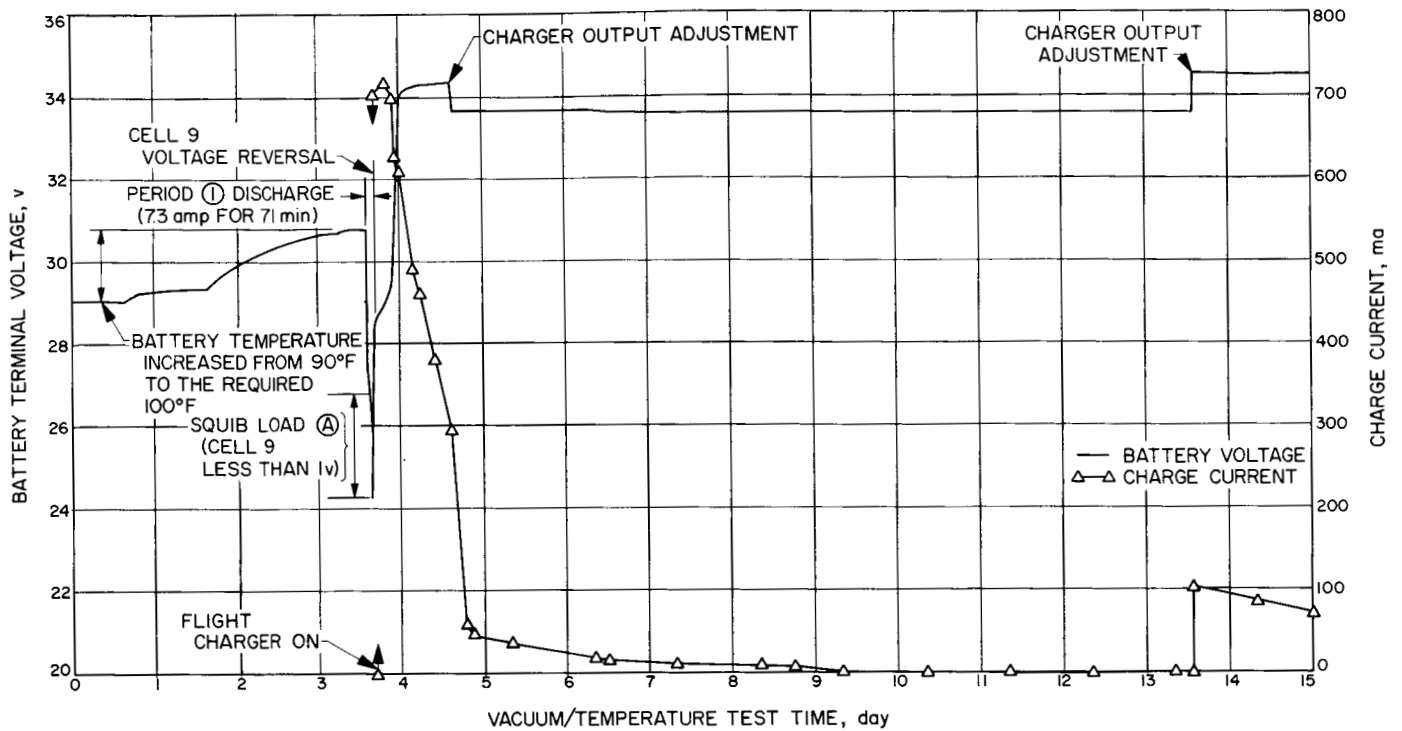
Fig. 39. Type approval battery 2 flight charging after launch and Sun acquisition

Fig. 40. Type approval battery 2 flight charging (15 to 45 days)

charge input. Therefore, on the 14th day of testing, the charger was reset using a modified procedure with 34.8 v and 5 ma as the calibration point. These charger adjust-ments were also made on TA battery 1 (Fig. 35) and TA battery 3 (Fig. 40). The charging operation continued at the final setting for an additional 38 days before the

Fig. 41. Type approval battery 2 flight charging (45 to 70 days)

charge current decreased to less than 10 ma. The initiation of the simulated midcourse maneuver load sequence was delayed until this charge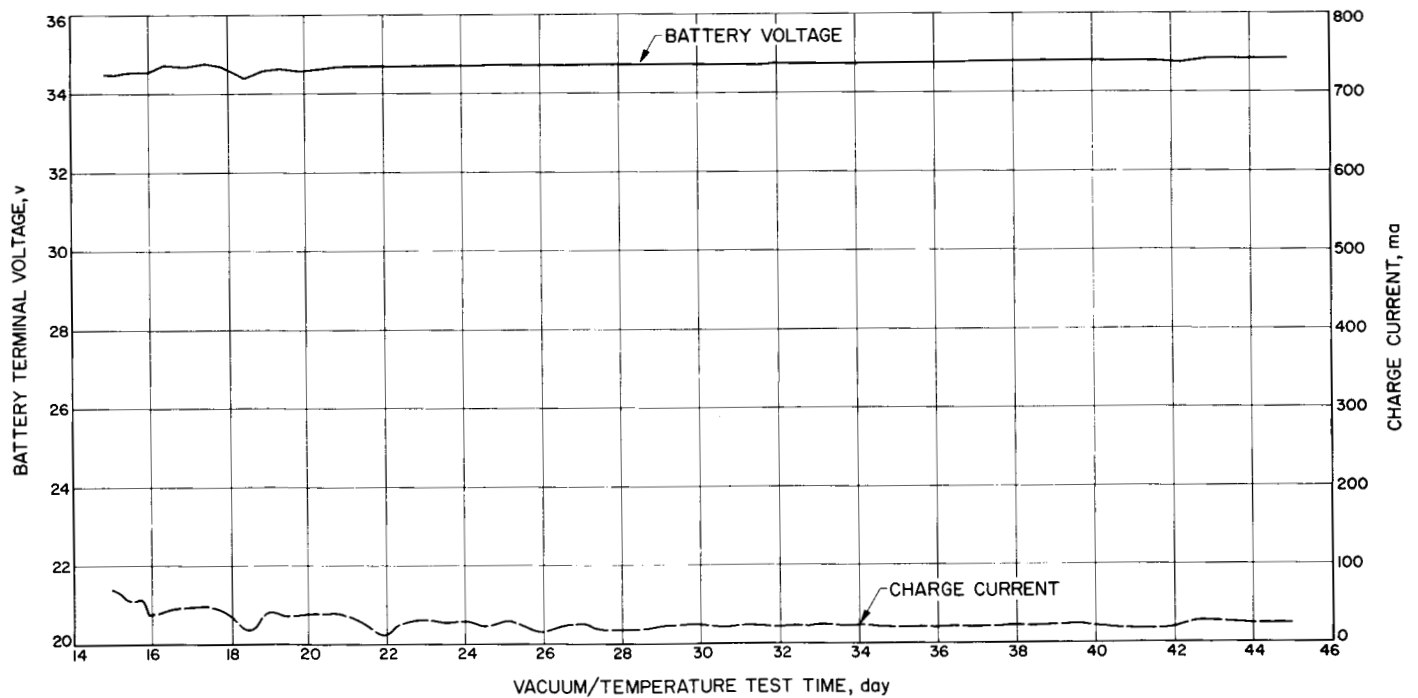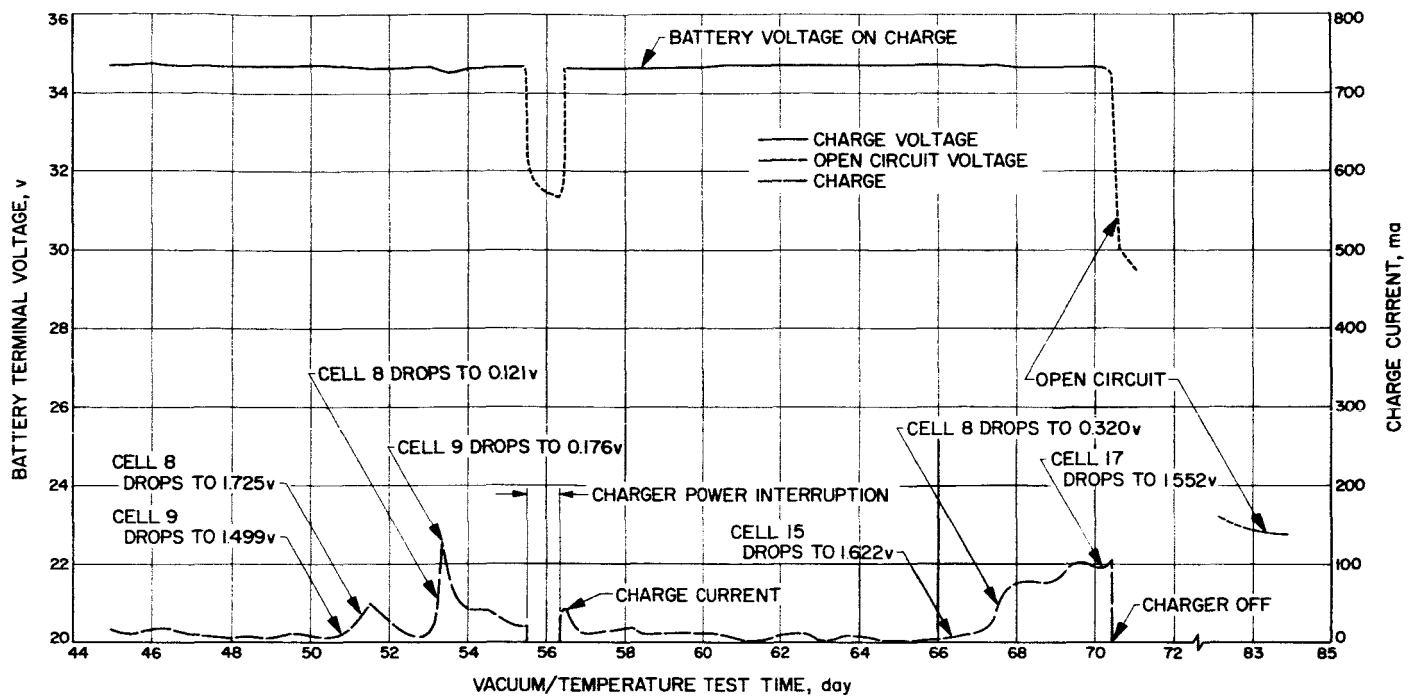 condition was obtained to be assured that the excessive discharge, at the beginning of the vacuum/temperature operation, had not damaged the battery. The midcourse maneuver load sequence period 2 (Fig. 32) was therefore scheduled to be concluded on the 53rd day, after placing the battery in the vacuum chamber. However, a review of the cell voltages prior to connection of the load disclosed that cells 8 and 9 had decreased significantly below the average cell voltage of 1.962 v for the remaining cells in the battery. These cell voltages were 1.725 and 1.555, respectively, and the charge current had increased to 50 ma (Fig. 41) and the battery terminal voltage had decreased approximately 0.1 v in keeping with the increased charge current. The charger output current/voltage relationship is shown in Fig. 19.

The cell voltages were recorded for the next 19 days and the values shown in Fig. 42 were obtained. Cell 8 voltage remained fairly constant at 1.51 to 1.56 v, until test day 69 when the voltage dropped abruptly to 0.320 v. On the 54th day of testing, cell 9 dropped sharply to 0.244 v and then gradually increased to 0.358 v on the 71st day of testing, just prior to removal of the battery from the test chamber. Cell 9 experienced polarity reversal during the discharge on the 3rd day after installa-

tion in the vacuum chamber. During the 67th test day, cell 15 dropped temporarily to 1.622 v and recovered to 1.853 v within 24 hr and then returned to 1.650 v the following day. On test day 71, cell 17 dropped to 1.552 v from 2.104 v. At this time the battery was removed from the vacuum chamber and testing was stopped. Electrolyte leakage in the vacuum chamber was observed.

Battery examination. Type approval battery 2 was returned to the manufacturer, where a post-mortem examination was conducted to determine the cause of the failures observed during testing. The 4- and 5-cell monoblocks were removed from their metal housing as the first step in the examination. The open-circuit cell voltages and the physical condition of the cell containers are shown in Table 10.

Two cells (6-6 and 6-7) had open-circuit voltages, indicative of fully charged cells. Each of these cells was discharged at the 20 amp rate to end voltages of 1.39 and 1.20 v, respectively, and each delivered 60.5 amp-hr.

Several cells from each assembly were selected for disassembly for a further examination of cell components. The negative plates were in excellent condition with no sign of erosion of active material from the grid. The edges of some negative plates had been flattened by impact with the cell case wall during the vibration tests.
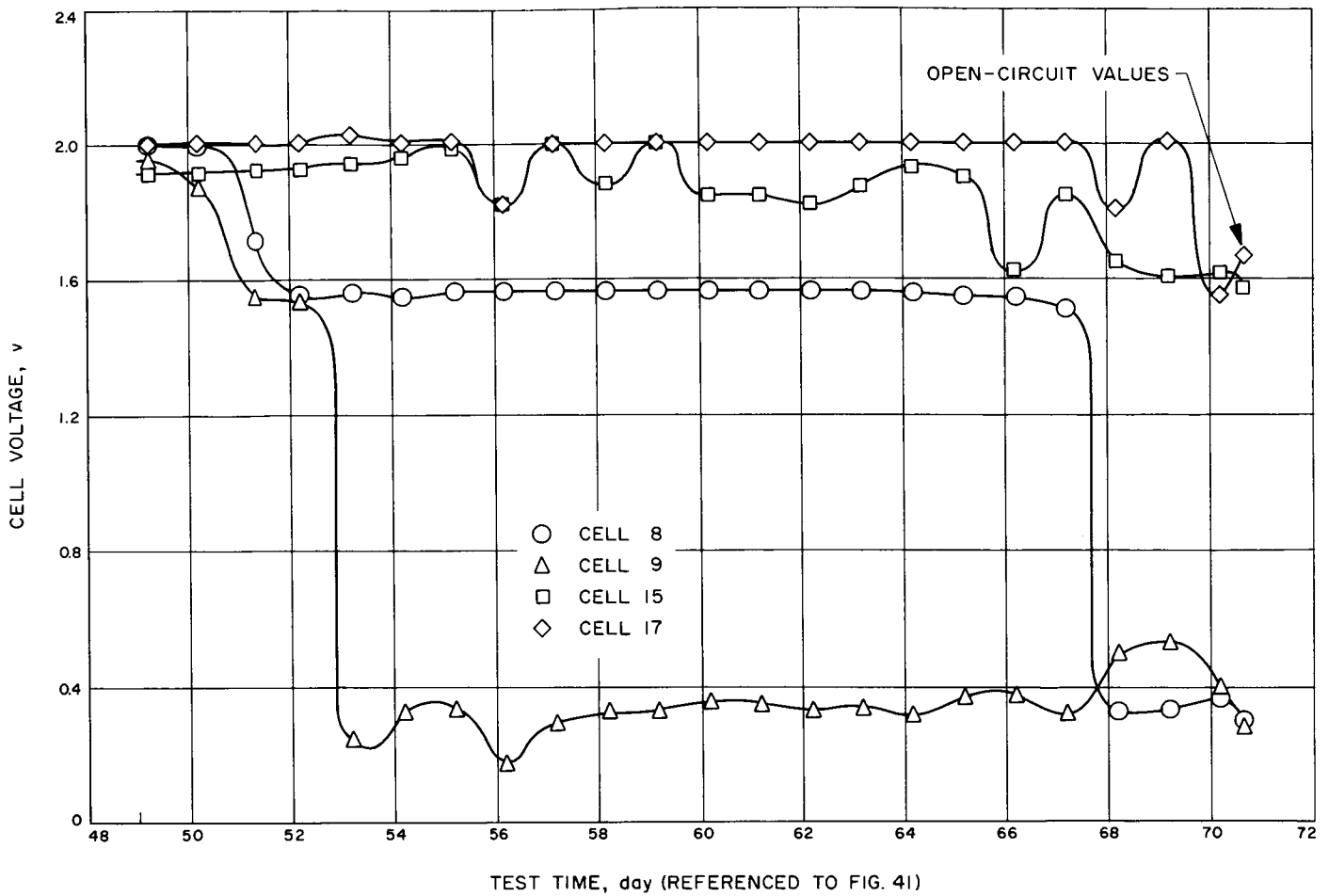
Fig. 42. Type approval battery 2 cell voltages during formation of internal shorts under charge

Table 10. Type approval battery 2 post-mortem examination

Assembly No.	Cell No.	Open-circuit voltage	Intercell wall[a]	Outside wall	Cell seal	Assembly No.	Cell No.	Open-circuit voltage	Intercell wall[a]	Outside wall	Cell seal
5	1	1.90		—	—	6	1	1.89		—	—
			Broken						Broken		
	2	0.03		—	—		2	1.88		—	—
			Broken						Broken		
	3	1.35		—	—		3	1.82		—	—
			Broken						Broken		
	4	0		—	—		4	0.21		—	—
			Broken & hot short						Broken		
	5	0.13		—	—		5	1.68	—	Broken	Broken
	6	0.46		Broken	Broken		6	1.87		Broken	—
			Broken						Broken		
	7	0.37		Broken	Broken		7	1.87		Broken	—
			Broken						Broken		
	8	0.43		Broken	Broken		8	0.07		—	—
			Broken						Broken & hot short		
	9	0.49		—	—		9	0.08		—	—

[a] The physical conditions of the intercell walls are listed between their respective cell numbers.

However, no grid wires were visible. The negative-plate lead wires and epoxy coating were in good condition. Positive-plate lead wires were heavily oxidized and their protective coatings were partially destroyed. Many positive-plate lead wires were broken at the juncture of the spot weld to the plate at the point where the lead wire coating terminated. The brown charred condition of the polystyrene case intercell walls, between cells 5-4, 5-5, and 6-8, 6-9 indicated the formation of internal shorts. The condition of the positive plates from several cells are shown in Table 11. Broken-plate lead wires may be the natural result of a sudden shift of the plate pack when a cell ruptures releasing the high internal pressure. Oxidation and weakening of the silver leads from the positive plates occurred during float charging.

Design recommendations. The condition of the silver lead wires on the positive plates indicated the desirability of providing a means of preventing or at least reducing the ability of the silver-plate lead wires to become oxidized. The solution selected was to apply a flexible

Table 11. Type approval battery 2 positive plate conditions determined by post-mortem examination

Assembly No.	Cell No.	Plate No.	Remarks
5	4	1, 2	Shorted to three adjacent negative plates in the area near location of charred hole in the intercell wall
	4	2, 3, 8, 9, 11	Both lead wires broken at plate
	4	4, 7	One of the two lead wires broken at plate
	5	5, 7	One of the two lead wires broken at plate
		11	Shorted through separator system to adjacent negative plate
	9	1, 2, 3, 4, 5, 6, 7	Both lead wires broken at plate
6	6	One	Both lead wires broken at plate on one plate; delivered 60.5 amp-hr at the 20-amp rate to end voltage of 1.39 v
	7	Five	Both lead wires broken at plate on five plates; delivered 60.5 amp-hr at the 20-amp rate to end voltage of 1.20 v
	8	All except one	Both lead wires broken at plate
	9	All except one	Both lead wires broken at plate

epoxy coating on the plate lead wire and that portion of the plate immediately surrounding the point where the lead wire and plate joined. The presence of shorted plates resulting from penetration of the separator system and the general appearance of the cellophane resulted in the decision to increase the cellophane portion of the separator system, from 4 to 5 layers. This decision was based on the condition of the cells in both TA 1 and TA 2 batteries.

c. Type approval battery 3 tests, 80°F.

Sun acquisition phase. The Sun acquisition sequence was simulated at the start of the temperature/vacuum test by turning on the flight charger. The battery terminal voltage and the charge current are shown in Fig. 43 for the first 34 hr. Battery temperature was within 80 ±2°F temperature range specified for the testing of battery 3. The charge current began tapering off as required and the charger output voltage stabilized accordingly. A comparison of the data of Figs. 43 and 19 (flight-charger characteristic), indicates proper system operation.

Midcourse maneuver phase. The data obtained during the midcourse maneuver load simulation are shown in Fig. 44. During the 45 min discharge at the 230 w level (Fig. 32), the battery voltage decreased from 28.47 v to 27.06 v. The squib load was not applied during the 230 w load time as described in the design specification; however, when it was applied, the wattage was adjusted upward to (230 + 272) 500 w to compensate for the smaller pre-load at that time. The minimum battery voltage under this large pulse load was 26.7 v, well above the required minimum of 25.8 v. Battery temperature was at a maximum of 86°F, during the period 2 discharge, due to the heat generated within the battery; however, the temperature was restabilized at 80°F, within a few hr after the discharge.

Cruise phase. Figure 45 is a plot of the battery terminal voltage and charge current for approximately 30 days after the midcourse maneuver. The high charge current present toward the end of the 3rd test day (Fig. 44) required a recheck of the charger calibration, which is noted during the first half of Fig. 45. Resetting of the charger control circuitry resulted in the significantly lower charge current, as noted during the latter half of Fig. 45. This current value is in close agreement with the design requirement of less than 10 ma of float current since the current value in Fig. 45 of approximately 20 ma is the sum of the current being drawn by the 0.2 w continuous load (Fig. 2) and the float charging current.
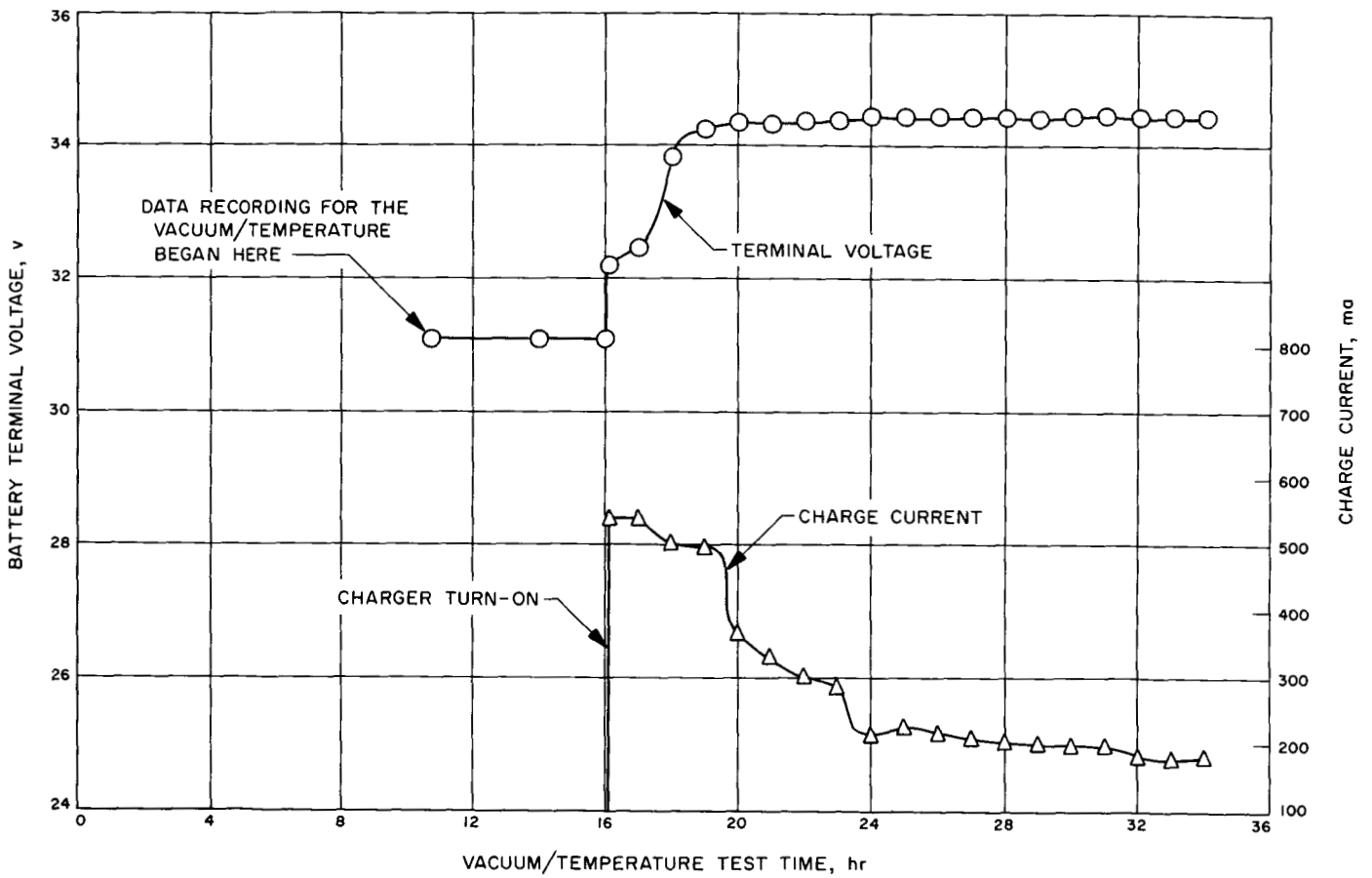
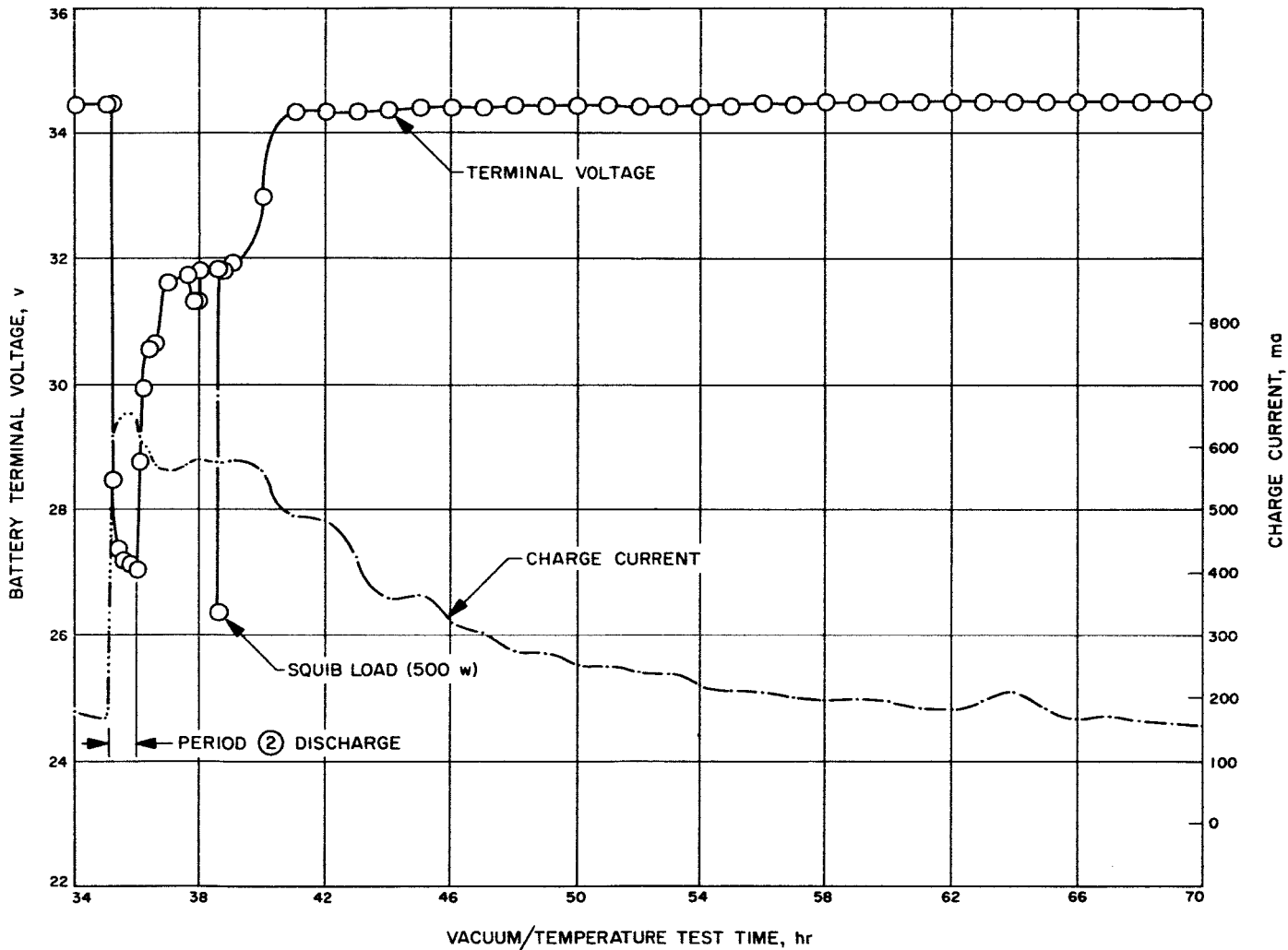**Fig. 43. Type approval battery 3 performance during Sun acquisition**

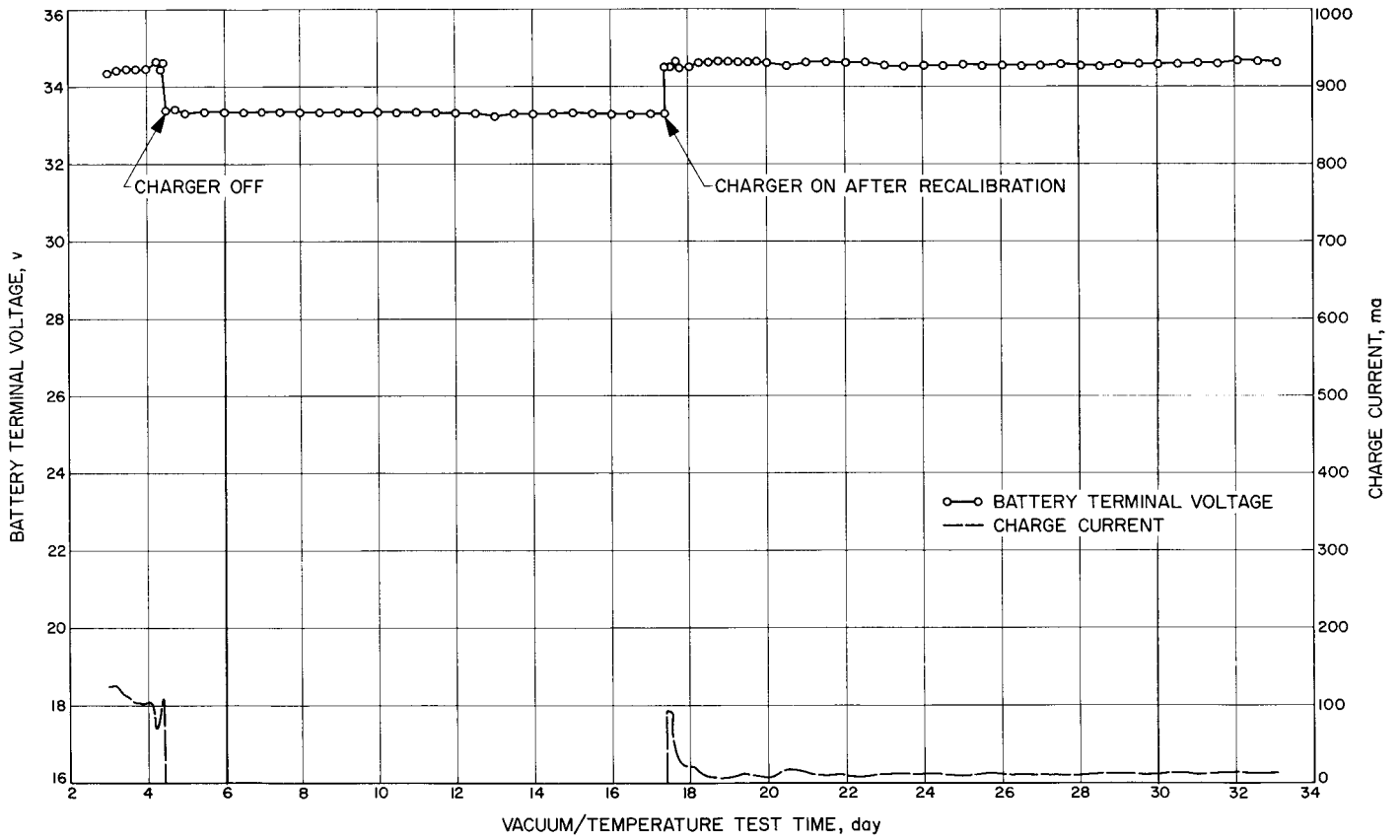Fig. 44. Type approval battery 3 performance during midcourse maneuver

Fig. 45. Type approval battery 3 cruise mode charging (3 to 33 days)

During the test period from the 33rd through the 62nd day, shown in Fig. 46, both battery voltage and charge current remained stable. During a portion of the 41st and 42nd days of the test, a temporary commercial power failure, operating the dc power supply, which in turn supplied the charger with the simulated solar panel voltage, was experienced. The dc supply required a manual resetting of its output before normal charging could be resumed.

The commercial power system was interrupted again on test day 77 (Fig. 47). The period three discharge on the 82nd test day was a one hr load of approximately 44 w. Because the flight charger was operating during this discharge, approximately 18 w were supplied by the charger and the balance by the battery; therefore, the battery voltage under load remained above 31.6 v. Battery temperature remained at 80 ±2°F.

The period 4, 5, and 6 discharges were also conducted with the battery charger on; therefore, sharing of the load occurred as indicated by the data presented in

Fig. 48. Battery temperature remained at 80°F. During the latter part of Fig. 48, beginning with the 116th test day and continuing through the 129th day (shown on Fig. 49), the charging current decreased slightly when the 0.2 w continuous load was temporarily turned off, to observe the operation of the charger and battery. Charger output voltage increased slightly as expected and the resultant charge current decreased to a value of less than 5 ma. The charger and battery responded normally when the small load was reapplied.

Data obtained during the 153rd test day are shown in Fig. 50. The charger was turned off prior to the period 10 discharge, to simulate the effect of loss of solar panel voltage which would occur during a Sun reacquisition maneuver. This discharge was at the 275-w rate for 15 min. When the load was first applied, the battery voltage dropped to 26.4 v, quickly recovered to 26.80 v and then gradually decreased 20 mv during the remaining 14 min. Approximately 30 min after completion of the discharge, the battery temperature reached a maximum of 84°F. The environmental chamber temperature
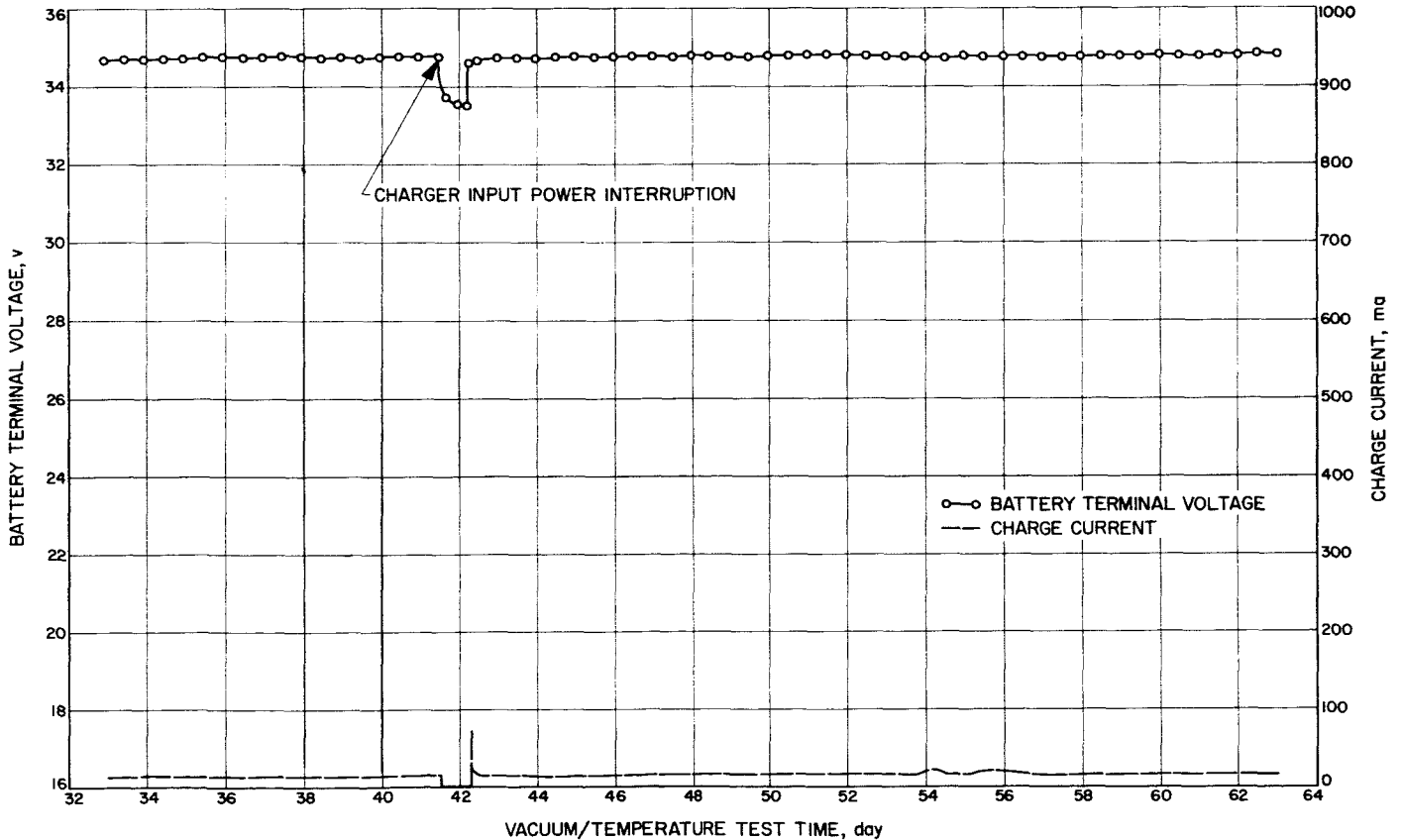

Fig. 46. Type approval battery 3 cruise mode charging (33 to 63 days)
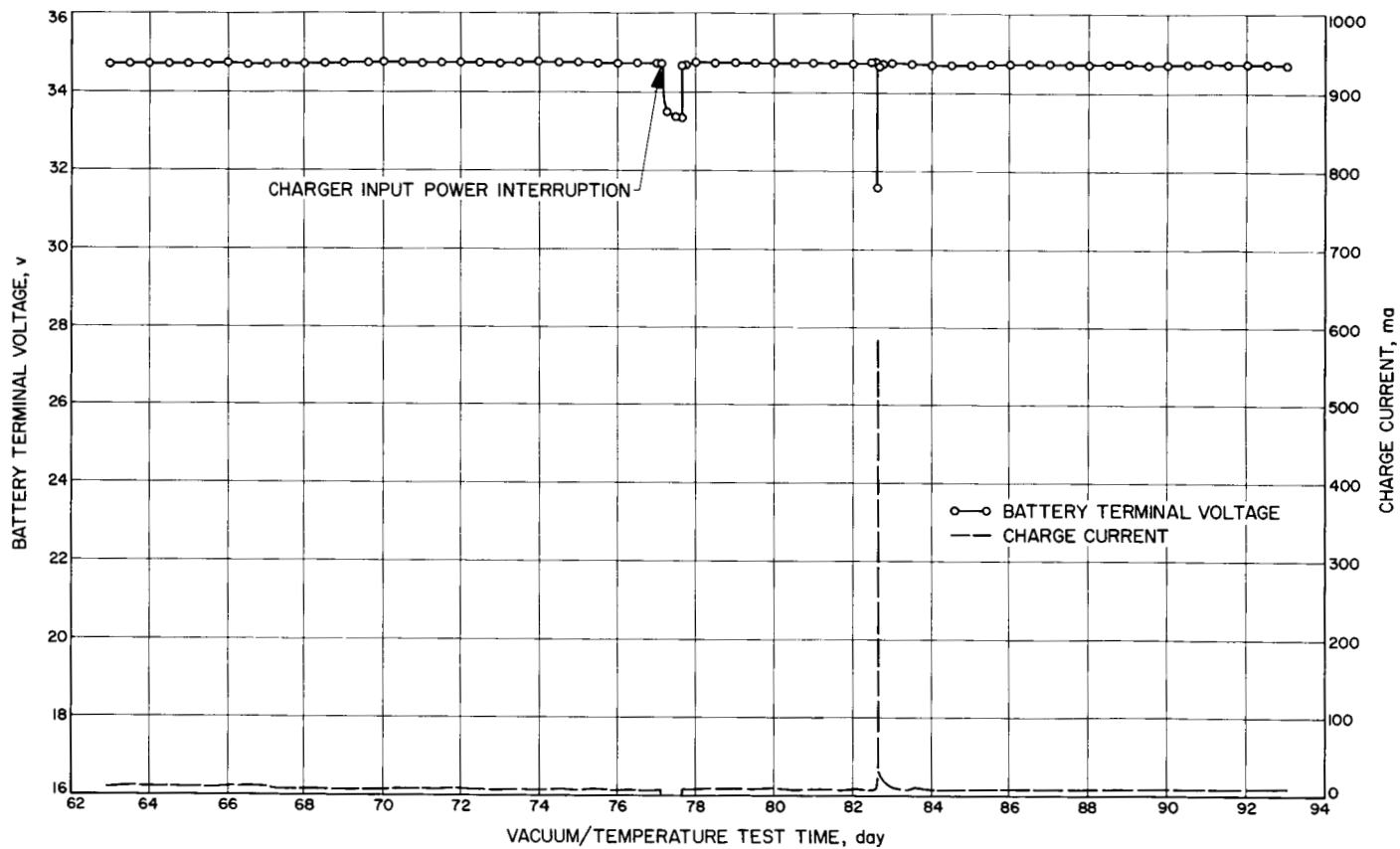
Fig. 47. Type approval battery 3 cruise mode charging and period 3 discharge (63 to 93 days)
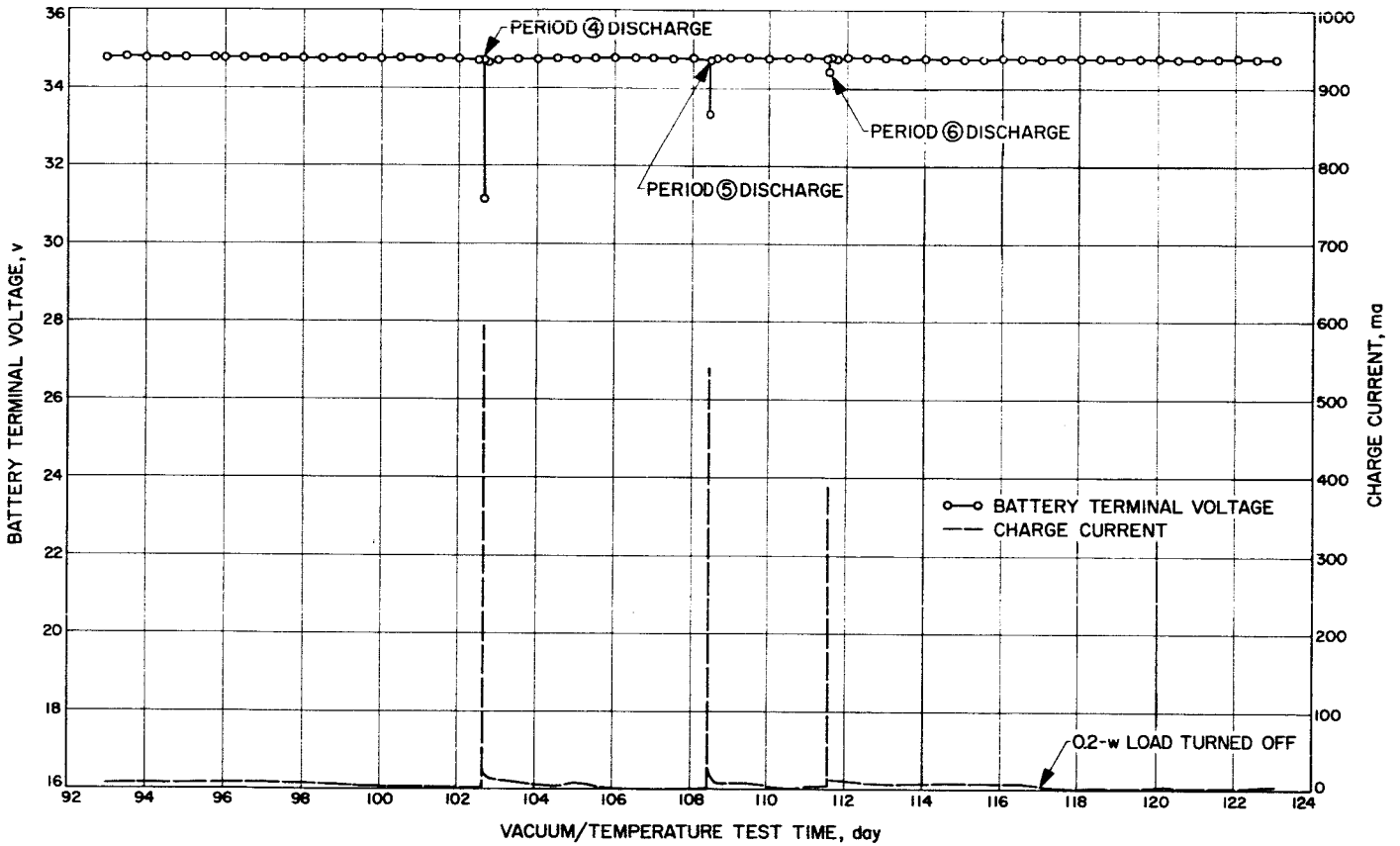
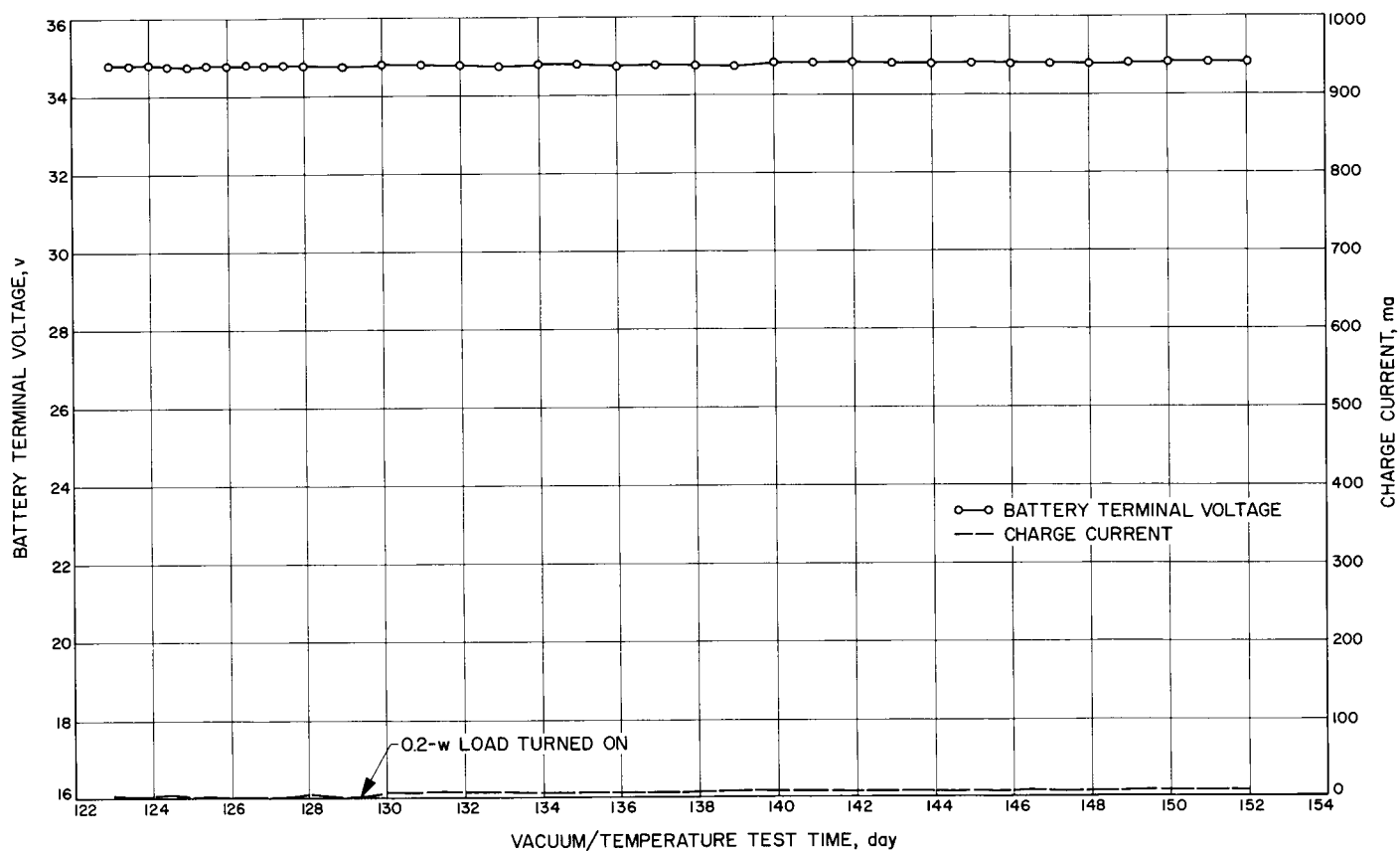Fig. 48. Type approval battery 3 cruise mode charging and periods 4, 5, and 6 discharges

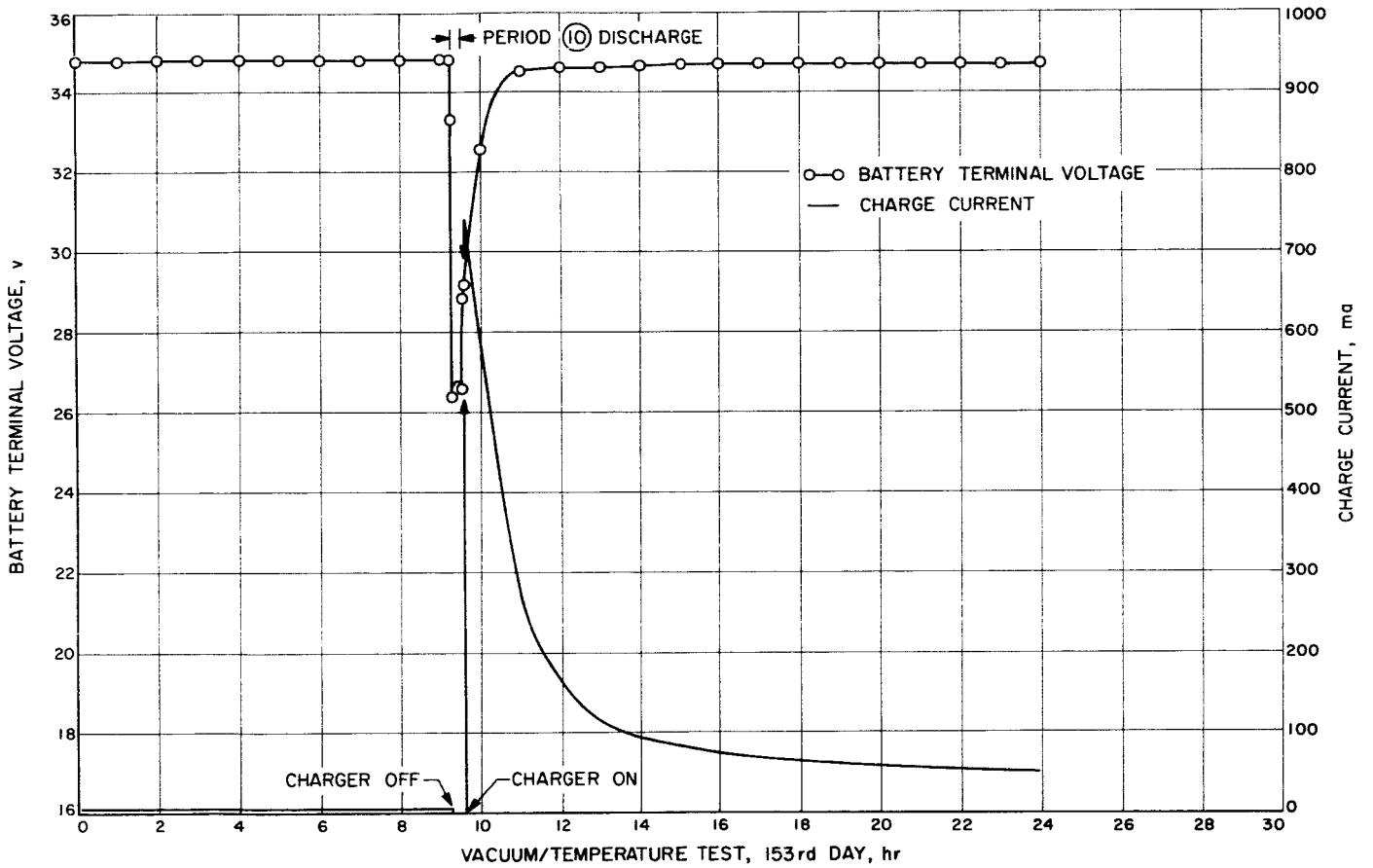**Fig. 49. Type approval battery 3 cruise mode charging with 0.2-w load off**

Fig. 50. Type approval battery 3 cruise mode charging and period 10 discharge

control system brought the battery temperature below 82°F within 8 hr. This delayed temperature response was slowed by the charging which was initiated at the conclusion of the discharge. Figure 50 shows that the initial charge current was 740 ma, and decreased rapidly to less than 100 ma within 4 hr.

Planet encounter phase. When the time for the period 7 discharge on the 156th test day arrived, the charge current had decreased to approximately 10 ma (Fig. 51). The charger was turned off prior to this final discharge to simulate the effect of the reduced solar panel voltage, which would be decreasing throughout the flight as the result of decreasing solar intensity. The battery was discharged for 18 hr at 32 w, with one squib load of an additional 136 w applied early in the 18-hr discharge. Battery voltage on the small load stabilized in the range of 27.7 to 27.8 v. However, the battery voltage during the squib load was a minimum of 25.63 v, almost 0.2 v below the required minimum of 25.8 v. When the load was removed from the battery at the end of 18 hr, the

open-circuit voltage was 28.57 v; however, this voltage continued to decrease rapidly over the next 4 days. Figure 52 indicates the rapid change in the open-circuit voltage of the battery. The cell numbers shown on Fig. 52 are located at the times at which those cells appear to have developed internal shorts. The TA 3 battery was removed from the vacuum/temperature test chamber after 161 days. Voltages measured at that time indicated there were only 6 cells which had not shorted. During the period that the battery was packed and shipped to the manufacturer for examination, the remaining cells shorted, resulting in a battery terminal voltage of 0.92 v.

Battery examination. Type approval 3 battery was returned to the manufacturer for an examination (postmortem) to determine the cause of the failures noted during the test program. Cell voltages were all below 0.5 v and the battery voltage was 1.02 v prior to disassembly of the cells. The presence of voltage between the metal chassis and the cell terminals indicated that several cells had broken and electrolyte leakage had
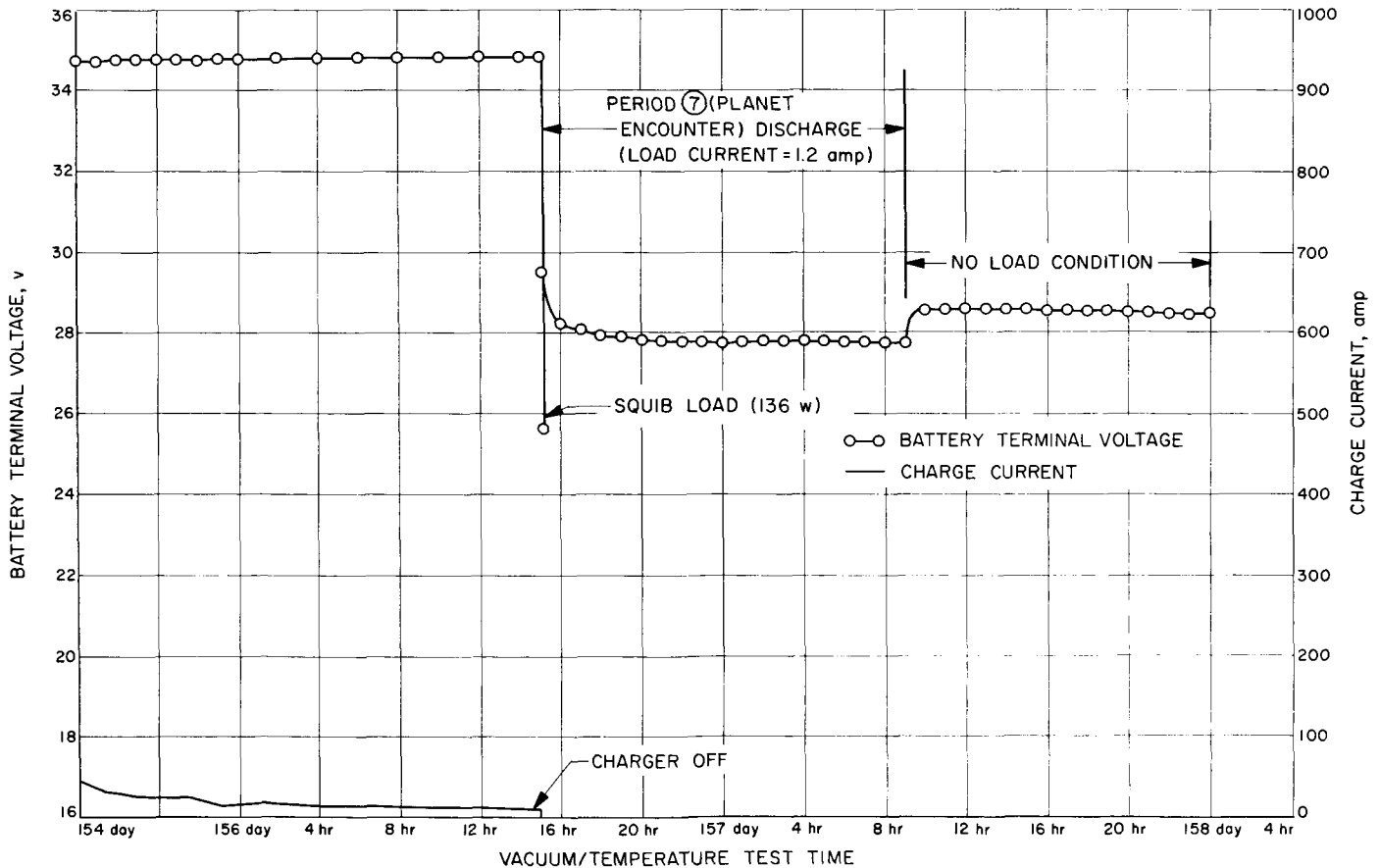

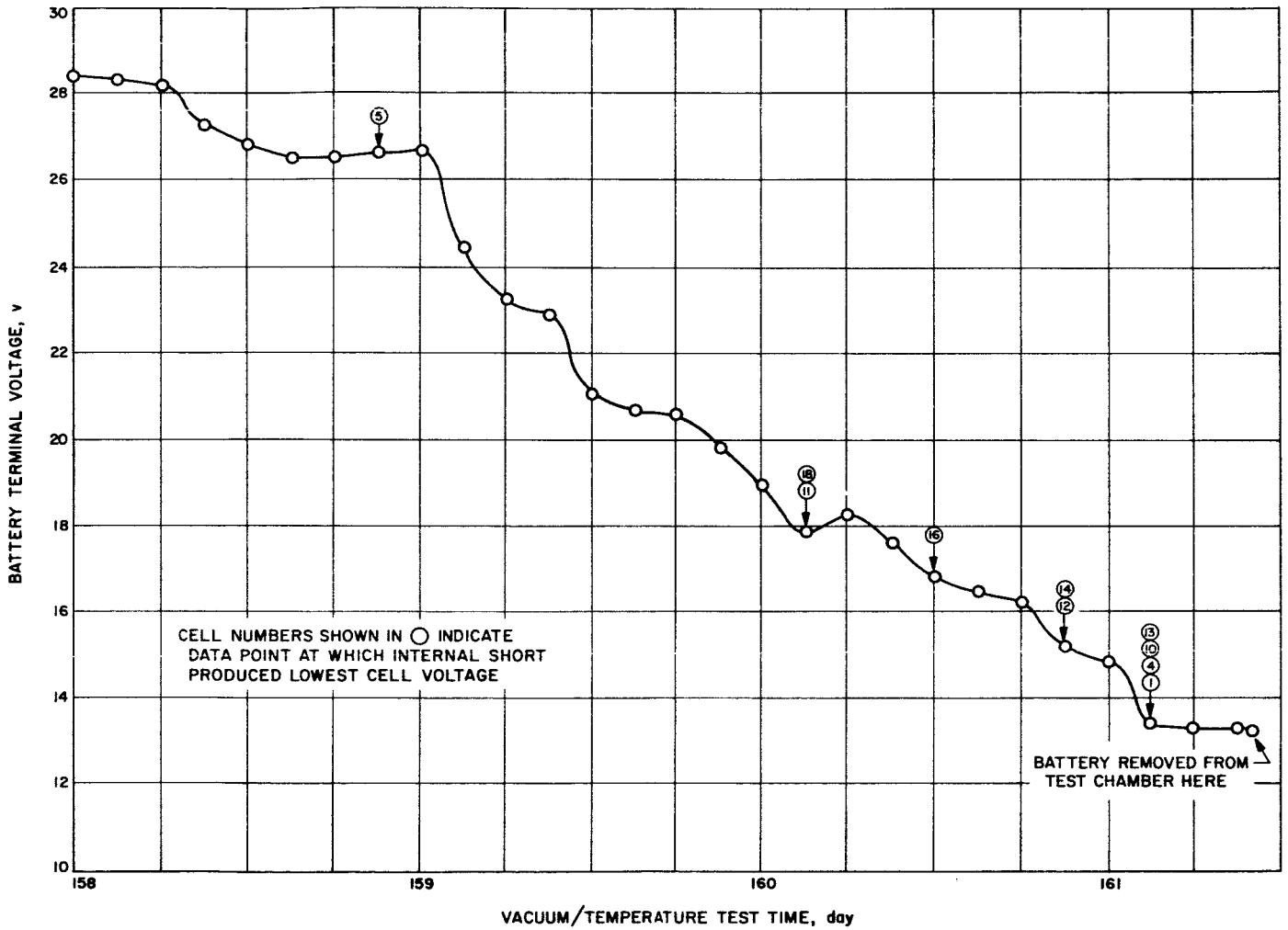Fig. 51. Type approval battery 3 performance during planet encounter

Fig. 52. Type approval battery 3 open-circuit voltage after planet encounter

occurred. Examination of the cell monoblocks disclosed the structural failures which are described in Table 12. Cracked cell walls resulted from excessive pressure buildup which was created as the result of cell shorting internally. After the shorting of the first cell the resultant chain reaction propagated similar damage throughout the battery. Further examination of cell components in both 9-cell assemblies disclosed the presence of zinc trees over the top of the separator, resulting in fully discharged positive and negative plates. Deterioration of the cellophane separator was observed in the fold area (corners) of some cells.

Design recommendations. The failures experienced with this battery are similar to those discussed for TA batteries 1 and 2. The design changes previously described were, therefore, considered satisfactory.

4. Summary of Type Approval Batteries

a. Summary of type approval battery 1 operation. The first cycle test conducted prior to the type approval test sequence produced 65 amp-hr on discharge and the battery accepted 63 amp-hr during charging. The discharge yield for this battery was less than TA 2 and 3 on the first cycle as a result of the procedure specifying an end of discharge voltage, which was higher than the subsequently corrected value.

The transportation vibration and handling shock tests were conducted with no immediately observable effect on the battery. Subsequent electrical tests were relied upon to detect internal effects which could be produced by these environments.

Battery performance during the 10-day temperature/humidity test was within the required limits.

The static acceleration test did not produce an identified effect on battery performance.

Battery performance during the high and low frequency vibration test was satisfactory.

The shock testing encountered difficulty in obtaining synchronization between the shock pulse and the peak-load pulse. No effect due to shock was observed on the battery, under the continuous discharge load. This test procedure was revised for the testing of the other TA batteries.

The battery test sequence was not properly conducted at the beginning of the vacuum/temperature test phase.

Table 12. Type approval battery 3 post-mortem examination

Assembly No.	Mono-block	Cell No.	Open-circuit voltage	Intercell wall[a]	Outside wall	Cell seal
7	5 cell	1	0.04	Broken	—	Leak at outside corner
		2	0.05	Broken	Broken	—
		3	0.04		—	—
		4	0.08	—	—	—
		5	0.12	—	—	—
		6	0.41	—	Broken	Leak at outside edge
	4 cell	7	0.09	—	Broken	—
		8	0.09	—	Broken	—
		9	0.09	—	—	—
9	5 cell	1	0	Broken	—	—
		2	0	Broken	—	—
		3	0	—	—	—
		4	0	Broken and burn hole	—	—
		5	0	—	—	—
		6	0	—	—	—
	4 cell	7	0	—	—	—
		8	0	—	—	—
		9	0	—	—	—

[a] The physical conditions of the intercell walls are listed between their respective cell numbers.

The discharging of the battery at that time was not considered detrimental to further battery testing. The flight charger was turned on and this simulated Sun acquisition sequence continued satisfactorily for 20 hr. Battery performance, during the midcourse maneuver and cruise mode load periods which followed, was also satisfactory. During the simulated planet encounter sequence, the battery terminal voltage dropped below the required minimum for several of the discharge periods. Comparison of cell voltages indicated the formation of internal cell shorts. The action of these cells during a subsequent period of open circuit confirmed this condition.

b. Summary of type approval battery 2 operation. The 72 amp-hr delivered on the first discharge and the acceptance of 65 amp-hr on the subsequent charge, both exceeded the minimum requirements for the pre-type approval checkout cycle.

The examination of this battery, following the transportation vibration test and that portion of the handling

shock test conducted in the shipping container, revealed electrolyte leakage in both of the 9-cell assemblies. Open-circuit cell voltages indicated that no cell shorting had occurred. Discharge of this battery at the 10-amp rate prior to shipment to the manufacturer yielded 67 amp-hr. The leaks were attributed to a previously detected design problem which had been corrected for later units. The battery was repaired by resealing the cell covers and was returned to JPL for continuation of the test program.

During the 10-day temperature/humidity test, the battery performance was acceptable for the open-circuit stand period and subsequent 30-min discharge.

Battery performance during discharge while subjected to static acceleration was acceptable.

Battery performance during discharge while subjected to low and high frequency vibration was acceptable.

Battery performance during the shock test, with a peak load of 460 w, was acceptable. The minimum discharge voltage was 26.4 v, with a 0.1 v dip resulting from the shock pulse.

Polarity reversal of cell 9, at the beginning of the vacuum/temperature test sequence, resulted from an error in the test procedure. The launch load period discharge was repeated at the beginning of the simulated space flight (vacuum/temperature) portion of the test. Charging to replace the energy removed during that discharge delayed the start of the midcourse maneuver load period. Difficulties with the charger calibration procedure also delayed the midcourse maneuver test phase. Deterioration of the voltage of two cells was observed near the end of the charging sequence. Float charging was continued for an additional 19 days and cell voltage variation and the accompanying increase in charger current resulted in the conclusion that several cells had developed internal shorts. Electrolyte leakage was observed in the vacuum chamber requiring the immediate removal of the battery.

c. Summary of type approval battery 3 operation. The discharge energy delivered on the first cycle, was 75 amp-hr and the charge accepted was 66 amp-hr, well above the required minimum of 60 amp-hr.

The transportation vibration and handling shock tests were conducted without any observed effect on the battery.

Battery performance during the 10-day temperature/humidity sequence, was according to the requirements. The battery remained in the test chamber in the open-circuit mode for an additional 36 hr. During this period, a malfunction in the chamber temperature control system resulted in a maximum chamber temperature of 135°F. When the battery was removed from the chamber, electrolyte leakage from one of the 9-cell assemblies was detected. This leak was repaired and the test program was continued.

During the static acceleration test, battery performance was acceptable and appeared to be unaffected by this environment.

Battery performance during the high and low frequency vibration tests was apparently unaffected.

Shock testing of the battery under a load of 460 w resulted in a 0.1-v dip in the terminal voltage.

Battery performance during the Sun acquisition, mid-course maneuver, and cruise phases of the vacuum/temperature test sequence was within the required limits. During the planet encounter phase, the battery voltage for the squib load was 0.2 v below the required minimum of 25.8 v. Battery voltage remained above 25.8 v for the balance of the planet-encounter discharge period. During the following 4 days, the open-circuit voltage measurements indicated that as many as 12 cells had developed internal shorts. TA battery 3 was removed from the test chamber after 161 days and the shorted cell condition was confirmed. During the interval that the battery was in transit to the manufacturer for examination, the remaining 6 cells shorted, resulting in a battery terminal voltage of 0.92 v.

VII. *MARINER II* BATTERY FLIGHT DATA

The *Mariner II* spacecraft development schedule was limited in time by the brief span of usable launch dates for a flight to Venus. The development of the battery for this flight was, therefore, restricted to a schedule which did not contain sufficient time to fully qualify the *Mariner II* battery design. Repeating the type approval test sequence described in this Report, using batteries of the *Mariner II* design, was not possible because of flight schedule restrictions.

The design changes resulting from the TA test program on the development model battery and the additional changes dictated by the *Mariner II* spacecraft system requirements were combined in the final battery design.
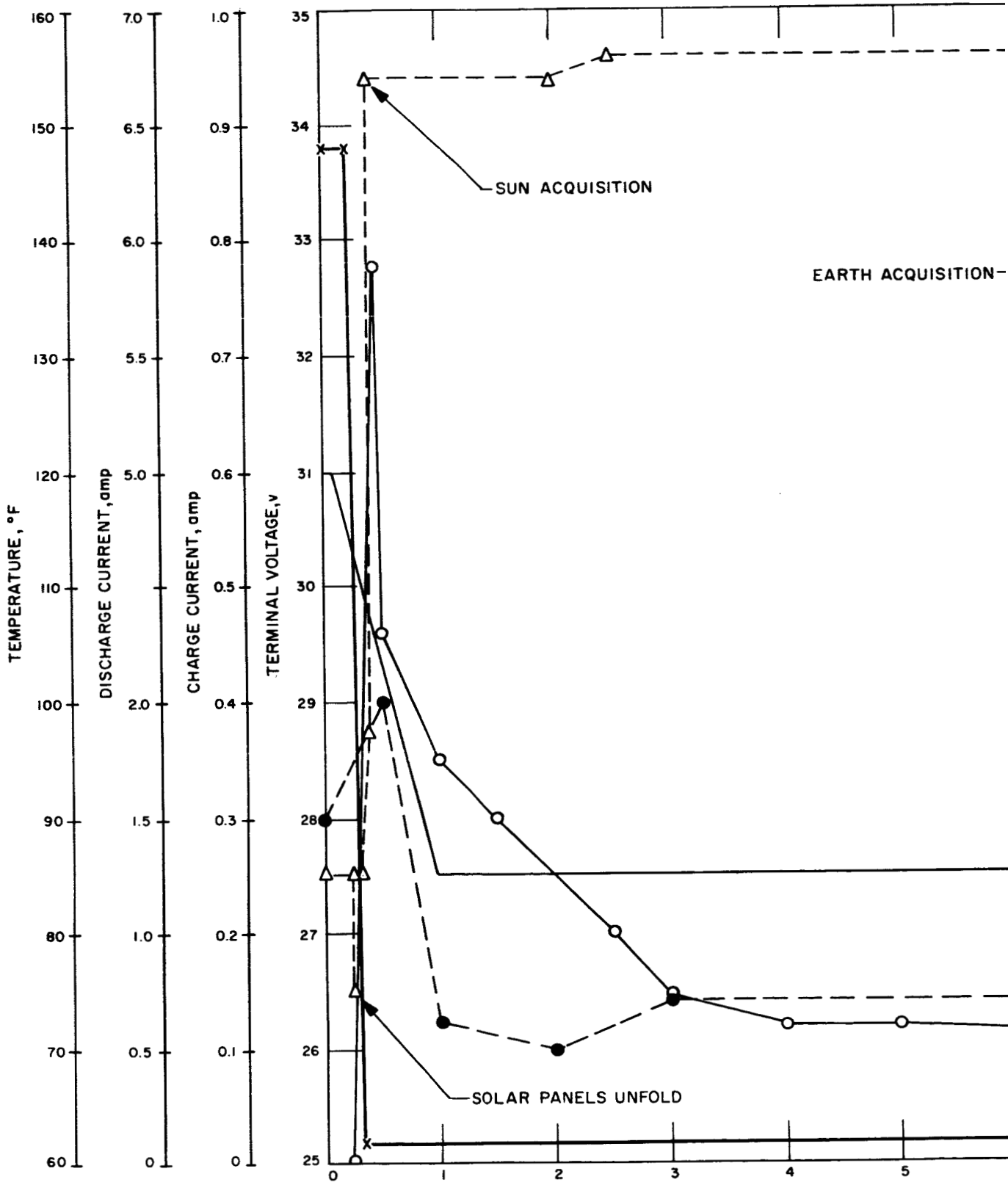
Fourteen batteries of the *Mariner II* design (Table 2) were built. Number 1 was a prototype battery, which was used to evaluate the electrical characteristics of this design. Numbers 2 and 3 were mock-ups for use in spacecraft weight, center of gravity and thermal tests. Numbers 4, 5, 8, 9 and 10 were used to support spacecraft systems tests. Number 6 was subjected to extensive shock and vibration testing. Numbers 7 and 11 were assigned to laboratory tests designed to evaluate capacity retention characteristics at various temperatures. Number 12, 14 and 15 were held in reserve as spares in support of the two spacecraft launches. Number 13 had a brief flight on *Mariner I*. Number 16 was flown in the *Mariner II* spacecraft.
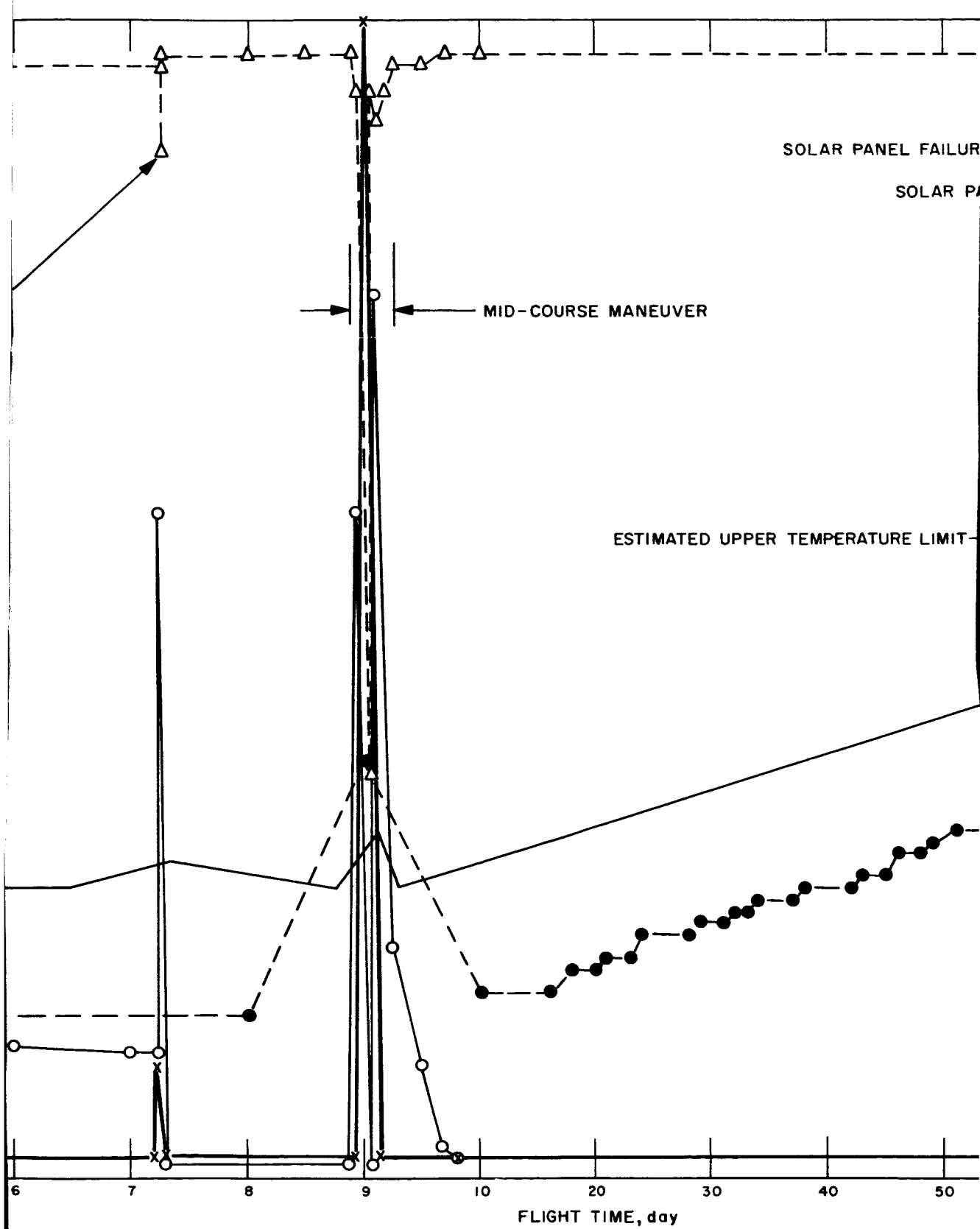
The *Mariner II* spacecraft was launched on August 27, 1962. The spacecraft telemetry system transmitted four measurements pertaining directly to the battery. These measurements were battery terminal voltage, battery temperature, battery charge current and battery discharge current. Figure 53 presents these four measurements in graphic form (necessarily condensed) for 129 days, starting at launch and progressing through Sun acquisition, Earth acquisition, the midcourse maneuver, planet (Venus) encounter, and for 20 days thereafter.

The minimum battery voltage during the flight was during launch, just prior to Sun acquisition, when it was 26.5 v. The maximum battery voltage of 34.7 v occurred during cruise charging. The battery temperature was slightly over 140°F at the end of the recorded data.

This battery met all spaceflight requirements and, in doing so, established several firsts in the history of batteries: (1) the first sealed *secondary* silver-zinc battery, (2) the first continuous charging of a sealed silver-zinc battery during spaceflight, and (3) the first silver-zinc battery to make a planetary spaceflight.
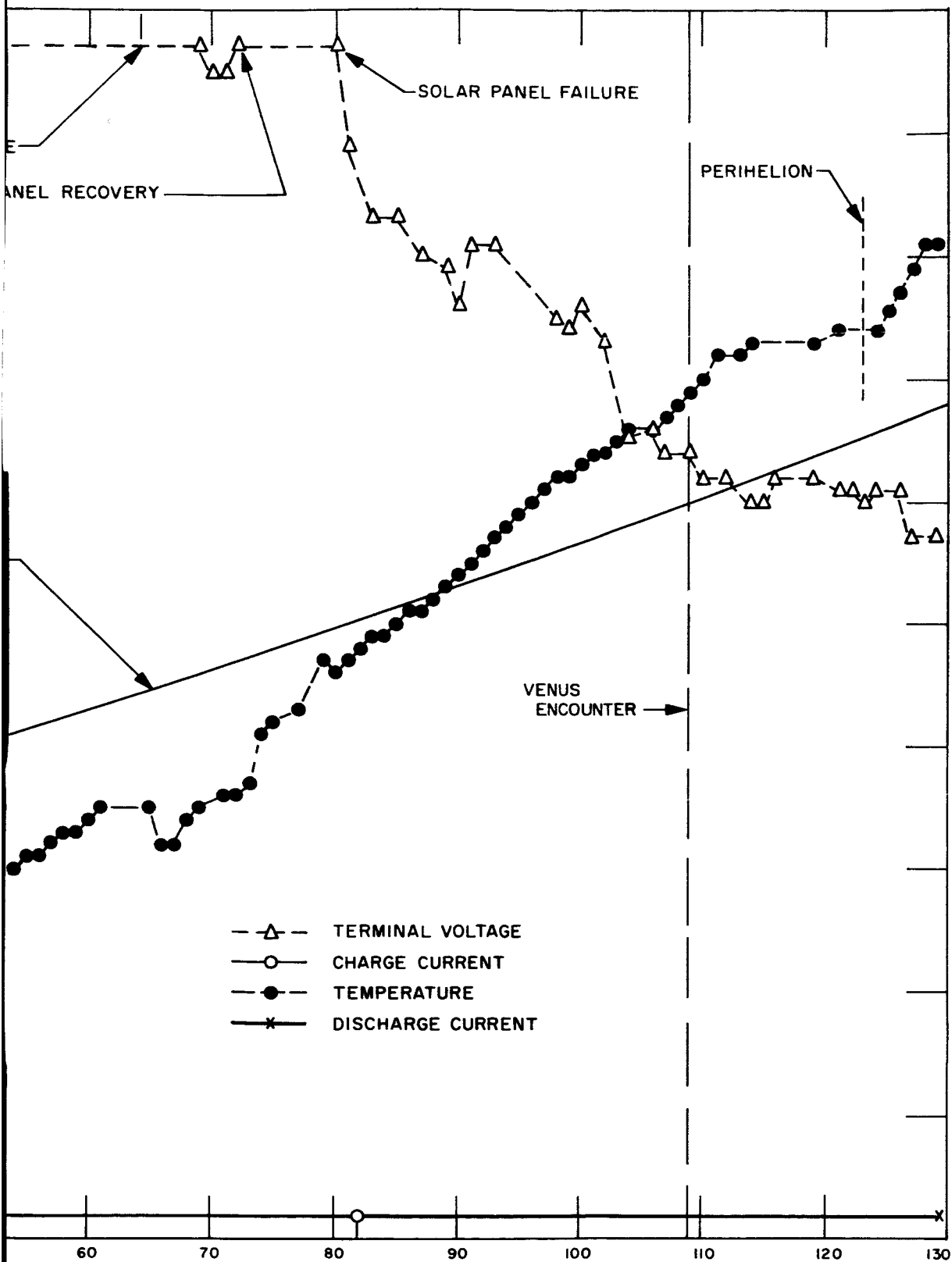
TEMPERATURE, °F

DISCHARGE CURRENT, amp

CHARGE CURRENT, amp

TERMINAL VOLTAGE, v

SUN ACQUISITION

EARTH ACQUISITION—

SOLAR PANELS UNFOLD

SOLAR PANEL FAILUR

SOLAR PA

MID-COURSE MANEUVER

ESTIMATED UPPER TEMPERATURE LIMIT—

FLIGHT TIME, day

2

SOLAR PANEL FAILURE

PERIHELION

ANEL RECOVERY

VENUS
ENCOUNTER →

— △ — TERMINAL VOLTAGE
—O— CHARGE CURRENT
— ● — TEMPERATURE
—✕— DISCHARGE CURRENT

60   70   80   90   100   110   120   130

Fig. 53. *Mariner II battery flight data*

3

REFERENCES

1. Schult, R. W., and Stafford, W. F., *The State of Development of Silver Oxide-Zinc and Nickel-Cadmium Batteries*, STL/TR-60-0000-09034, Space Technology Laboratories, Los Angeles, California, February 1960.

2. Howard, P. L., "The Silver Oxide-Cadmium Secondary Battery," Paper CP 61-346, Presented at AIEE Conference, New York City, New York, February 1961.

3. Whitney, C. B., "Evaluation of Silver-Cadmium Batteries For Satellite Applications," Test No. D2-90023, Boeing Airplane Company, Seattle, Washington, August 21, 1961.

4. The Electric Storage Battery Company, Missile Battery Division, "Service and Operating Introductions For The Sealed Silver-Zinc Battery Type 1SS25-1," Raleigh, North Carolina, March 27, 1961.

ACKNOWLEDGMENTS